75-49

4077

GEOTECHNICAL ENGINEERING

THE DESIGN OF HIGHWAY CUTS IN INTERMEDIATE QUALITY ROCK

Rock Testing Techniques Related to the Performance Of Highway Cuts in Shales and Sandstones

by

R. E. GOODMAN

F. E. HEUZÉ

R. K. THORPE

J. M. CHATOIAN

CALIFORNIA DEPARTMENT OF TRANSPORTATION
CONTRACT NO. HPR-PR-1-(11) DO346
REPORT NO. TE-75-1

DEPARTMENT OF CIVIL ENGINEERING
UNIVERSITY OF CALIFORNIA, BERKELEY

TRANSPORTATION MATERIALS
& RESEARCH LIBRARY

UNIVERSITY OF CALIFORNIA · BERKELEY

Clibpdf - www.fastio.com

Geological Engineering

THE DESIGN OF HIGHWAY CUTS IN INTERMEDIATE QUALITY ROCK

Rock Testing Techniques Related to the Performance of Highway Cuts in Shales and Sandstones

by

R. E. Goodman
F. E. Heuzé
R. K. Thorpe
J. M. Chatoian

California Department of Transportation
Contract No. HPR-PR-1-(11) D0346)

August, 1974

Department of Civil Engineering
University of California, Berkeley

ClibPDF - www.fastio.com

TECHNICAL REPORT STANDARD TITLE PAGE

1. REPORT NO. b	2. GOVERNMENT ACCESSION NO. b	3. RECIPIENT'S CATALOG NO. b
4. TITLE AND SUBTITLE The Design of Highway Cuts in Intermediate Quality Rock		5. REPORT DATE
		6. PERFORMING ORGANIZATION CODE
7. AUTHOR(S) R.E. Goodman, F.E. Heuzé, R.K. Thorpe, J.M. Chatoian		8. PERFORMING ORGANIZATION REPORT NO. CA-DOT-TL-2137-1-75 RTA13945-194051-UCB
9. PERFORMING ORGANIZATION NAME AND ADDRESS Geological Engineering Group, Civil Engineering Department University of California, Berkeley 94720		10. WORK UNIT NO. b
		11. CONTRACT OR GRANT NO. D0346
12. SPONSORING AGENCY NAME AND ADDRESS Department of Transportation Transportation Laboratory Sacramento, California 95825		13. TYPE OF REPORT & PERIOD COVERED Final
		14. SPONSORING AGENCY CODE b

15. SUPPLEMENTARY NOTES

This study was conducted in cooperation with the U.S. Department of Transportation, Federal Highway Administration (Federal Program No. HPR-PR-1-(11) D0346)

16. ABSTRACT

The report discusses testing techniques helpful in forecasting the behavior of highway cuts in shales and sandstones intermediate in physical properties between hard rocks and soils. The investigation included borehole loading tests in situ, and laboratory measurements of durability, strength, and rock quality. Equipment and procedures for testing together with typical results are presented for a number of techniques including NX borehole jack measurements; slake durability tests; point load strength determinations; radial permeability tests; and direct shear tests. Field studies and samples for laboratory studies were derived from three highway cuts within 50 miles of Berkeley.

17. KEY WORDS Rock cuts, California, sandstones, shales, weathering, mechanical properties, in-situ tests, bore-hole jack, shear testing, permeability, durability, deformability	18. DISTRIBUTION STATEMENT Unlimited

19. SECURITY CLASSIF. (OF THIS REPORT) Unclassified	20. SECURITY CLASSIF. (OF THIS PAGE) Unclassified	21. NO. OF PAGES 128	22. PRICE b

HMRT 1242 ORIG 9 72)

ClibPDF - www.fastio.com

ABSTRACT

The report discusses testing techniques helpful in forecasting the behavior of highway cuts in shales and sandstones intermediate in physical properties between hard rocks and soils. The investigation included bore hole loading tests in situ, and laboratory measurements of durability, strength, and rock quality. Equipment and procedures for testing together with typical results are presented for a number of techniques including: NX bore hole jack measurements; slake durability tests; point load strength determinations; radial permeability tests; and direct shear tests. Field studies and samples for laboratory studies were derived from three highway cuts within 50 miles of Berkeley.

ClibPDF - www.fastio.com

TABLE OF CONTENTS

		Page
ABSTRACT		i
LIST OF FIGURES		iv
LIST OF TABLES		vi
PREFACE		vii
Chapter 1.	INTRODUCTION	1
Chapter 2.	FIELD STUDIES	3
2.1	Locations of Sites Selected for Study	3
2.2	General Geology of the Study Sites	3
2.3	Sampling and Storage of Specimens	12
2.4	Rock Deformability Tests in the Field	13
Chapter 3.	LABORATORY INDEX TESTS	17
3.1	Radial Permeability Test	17
3.2	Slake Durability Tests	30
3.3	Point Load Strength Testing	43
Chapter 4.	LABORATORY SHEAR TESTS	47
4.1	Shear Tests on Specimens Selected for the Core Box	47
4.2	Large Specimen Direct Shear Testing	49
Chapter 5.	DISCUSSION AND RECOMMENDATIONS FOR FURTHER STUDIES	62
5.1	Results of the Test Program	62
5.2	Application of the Test Methods Discussed to the Design of Excavations in Intermediate Quality Rocks	63
5.3	Recommended Future Investigations	74
Appendix 1	GEOLOGICAL LOGS OF BORINGS	76
Appendix 2.1	CURVES OF BOREHOLE JACK (NX-JACK) TEST RESULTS	81

ClibPDF - www.fastio.com

		Page
Appendix 2.2	COMPUTER PROGRAM FOR NX-JACK TEST ANALYSIS, AND A TYPICAL OUTPUT INCLUDING A PRINTER PLOT	93
Appendix 3	DETAILED PROCEDURES FOR RADIAL PERMEABILITY TESTS	101
Appendix 4	DIRECT SHEAR TESTING WITH THE (σ,u) MACHINE	117
Appendix 5	DATA SHEET FOR LARGE SHEAR TESTS	124
REFERENCES		127

ClibPDF - www.fastio.com

LIST OF FIGURES

Figure		Page
2.1a	Site locations	4
2.1b	Location of site 1	5
2.1c	Location of site 2	6
2.1d	Location of site 3	6
2.2	General geologic map of site 1	9
2.3	General geologic map of site 2	10
2.4	General geologic map of site 3	11
2.5a	NX-jack test set up	15
2.5b	Close up of NX-jack	15
2.6	Typical plate pressure versus wall deformation curve for borehole jack tests	16
3.1	Radial permeability test apparatus	19
3.2	300 psi radial permeameter	20
3.3a,b	Radial permeability test equipment	21
3.4	Standard sample for use in the radial permeability test	22
3.5	Sample test results	26
3.6a,b,c	Failed samples	28,29
3.7a,b,c,d	Logs of point-load strengths and slake durability	37-40
3.8	Slake durability machine and point-load apparatus	41
4.1	Shear machine for samples up to 5 inches x 5 inches	52
4.2	Potted samples of rock core before shear test	52
4.3	Shear machine for samples up to 11 3/4 inches x 17 3/4 inches	55
4.4	Half of shear sample no. 1 (sandstone). Potted in plaster	56
4.5	Shear test data for large specimen of sandstone	60
4.6	Shear test data for soft claystone	61
5.1a	Geologic sketch map and cross-section of rock cut on Highway 24	65

ClibPDF - www.fastio.com

Figure		Page
5.1b	Photograph of cut of figure 5.1a used together with another similar photo	66
5.2	Extrapolated shear test curves	70
5.3	Determination of a single overall friction angle $\phi_{equivalent}$ for rock of intermediate quality (ϕ = 26° in sliding on smooth surfaces)	71
A3.1	Drill press set up used to drill the axial hole	110
A3.2	Alternate sealing and tube retaining system	111
A3.3	Radial permeameter top plate	112
A3.4	Deairing the axial hole	113
A3.5	Radial permeability data sheet	114
A3.6	Pipette flow measuring system	115
A3.7	Pipette valve and brackets	116
A4.1	Schematic section through direct shear machine	121
A4.2	Sealing scheme for water-tight test chamber	122
A4.3	Photographs of direct shear machine	123

ClibPDF - www.fastio.com

LIST OF TABLES

Table		Page
2.1	Summary of NX-jack borehole deformability measurements	14
3.1	Typical data sheet	25
3.2	Typical data sheet - slake durability test	35
3.3	Typical data sheet - point load test	36
4.1	Summary of small scale shear tests	50,51
4.2	Summary of large scale shear tests on intact samples	59
5.1	Peak shear strength roughness parameter J_R calculated for shear test results on discontinuity surfaces	72
5.2	Computation of Barton's $\tau - \sigma$ curves for shear tests on discontinuity surfaces	73
A3.1	Sample calculations	109

ClibPDF - www.fastio.com

PREFACE

This research was performed under contract with the California Department of Transportation. Mr. Marvin L. McCauley was Project Monitor. This study was conducted in cooperation with the U.S. Department of Transportation, Federal Highway Administration, Federal Program Number HPR-PR-1(11) D0346.

Professor Richard E. Goodman, of the Civil Engineering Department at the University of California, Berkeley was Principal Investigator in charge of the project. Dr. Francois E. Heuzé was also a Faculty Investigator. Messrs. Richard K. Thorpe and John Chatoian, Research Assistants, completed the research group.

Miss Debbie Honigman typed the manuscript and Mrs. Gloria Pelatowski drafted the figures. Their help is gratefully acknowledged.

The contents of this report reflect the views of the authors who are responsible for the facts and the accuracy of the data presented herein. The contents do not necessarily reflect the official views or policies of the State of California, or of the Federal Highway Administration. This report does not constitute a standard specification or regulation.

ClibPDF - www.fastio.com

Chapter 1. INTRODUCTION

In many highway projects, the design engineer is faced with two problems. First, a large number of cuts must be designed; thus one cannot usually conduct a very thorough study of each individual case. Second, California rock formations often have "intermediate" strength properties; they are neither soils, nor hard rocks. Powerful methods of slope analysis, using limit equilibrium analysis, finite element analysis, or three-dimensional graphical techniques (Duncan and Goodman,* 1968. Heuzé and Goodman, 1971. Wright, 1971) cannot readily be used.

Consequently one must develop special design procedures for working in these materials. The procedures should hopefully be based upon results from simple, inexpensive, and easily performed tests. Correlations must also be developed between various test results and the relevant properties of the rock mass.

This report marks the beginning stage of what is hoped will be a continuing committment by the California Transportation Department and the University of California to study the characteristics of these materials and to develop suitable analysis techniques for transportation construction. The approach adopted in this first research project was to inquire into new methods of rock testing appropriate to classification and design of excavations in intermediate quality rocks. The investigation encompassed the following:

1. Field work, including NX-jack rock deformability testing in boreholes as well as sampling and field mapping;
2. Laboratory work searching for quality measurements and index properties of core samples; these included radial permeability, point load strength, and slake durability tests.

*See alphabetic list of references at the end of this report.

ClibPDF - www.fastio.com

3. Laboratory shear tests under controlled normal load and controlled shear displacement, or shear load.

It is hoped in later research to demonstrate relationships between cut performance and properties derived from such tests.

In agreement with the Project Monitor, three field sites were chosen in shales and sandstones, within a radius of 50 miles from Berkeley; they were respectively on Highway 680 (at the Sheridan Road exit), on Highway 4 (near the John Muir Mansion) and on Highway 24 (at the east end of the Caldecott Tunnel). The cut on Highway 680 was part of a large number of California highway cuts investigated previously by the Division of Highways (Mearns, Hoover and McCauley, 1973). The cuts on Highways 4 and 24 were not part of this group, but were fully representative of the conditions to be studied in this work.

Two sites on Highway 1, near Pacifica, in decomposed granite, were originally proposed but abandoned after discussions with the Project Monitor.

The rest of the report is organized in 4 chapters.

Chapter 2: Field Studies

Chapter 3: Laboratory Index Tests

Chapter 4: Laboratory Shear Tests

Chapter 5: Discussion and Recommendations for Further Studies

ClibPDF - www.fastio.com

Chapter 2. FIELD STUDIES

2.1 Locations of Sites Selected for Study

Three roadcuts were selected to obtain samples for testing and evaluation. Figure 2.1a, a map of the San Francisco Bay Area, shows their locations. Site 1 is located on Interstate Highway 680, about one-fourth mile south of the Sheridan Road interchange in Alameda County (figure 2.1b). The Sheridan Road interchange is about five miles southwest of the Sunol exit. The site is on the north side of the freeway and is the first roadcut south of Sheridan Road. Site 2 is a roadcut on State Highway 4, just west of the town of Martinez, in Contra Costa County (figure 2.1c). It is about a quarter of a mile west of the Alhambra Avenue interchange, on the north side of the freeway. The third site is on State Highway 24, about 6 miles east of Oakland, (figure 2.1d). It is located at the eastern end of the Caldecott Tunnel, in Contra Costa County and on the south side of the freeway, adjacent to the freeway offramp to Fish Ranch Road.

2.2 General Geology of the Study Sites

Site 1: The roadcut at site 1 is cut into a hill consisting of a light grey, fissile shale. The cut strikes N78E and is about 150 feet high on a slope of about 60°; it has a 30 foot wide bench. The shale strikes N58°-64°E and dips about 38° to the south. It weathers to a light brown and forms a soil comprised of small, angular chips of shale about 1/8 of an inch long and smaller. The soil zone is more than 12 inches thick on the hill above the cut and less than 2 inches thick on the cut face. There are very few outcrops on the gently rolling hill into which the slope is cut. Tension cracks are present on the cut face above the bench. Small scarps, about 1 to 2 feet high, have developed in some areas (figure 2.2). Above the cut is an arc-shaped zone of tension

ClibPDF - www.fastio.com

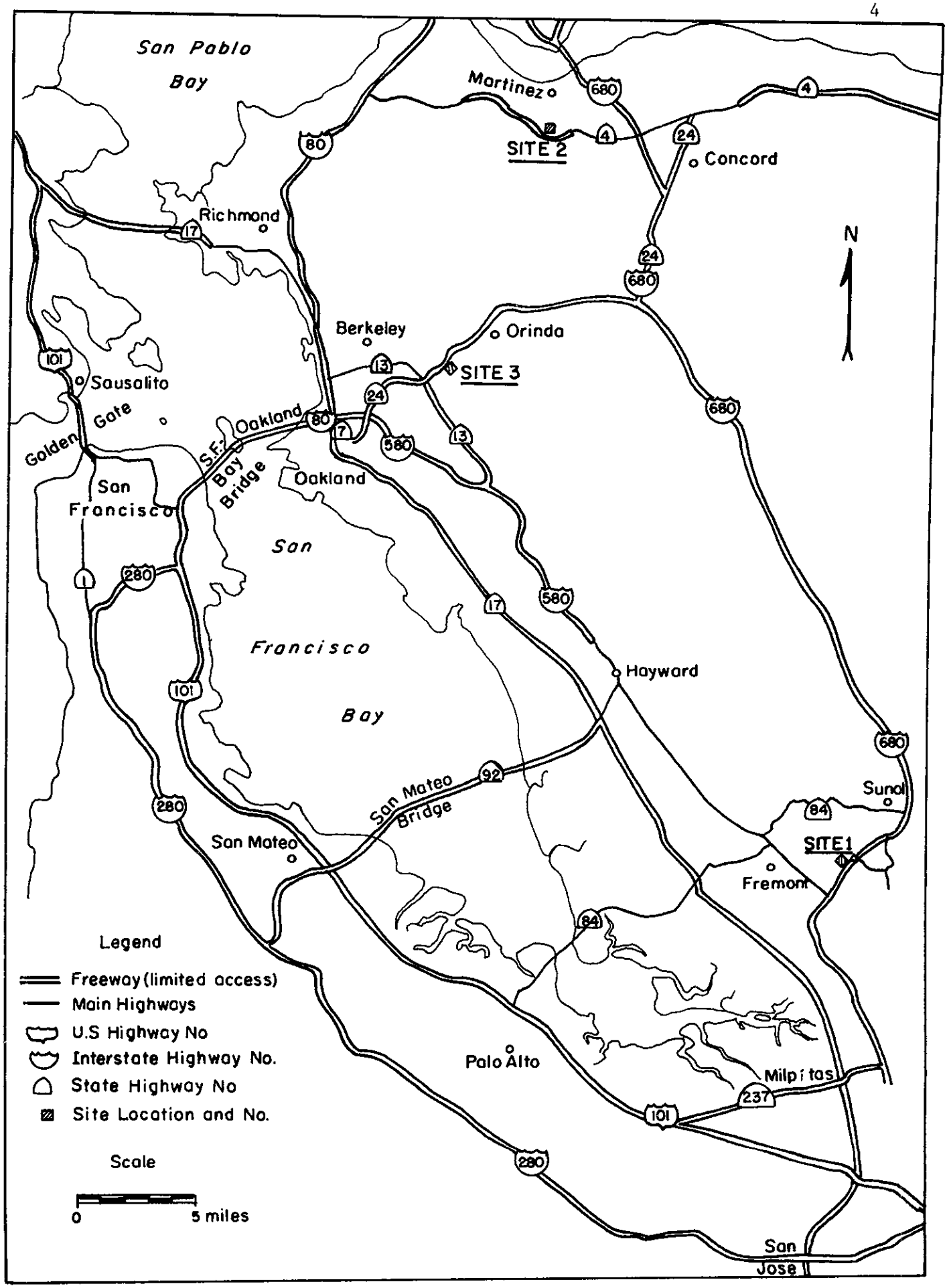

Figure 2.1a. Map of San Francisco Bay Area showing the site locations.

ClibPDF - www.fastio.com

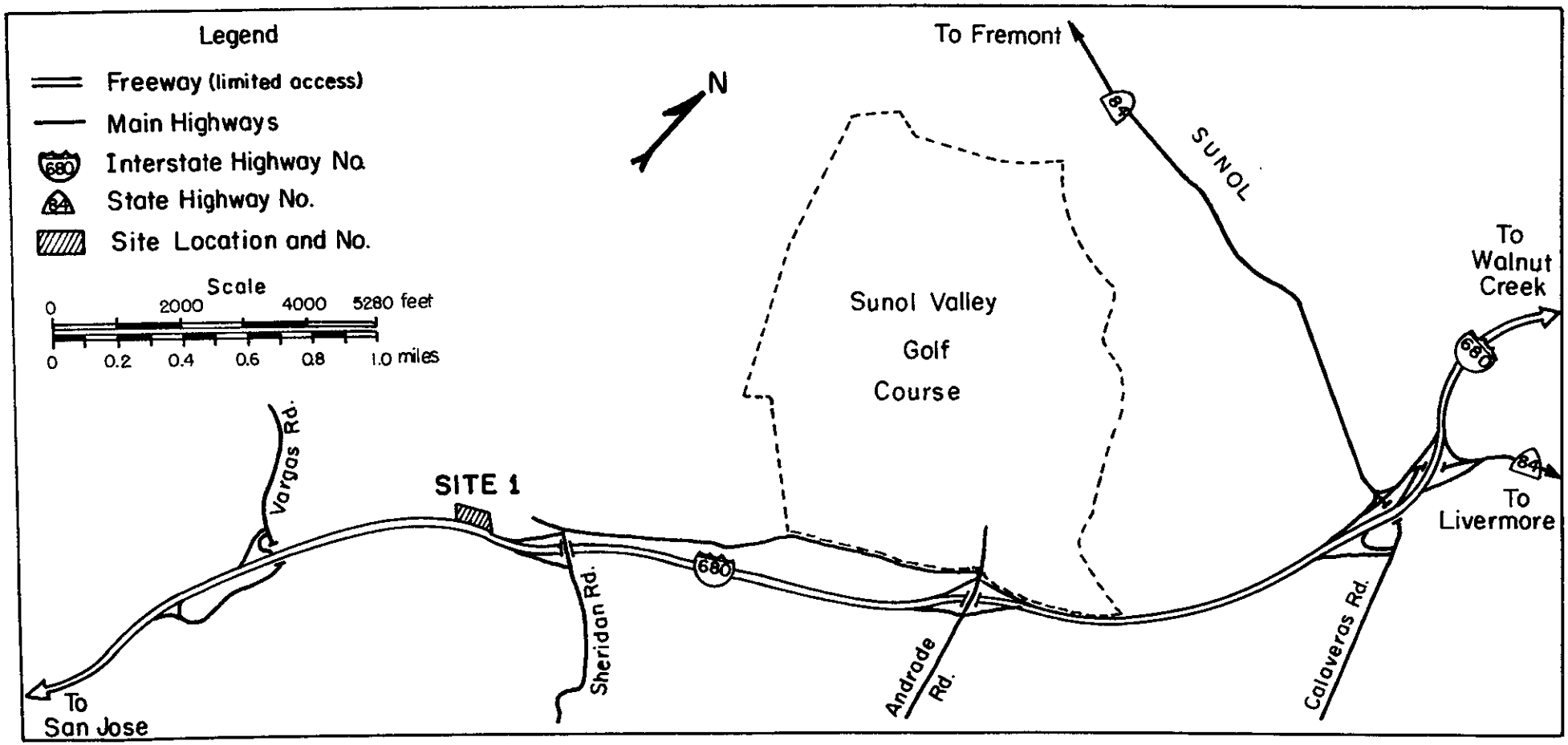

Figure 2.1b. Location of Site 1.

ClibPDF - www.fastio.com

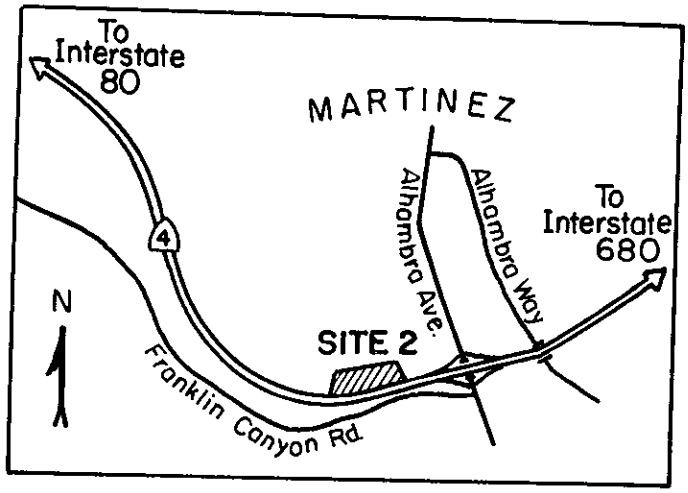

Figure 2.1c. Location of Site 2.

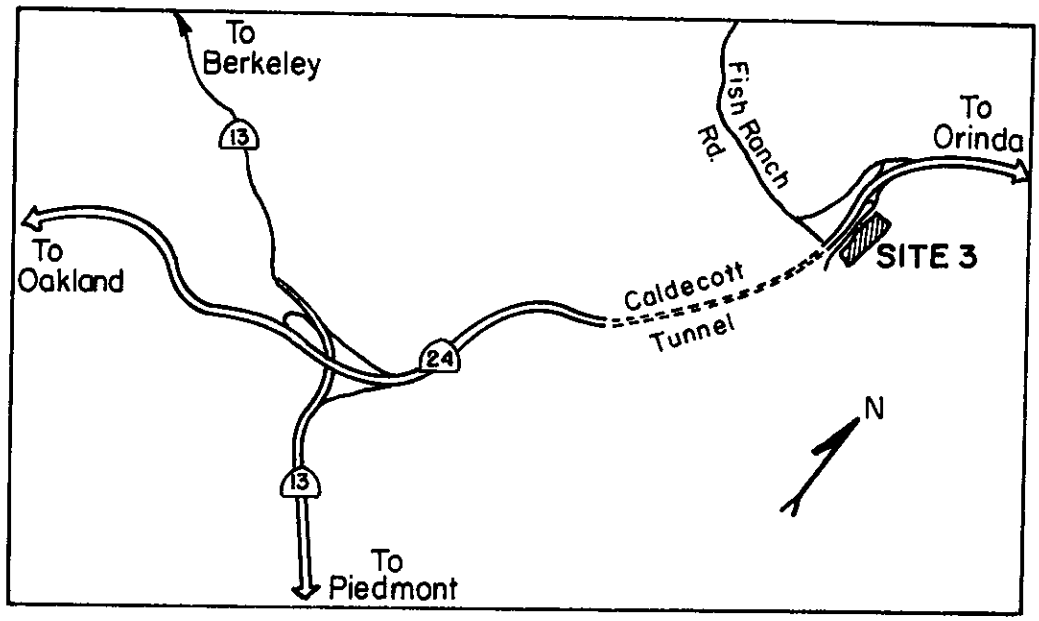

Figure 2.1d. Location of Site 3.

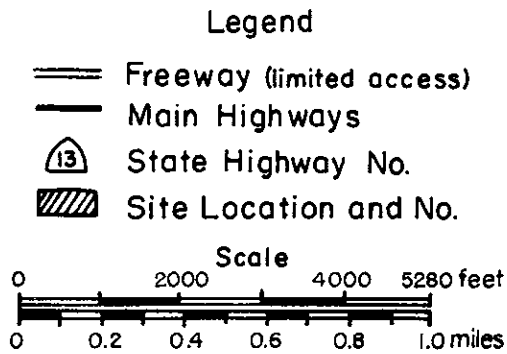

ClibPDF - www.fastio.com

cracks in which the openings are up to 2 inches wide. There is a small scarp, ranging from 6 to 12 inches high, along the back of this zone.

A vertical borehole was drilled, on the bench,to a depth of 35 feet (figure 2.2). Cores obtained from the drilling operation consist entirely of a light brown to dark grey shale. The cores are very soft and clayey near the surface and generally become harder with depth. Sample color changes from dark grey to light brown as the degree of weathering increases. When allowed to dry, all samples develop randomly oriented cracks. Cracking is much more intense in the highly weathered samples (upper 4 feet). Bedding planes, dipping about 30°, are first noticed in cores recovered from about 12 feet down. Fracture planes oriented both perdendicular to and sub-parallel to the bedding plane also become apparent at this depth. Most fracture planes contain a dark reddish-brown, non-calcareous coating. Calcareous staining occurs together with the reddish-brown coating at 20 feet. At 34 feet, the reddish brown coating is absent. Instead, the fractures are mineralized with a thin coating of quartz.

Site 2: The roadcut at site 2 is cut in a massive, light tan, fine-to-very fine grained feldspathic sandstone. The cut strikes N90E; it is about 200 feet high on a 1:2 slope with a 20 foot wide bench at mid height. Very fine grained, sub-angular to sub-rounded quartz comprises about 60 to 65 percent of the rock, very fine grained feldspar about 25 to 30 percent, and ferro-magnesium and minor accessory minerals about 10 percent. It is moderately well cemented. Small, rounded outcrops crop out through the thin, silty soil cover on the cut face. Above the cut, the soil cover is thicker and there are very few outcrops. To the west of the boreholes is a thick sequence of calcareous mudstones. It strikes about N55W and dips at about 45 to 60 degrees to the northeast. Neither borehole encountered this unit.

ClibPDF - www.fastio.com

Two boreholes, numbers two and three, were drilled to depths of 28 and 21 feet, respectively. Cores recovered from the two holes are mostly a light yellowish-brown, very fine grained, massive siltstone. It is highly altered and ranges randomly from moderately cemented to very poorly cemented. Samples fresh enough to analyze are comprised of 55 to 70 percent very fine grained, sub-angular to sub-rounded, well sorted, clear quartz; 25 to 35% very fine grained altered feldspar; (now a yellowish-brown clay); 5 to 9% sub-rounded black minerals, slightly larger than the quartz grains; and minor amounts of accessory minerals, including very fine-grained, sub-rounded garnet.

A light, yellowish-grey to yellowish-brown clay is present in two locations in borehole 2. Cores of this material were recovered from depths of 6 and 24 to 28 feet. It is very soft and pulls apart easily, revealing an intense network of slickensided discontinuities. The shear fractures dip from 15 to 30 degrees. There is no surficial expression for these shear zones on the cut face or the hill above it.

Site 3: The roadcut at site 3 is cut into a thick, steeply dipping sequence of grey, feldspathic sandstones and pebble-cobble conglomerates interbedded with reddish-brown shales (figure 2.4). The cut strikes N2E; it is about 250 feet high with 3 benches. The angle of the rock cut is 51°. The beds trend approximately N70W, dipping about 85 degrees to the east. A grey, fine grained, well lithified, feldspathic sandstone is the predominant unit. Within this unit are zones of coarse grained sandstones and conglomerates. The zones range in thickness from a few inches to several feet thick. Clasts in the conglomerate consist of sub-angluar to sub-rounded milky quartz, red chert, and volcanic rocks. The clasts range in size from pebble to cobbles. The matrix is a grey fine to medium grained, feldspathic sandstone. Some of the sandstone units show lateral gradations in grain size. In these units

ClibPDF - www.fastio.com

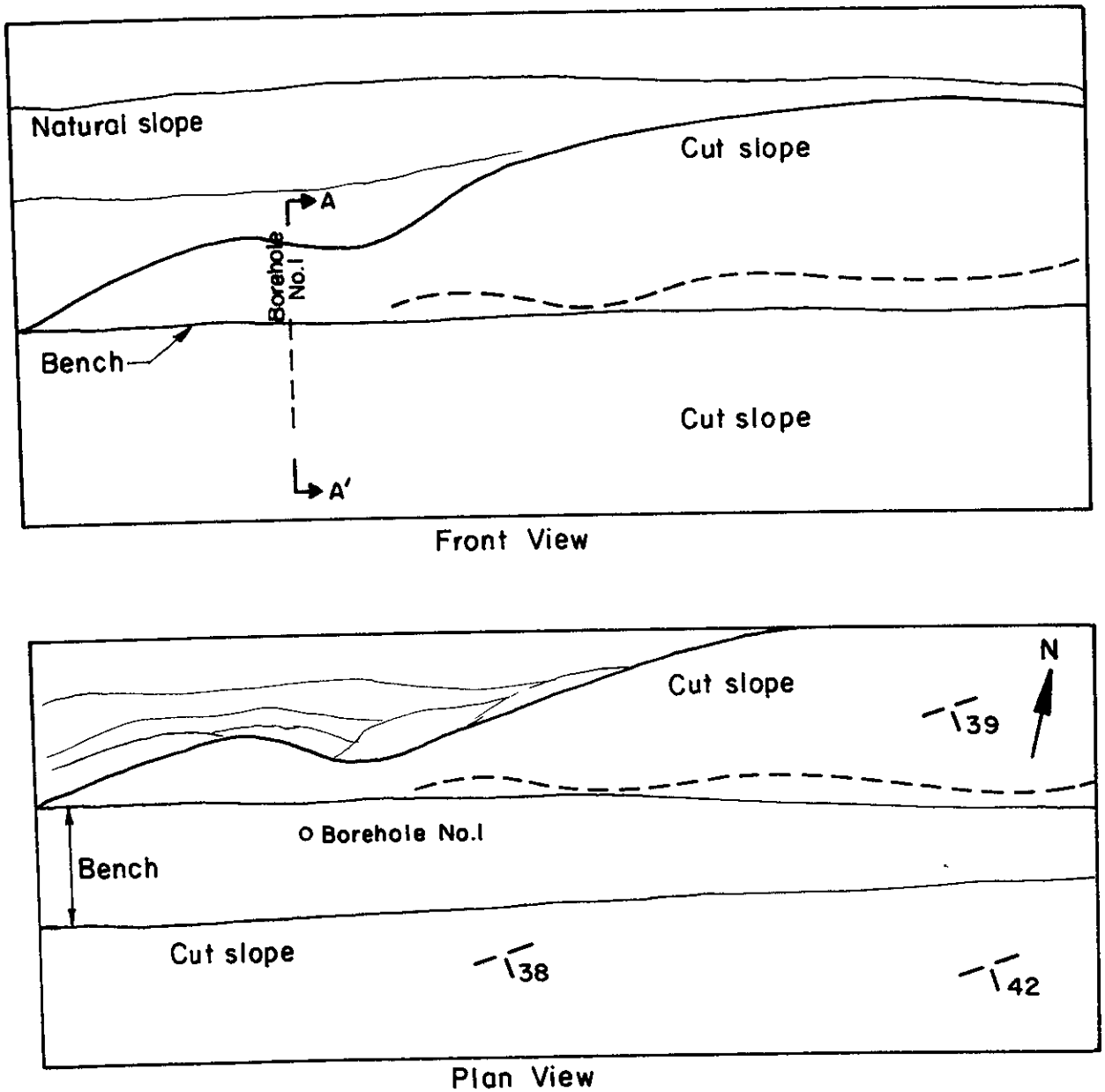

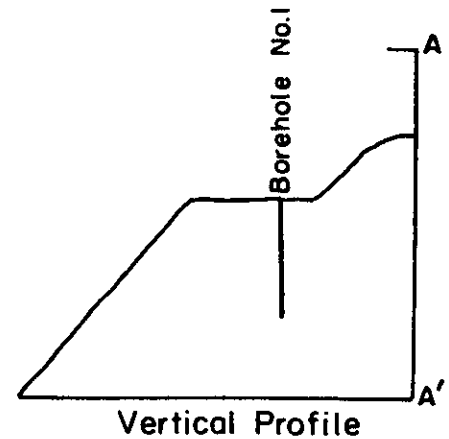

Rock is light grey fissile shale

Legend

tension cracks

strike and dip, approximate

30

0 20 40 60 ft.

Figure 2.2. General Geologic Map of Site 1. Roadcut (north side of freeway) west of Sheridan Road, on Highway 680, Alameda County.

ClibPDF - www.fastio.com

ClibPDF - www.fastio.com

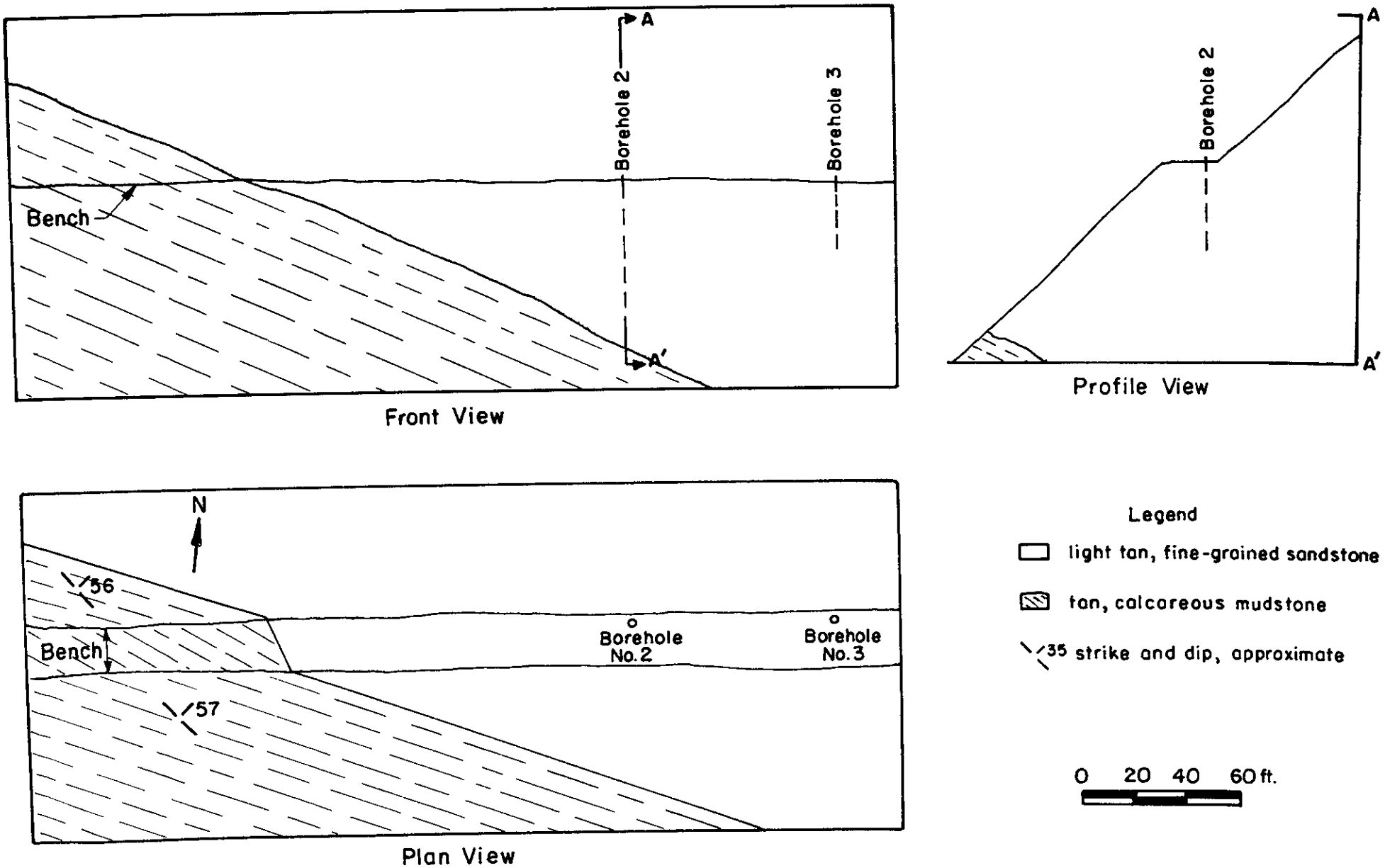

Figure 2.3. General Geologic Map of Site 2. Roadcut west of Alhambra Road, on Highway 4, Martinez, Contra Costa County.

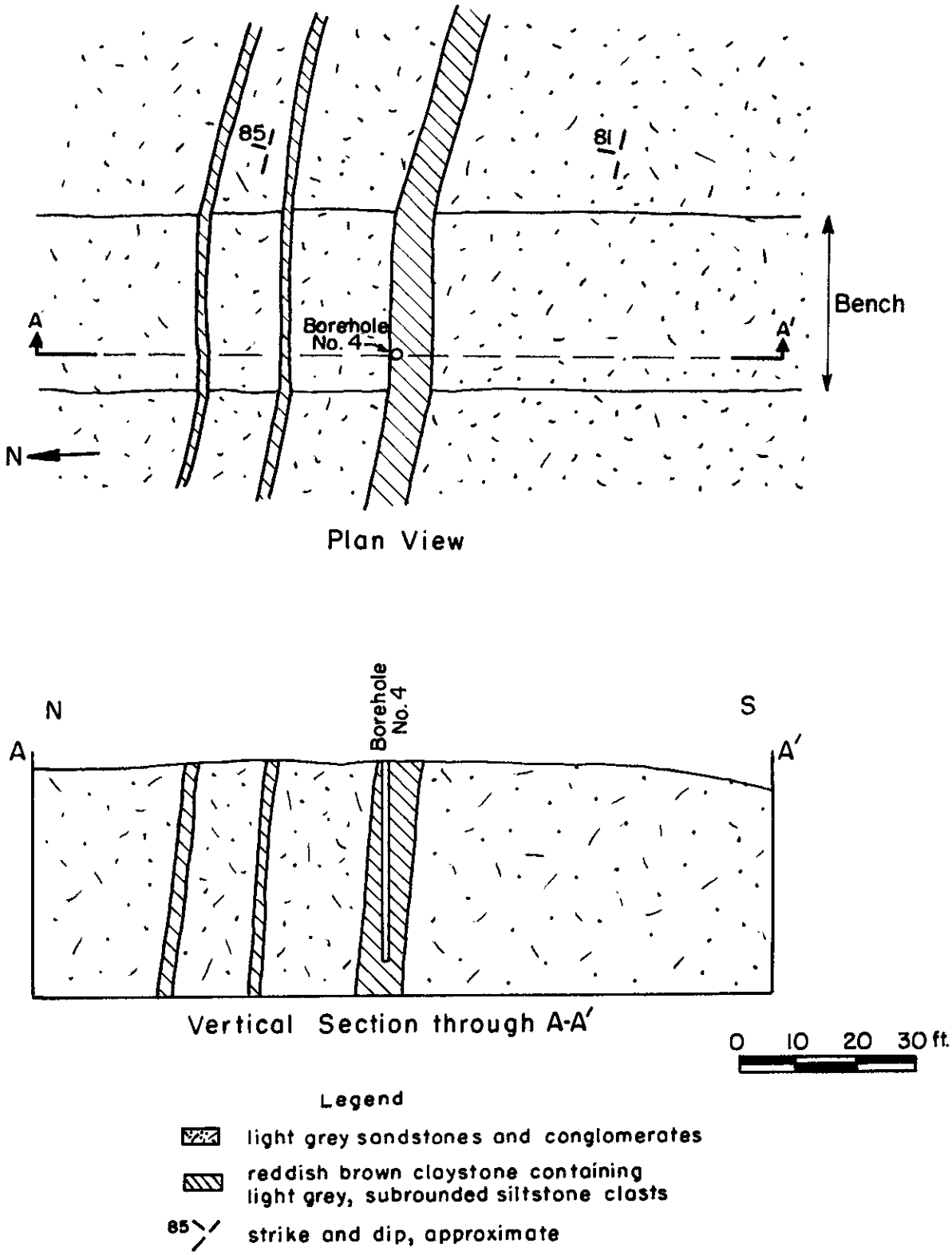

Figure 2.4. General Geologic Map of Site 3. Roadcut (south side of freeway) at east end of the Caldecott Tunnel, Contra Costa County.

ClibPDF - www.fastio.com

grain sizes range from pebble-sized at the base to medium or fine grained at the top.

A reddish-brown mudstone is interbedded with the sandstones and conglomerates. Individual beds range in thickness from one to three feet. Small, sub-angular to sub-rounded clasts of grey, very fine-grained feldspathic sandstone are found throughout the mudstone. They have the same composition as the fine grained sandstones at the site.

The mudstone has been weathered to a reddish-brown soil. Beneath the surface, and along rill banks, it forms small blocky fragments, smaller than 1/4 of an inch in diameter. These fragments form talus slopes 2 to 3 inches high along the rill banks. Rills and gullies occur along the cut slope. They are most pronounced along the interface between sandstone and mudstone beds, forming channels up to one and a half feet deep and 1 to 3 feet wide.

2.3 Sampling and Storage of Specimens

Core samples were recovered from the four boreholes by a 3.25 inch (OD) diamond core barrel five feet in length. The diameter of the core samples is approximately two inches. This dimension, along with the core lengths, varied considerably. In some instances, only rubble was retrieved. The samples were cleaned, logged, and stored in cardboard core boxes by the Transportation Laboratory's geologists. Our geological descriptions of the cores are included in Appendix 1. Upon receipt of the core boxes in the laboratory, the samples were sealed in plastic bags and stored in a 100 percent humidity room throughout the duration of testing.

Surface samples were obtained for direct shear tests. The rock samples were stored at room temperature and sealed in plastic bags. High humidity storage was not deemed necessary since the samples had been previously exposed to air at the ground surface.

ClibPDF - www.fastio.com

2.4 Rock Deformability Tests in the Field

a) The NX-jack: The NX-borehole jack is an instrument capable of applying unidirectional pressure to the wall of a borehole. The instrument, the testing procedure, and the data analysis have been thoroughly discussed in published literature (Goodman, Van, Heuzé, 1968; Heuzé, Goodman, Bornstein, 1971). Previous experience was primarily with fairly hard rocks with deformabilities of one to several millions of psi. However, it seemed that the instrument should also be used to investigate the softer rocks (10^5 psi $< E < 10^6$ psi) considered in this study.

b) NX-jack tests and results: Tests were performed in boreholes on all three field sites discussed at the beginning of the report. The typical set-up is shown in figure 2.5 with a close up of the instrument. Figure 2.6 is a typical pressure versus deformation graph (plotted by CALCOMP). The test results are given in detail in Appendix 2.1 and are summarized in Table 2.1, consisting of a set of pressure - deformation curves. Appendix 2.2 contains the listing of a computer program written during this project to analyze test results. The program was used to process and plot curves presented in Appendix 2.1. Typical printer plots of satisfactory quality are also included in Appendix 2.2.

The tests were performed at different depths and at different orientations with respect to highway alignment. In most cases the jack performed satisfactorily. In places where the borehole wall had been damaged during drilling or subsequently, the test results reflect this damage (Highway 680 site - depth 18 feet for example). The test results are further discussed in Chapter V.

ClibPDF - www.fastio.com

TABLE 2.1
SUMMARY OF NX-JACK BOREHOLE DEFORMABILITY MEASUREMENTS

LOCATION	DEPTH FROM COLLAR FT.	ORIENTATION W/R TO HWY.	PRESSURE* RANGE(PSI)	E**(1ST LOAD) 10^5 PSI	E(1ST UNLOAD) (10^5 PSI)	E(RELOAD) 10^5 PSI)	REMARKS
HWY 24 (Hole 4)	6		80-500	0.36-0.46	0.72-0.36	0.48-0.63	
"	8		80-1200	0.32-0.46	-	-	
"	11		60-500	0.36-0.48	0.93-0.39	-	
"	15		80-500	0.25-0.39	0.63-0.36	0.32-0.56	
HWY 4 (Hole 3)	7		50-200 200-850	0.21-0.28 0.42-0.77	1.40-0.72	1.10-1.50	Trials 1&2 are the same results
"	9		30-350 350-500	0.10-0.13 0.21-0.23	-	-	Results usable for 1st loading only
HWY 680 (Hole 1)	6		60-650	0.20-0.27	0.56-0.32	0.39-0.56	
"	10		100-900	0.31-0.46	0.46-0.42	0.63-0.84	
"	14		160-500	1.40-1.70	2.10-1.70	-	
"	17		100-400	0.16-0.23	-	-	Results usable for 1st loading only
"	18		70-160	≃ 0.05	-	-	Hole was caved-in next to test location

* This is the average unidirectional pressure under the jack plate. The hydraulic efficiency (jack plate pressure/ hydraulic line pressure) of the particular jack was 0.55. It is the line pressure which is shown on the plot of test results. It pertains to the first loading only. Values of E(unload) are those of the straight line portions of the records.

**Moduli ranges shown are obtained by smoothing out the "bumps" in the curves.

ClibPDF - www.fastio.com

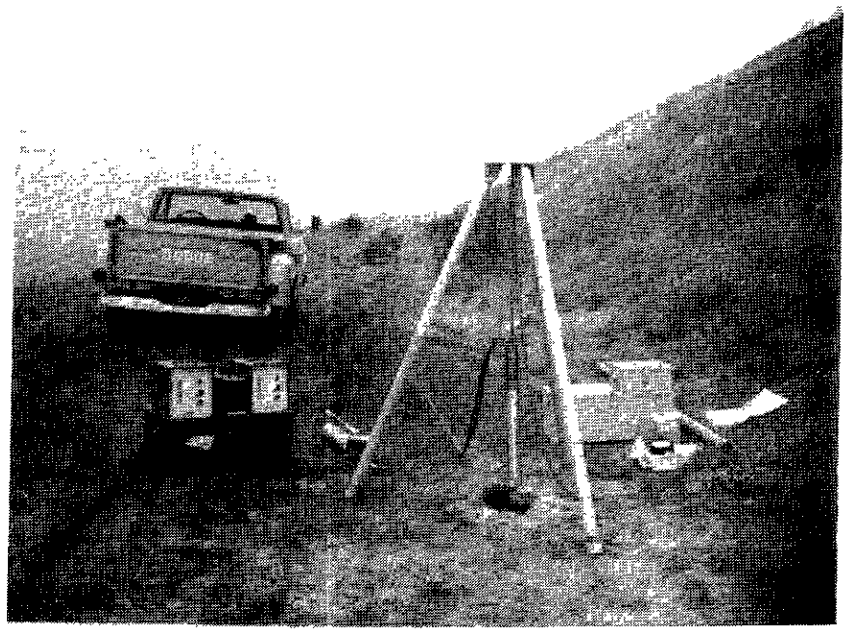

a) NX-Jack Test Set Up

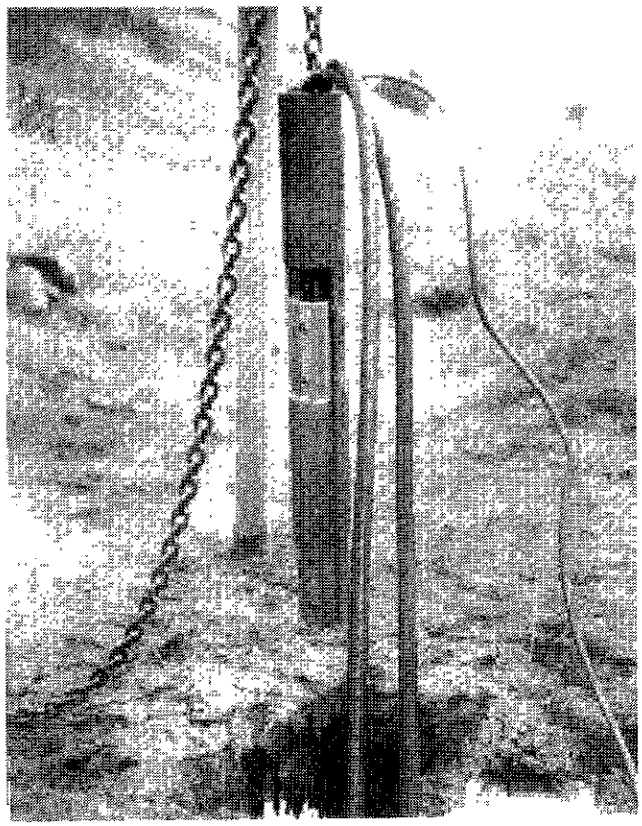

b) Close Up of NX-Jack

Figure 2.5

ClibPDF - www.fastio.com

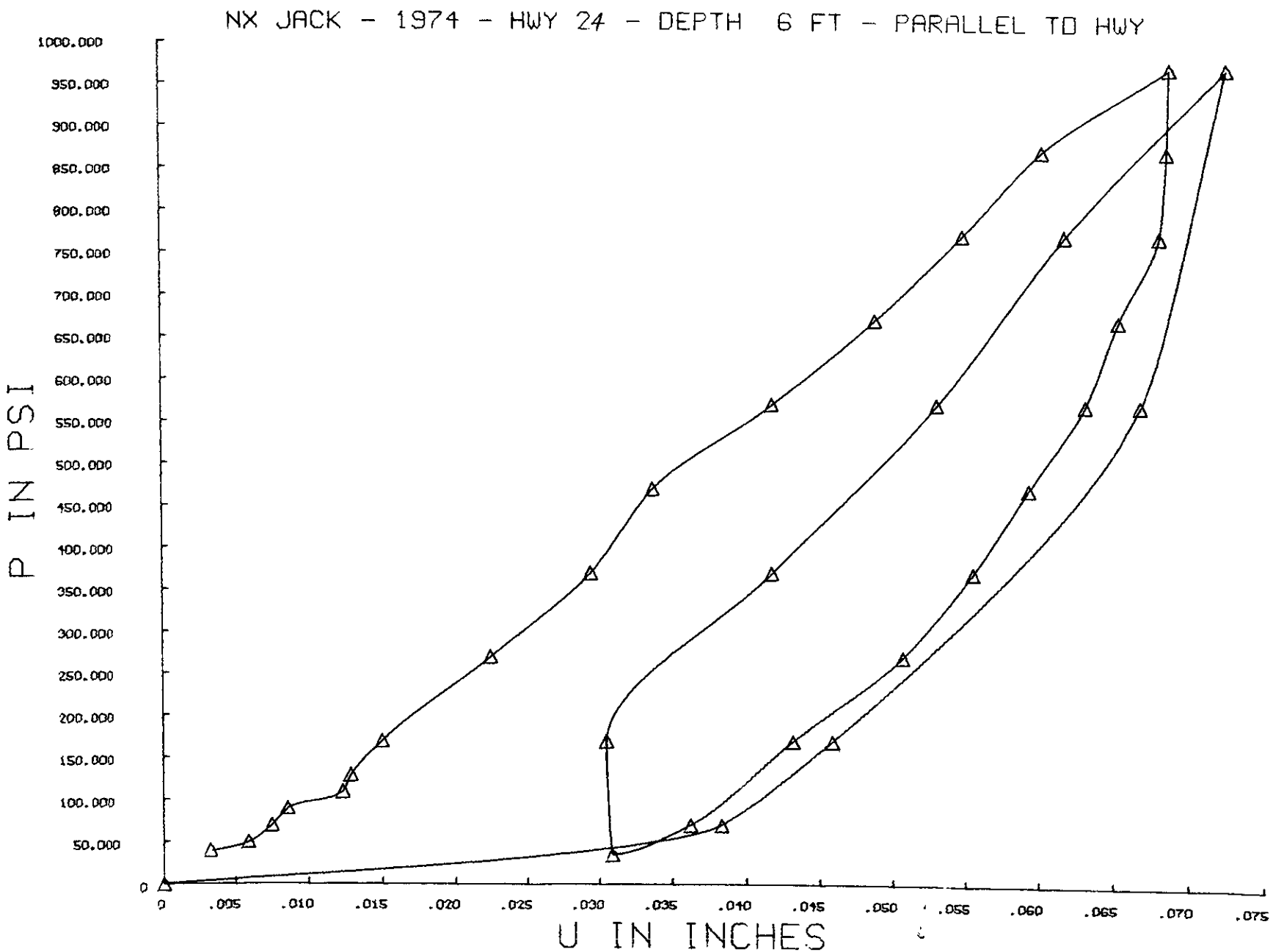

Figure 2.6 Typical Plate Pressure Versus Wall Deformation Curve for Borehole Jack Tests. (The complete set of curves is in Appendix 2.1).

ClibPDF - www.fastio.com

Chapter 3. LABORATORY INDEX TESTS

Laboratory tests on core samples, and in some instances blocks picked from the outcrop, were pursued in order to try several techniques of assessing rock quality and durability. Like the borehole jack tests, these are new, quick, and potentially valuable methods whose applicability for indexing weak rocks needs to be studied. First the radial permeability test will be discussed followed by durability and point load tests.

3.1 Radial Permeability Tests

a) Introduction: The radial permeability test, figures 3.1 to 3.3, was developed by J. Bernaix (1969) while investigating the mechanical properties of the rocks at Malpasset Dam Site, France. His study was undertaken after various unsuccessful geological and mechanical investigations of the foundation rock had been carried out to determine the cause of the dam failure. Standard mechanical tests did not produce any evidence of intrinsic weakness of the rock. However, a detailed study of the rock in thin sections revealed an intense system of fractures.

Bernaix's research was directed towards determining the quantitative effect of the system of fractures on rock properties. Different rock types from various localities were tested and compared. It was found that the radial permeability test could be used to provide a quantitative evaluation of the fracture intensity of a rock. Based upon this test, the behavior of the Malpasset rock is quite different from that of most of the rocks tested whereas, by applying classical criteria for assessing rock quality it was not possible to distinguish one from another.

The radial permeability test was used in this project to evaluate its suitability as an index test when working with intermediate quality rocks. Our permeameter, designed as part of the project work by the investigators, is modified from Bernaix's original concept to include a load cell and three

ClibPDF - www.fastio.com

loading screws for application of axial force to the specimen, figure 3.2. Calibration of the diaphram load cell, which forms the bottom of the permeameter, figure 3.3b,enables us to control and monitor the axial load on the sample and to monitor axial swelling during the test.

b) Procedures: The radial permeability test requires cylindrical samples 2 to 2-1/2 inches in outer diameter with an axial hole 3/8 inches in diameter extending to within 3/4 inch of the bottom (figure 3.4). A nipple is cemented into the top of the inner hole and water is either introduced or discharged from the central hole, through the nipple, according to the test mode. In the "convergent" test mode, the water on the outside is maintained at a pressure up to 300 psi, causing radial flow to the inner surface, which is maintained at atmospheric pressure. In the "divergent" test mode, the water pressure around the outer surface is atmospheric while the inner hole has pressure up to 30 psi, causing radial flow from the center of the sample outwards. Under convergent flow, there is a compressive body force, due to the flow, which is proportional to the pressure difference; conversely, during divergent flow tensional body forces are created. Bernaix found that the ratio of convergent to divergent permeabilities at specified pressures (50 bars and 1 bar respectively) serves as a fissuring index because the permeability is highly stress dependent in fissured rocks.

Flow is radial in the central portion of the sample over a length ℓ, equal to that of the central cavity. Flow through the ends is disregarded. Bernaix (1969, p. 64) checked this approximation and determined that it introduces "...only a very small error, considering the fact that we study mainly the variations of permeability."

According to Darcy's Law,

$$Q = k \frac{h}{L} A \qquad (1)$$

ClibPDF - www.fastio.com

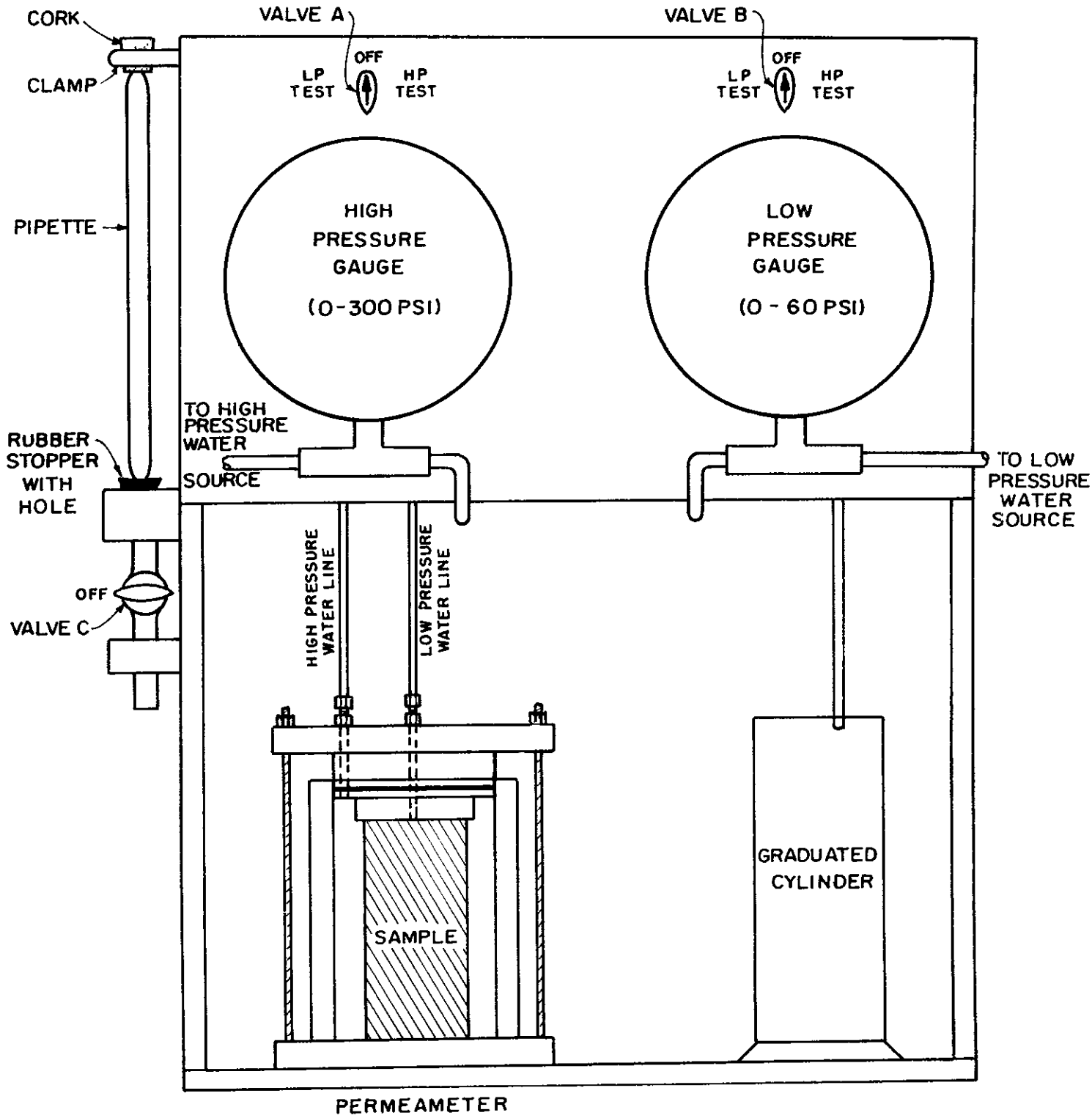

Figure 3.1. Radial permeability test apparatus.

ClibPDF - www.fastio.com

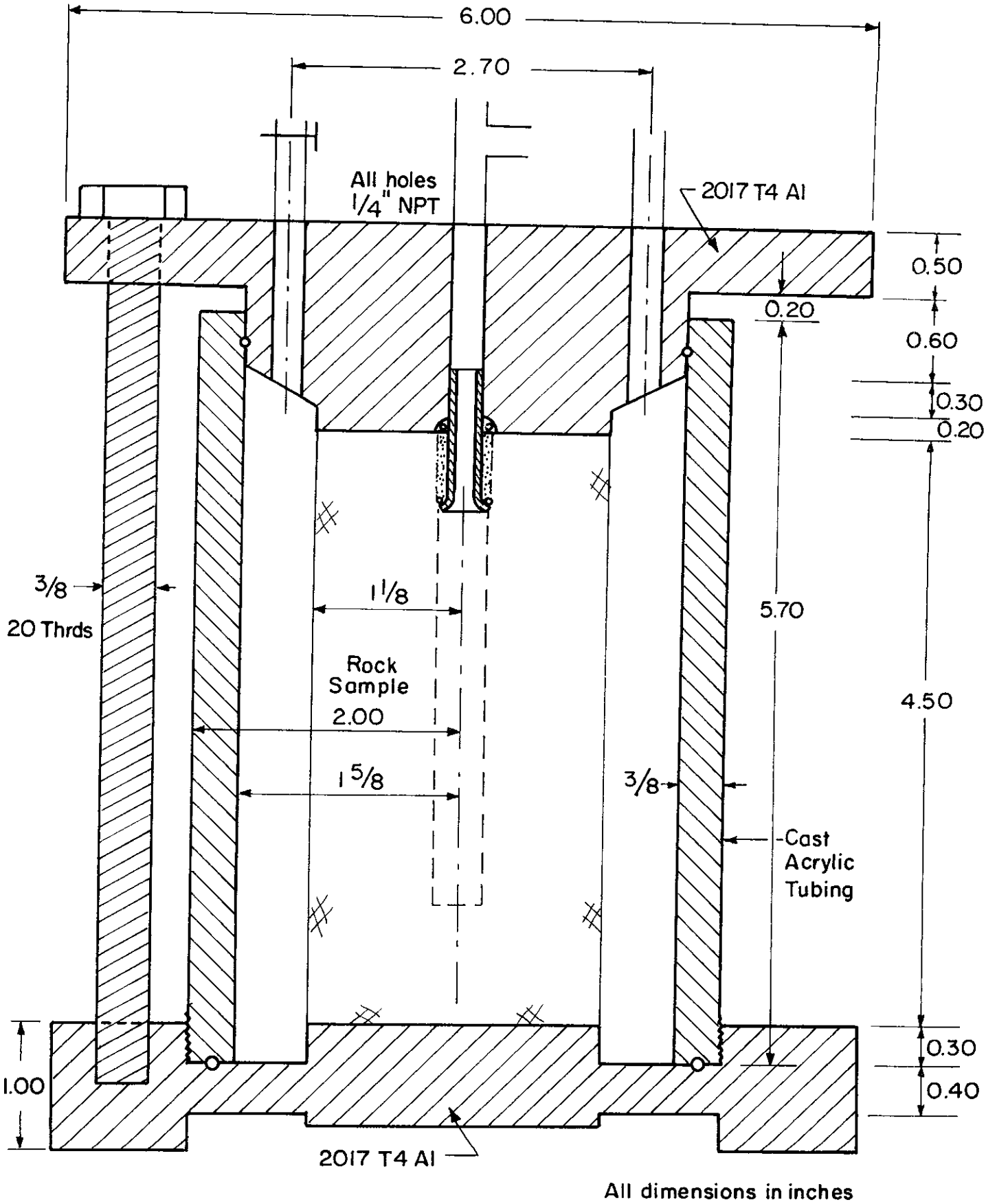

Figure 3.2. 300 psi. Radial permeameter.

ClibPDF - www.fastio.com

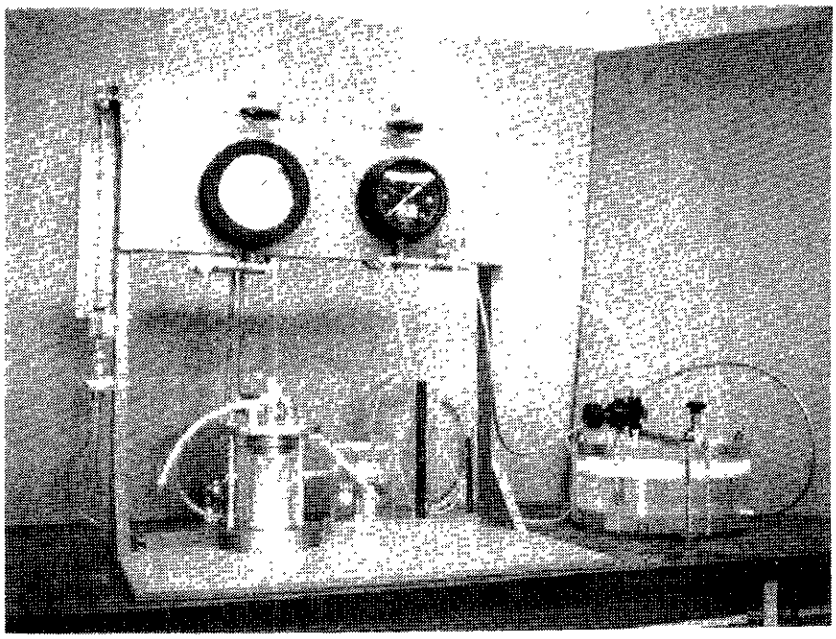

Figure 3.3a. Radial Permeability Test Equipment

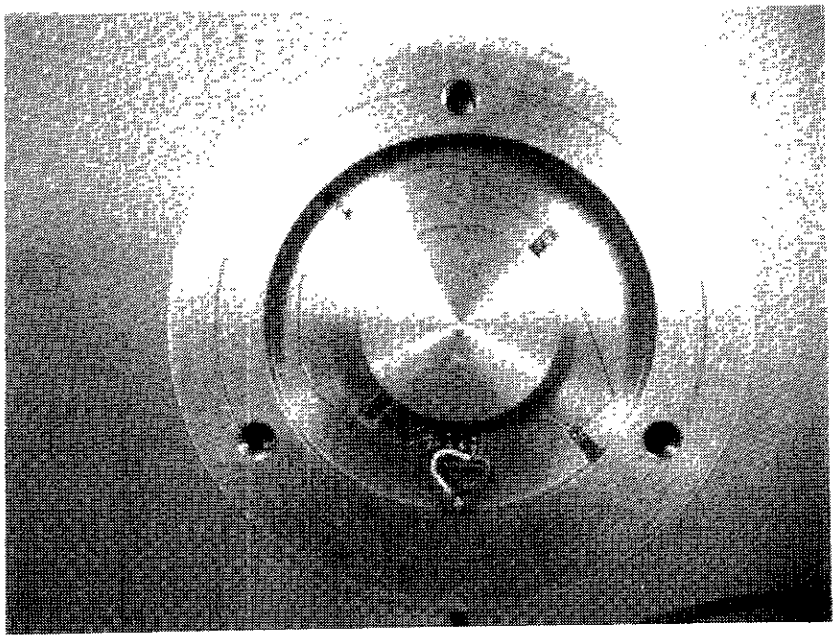

Figure 3.3b. Base of the Radial Permeameter Showing the Load Cell

ClibPDF - www.fastio.com

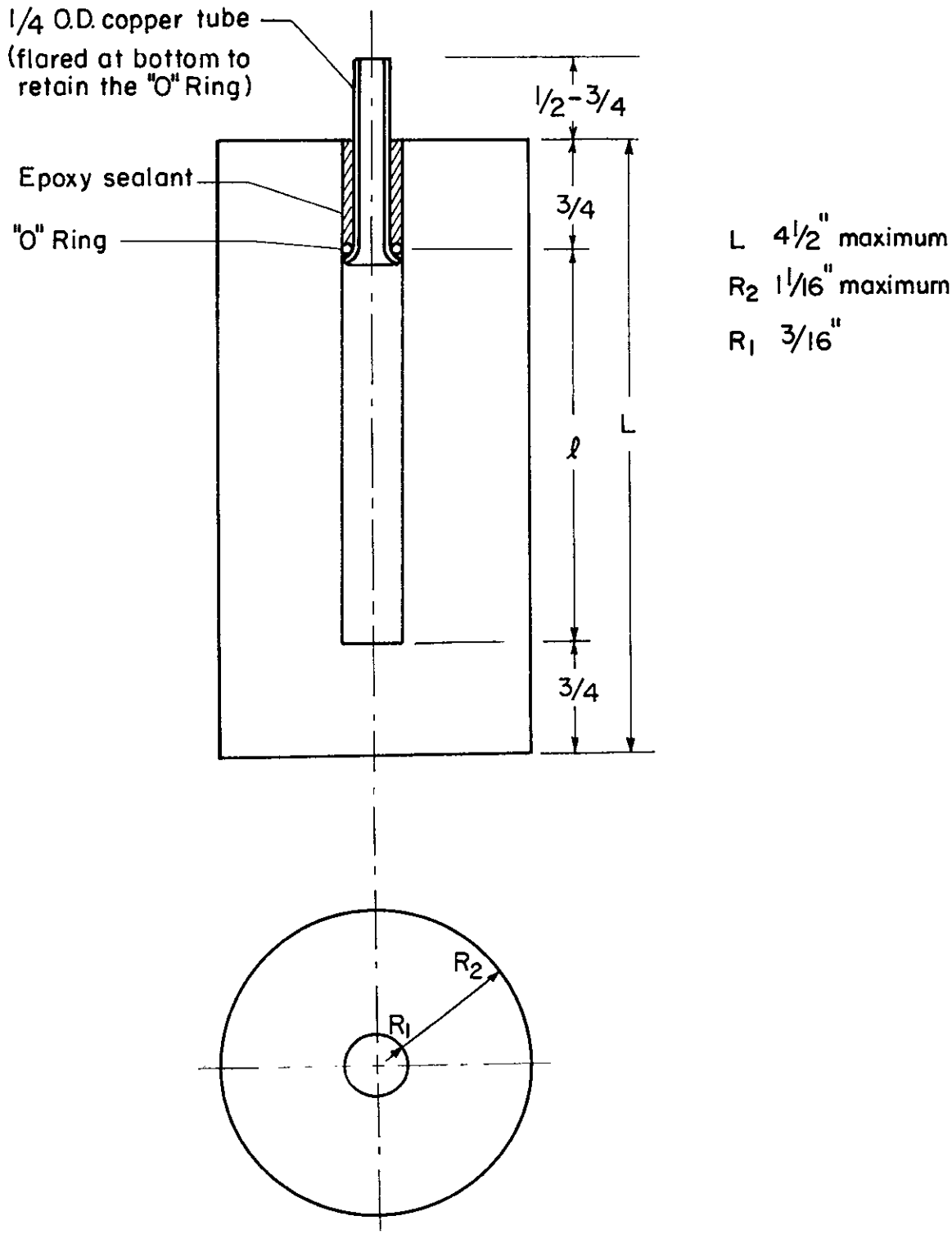

Figure 3.4. Standard sample for use in the radial permeability test.

ClibPDF - www.fastio.com

where

Q = flow rate

k = permeability constant

h = head loss across L

A = area through which flow takes place

L = length of flow path

The flow rate across a coaxial cylinder of radius r is

$$Q = k(2\pi r\ell)\frac{dp}{dr} . \tag{2}$$

Bernaix developed a formula for determining k by rewriting formula (2) in the form

$$\frac{dr}{r} = \frac{k(2\pi\ell)}{Q}\,dp$$

and integrating over the length of the path taken by the water

$$\int_{R_1}^{R_2}\frac{dr}{r} = \int_{o}^{P}\frac{2\pi\ell k}{Q}\,dp$$

$$\mathrm{Ln}\,\frac{R_2}{R_1} = \frac{2\pi\ell kP}{Q} .$$

From this, he obtained

$$K = \frac{Q}{2\pi\ell P}\,\mathrm{Ln}\,\frac{R_2}{R_1} \tag{3}$$

and concluded that the seepage gradient

$$\frac{dp}{dr} = \frac{P}{r\mathrm{Ln}\ R_2/R_1}$$

is not uniform in the sample. In fact dp/dr is independent of the direction of flow and remains proportional to the seepage pressure P.

In our tests, the volume rate of flow, Q, is measured by timing the filling of a pipette, after steady flow has been established. The static water pressure (P) is supplied from a nitrogen pressured water chamber and is measured with a

ClibPDF - www.fastio.com

Bourdon gage. The permeability k (dimensions of velocity) is calculated from equation 3. Appendix A3 contains detailed descriptions of procedures for specimen preparation, test set-up, and test methods.

The time required to run the test, including sample preparation, is dependent upon the permeability of the sample. During our testing program the average time was about 3 1/2 to 4 hours. When a standarized procedure for sample preparation and testing is followed and, especially, if numerous samples can be prepared at one time, the total time should be reduced by one-half to one hour. Table 3.1 is a typical data sheet from a radial permeability test; it yields the log permeability versus pressure plot shown in figure 3.5.

c) Test results: The test results were not reproducible. After running a test an a sample through a range of pressures a new test often gave different permeabilities; this behavior may be related to a path dependence of the permeability owing to non recoverable effects during tests, including erosion of material from fractures and fracture propagation. Furthermore, if the flow rate is monitored over an extended period, e.g., 2 hours, while maintaining a constant water pressure, the rate of flow may vary, decreasing with some samples and increasing with others. A decrease in permeability with time is probably due to the closing of fractures, and pores caused by swelling or particles clogging the opening. An increase of permeability with time reflects the opening of fractures, again due to erosion or fracture propagation. In Bernaix's experiments with unweathered hard rocks test results were reproducible and did not

ClibPDF - www.fastio.com

University of California

RADIAL PERMEABILITY TEST

Rock Mechanics Laboratory

Table 3.1 TYPICAL DATA SHEET

Sample Description: Med-dark brown, pebbly mudstone; pebbles are grey, subrounded siltstone up to 1/4" in diameter.
Location: Floyd Hill
Boring No. 7 Sample Depth 38

No visible fractures

Test No. 3
Date: 8/21/74
Tested by: JMC
Strain Indicator No. --
Gate Factor: --
Sample Dimensions (cm):
L 11.11 L_1 1.91
ℓ 7.30
R_1 .48 R_2 2.51

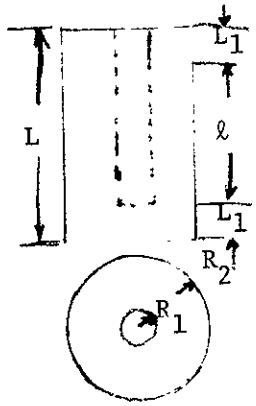

Test	Strain Indicator Reading (Micro Inch/Inch) Static	Strain Indicator Reading (Micro Inch/Inch) Steady State	Water Pressure (lb/in^2) Static	Water Pressure (lb/in^2) Steady State	Head (cm)	Q (cc)	Time (sec)	k cm/sec	Remarks
Conv.			30	30	2109.2	100	516.8	3.30×10^{-6}	Clear water in burrette
			50	50	3515.9	100	421.1	2.43×10^{-6}	Clear discharge water
			75	75	5273.8	100	385.4	1.77×10^{-6}	Clear discharge water
			100	100	7031.7	100	370.7	1.38×10^{-6}	Clear discharge water
			125	125	8789.6	100	362.2	1.13×10^{-6}	Clear discharge water
			150	150	10547.6	100	358.3	9.52×10^{-7}	Clear discharge water
			175	175	12303.4	100	356.8	8.20×10^{-7}	Clear discharge water
			200	200	14063.4	100	354.8	7.21×10^{-7}	Clear discharge water
			225	225	15821.3	100	348.2	6.53×10^{-7}	Clear discharge water
			250	250	17579.3	100	341.1	6.00×10^{-7}	Clear discharge water
			275	275	19337.2	100	327.5	5.68×10^{-7}	Clear discharge water
			297	297	20884.1	100	313.3	5.50×10^{-7}	Clear discharge water
Div.			5	5	351.6	25	433.5	5.90×10^{-6}	Clear discharge water
			10	10	703.2	25	196.9	6.50×10^{-6}	Clear discharge water
			15	15	1054.8	50	238.5	7.15×10^{-6}	Clear discharge water
			20	20	1406.3	50	161.61	7.92×10^{-6}	Clear discharge water
			25	25	1757.9	100	236.9	8.64×10^{-6}	Water slightly murky

ClibPDF - www.fastio.com

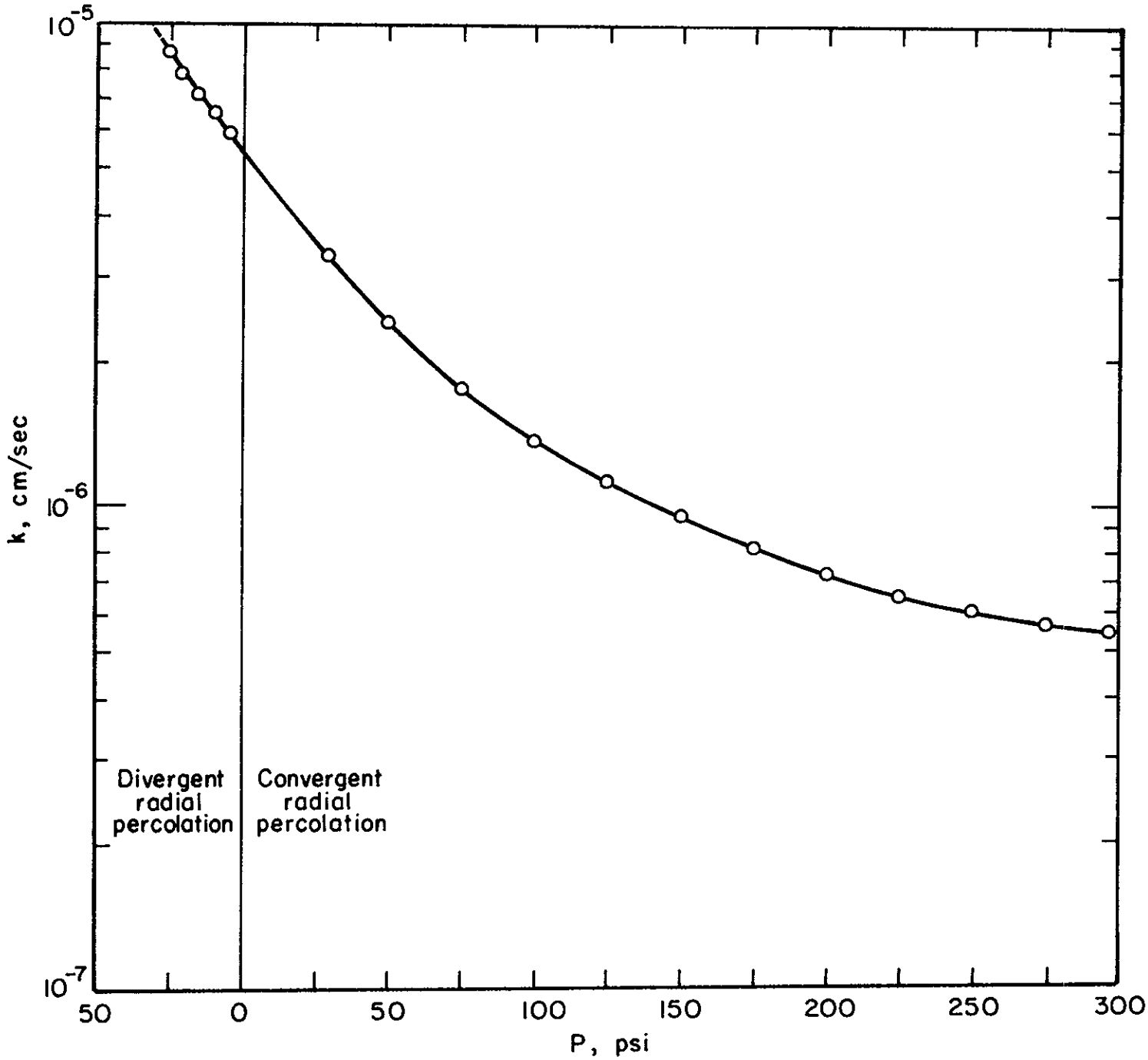

Figure 3.5. Sample test results.

ClibPDF - www.fastio.com

vary with time. These non-linear and time-dependent effects may therefore offer parameters useful in evaluating the engineering properties of intermediate quality rocks. Further testing will be needed to establish the necessary correlations.

Problems occurred during both sample preparation and testing. Several core samples were too fragile to use as test specimens. This was especially true of the more weathered claystones. No tests were run on cores from borehole 2 (site 2) as samples throughout the core length were too highly weathered and fractured to remain intact during sample preparation. Samples were restrained axially but they still failed during cutting and drilling operations.

Specimens from borehole 4 (site 3) posed a different problem. These dark-brown, pebbly mudstone specimens were highly fractured and required both sulfur end caps and wire screen wrapped around the sample to provide axial support.

Most samples failed during testing. Failures resulted when fracture plane cavities were eroded by the flowing water (figure 3.6a, 3.6b and 3.6c). Fracture propagation in divergent tests may have been a factor in some tests. As noted test results were not reproducible, possibly owing to erosion along fractures. This cause is supported by observations of discoloration of the water in many tests including those where test samples exhibited no macro-fractures. Swelling of clays in the samples may have occurred. If it did, the permeability would most certainly have been affected.

d) Further studies: Further testing is needed to properly evaluate the use of the radial permeameter to determine rock quality indices for intermediate quality rocks. Areas of needed investigation include: 1) running many tests on samples taken from the same rock or samples taken within close proximity

ClibPDF - www.fastio.com

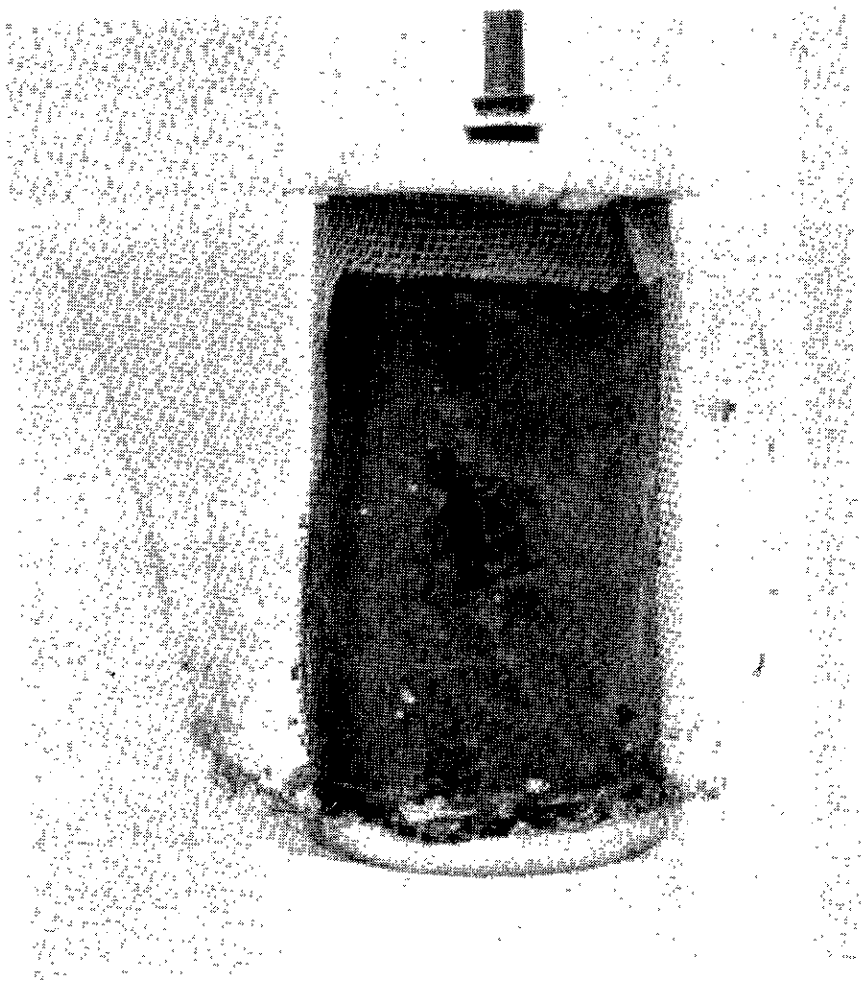

Figure 3.6a. Failed Sample. Failure resulting from erosion along fracture plane. (Note cavity in the central portion of the sample). Borehole #4, Site 3, Depth 10 feet.

ClibPDF - www.fastio.com

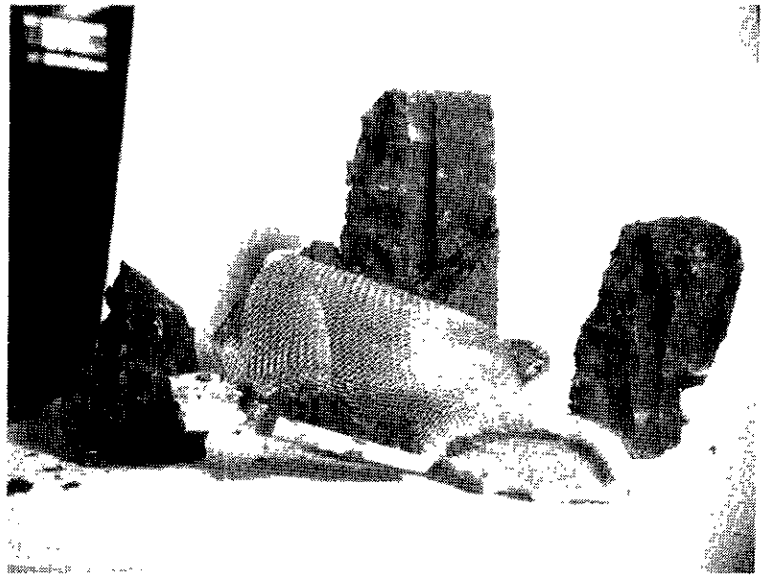

Figure 3.6b. Failed Sample. Failure occurred during the divergent test when the water pressure (5 psi) opened the pre-existing fractures. Borehole 4, Site 3, 29 feet.

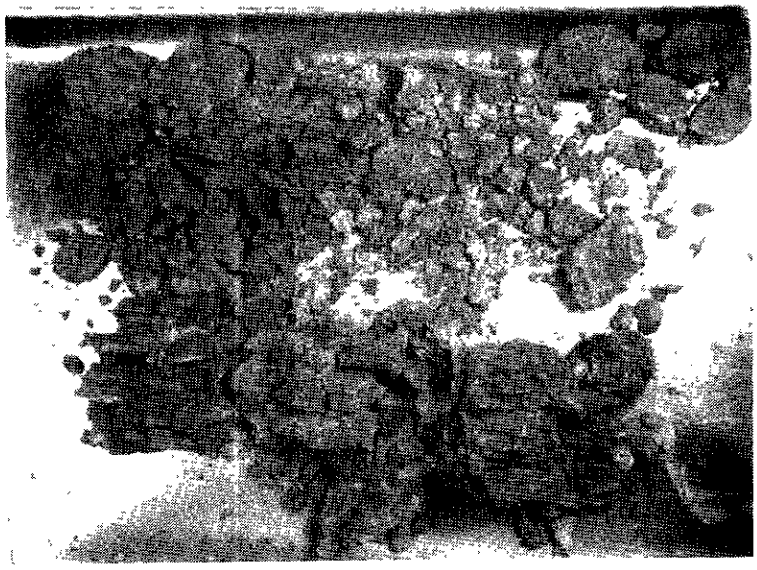

Figure 3.6c. Failed Sample. Failure occurred as soon as the sample was subjected to water under pressure (convergent test at 25 psi). Note the difference in fracture orientation and intensity between this and the preceeding sample (figure 3.6b). Borehole 4, Site 3, 22 feet.

ClibPDF - www.fastio.com

to study the scatter of test results. Samples within each suite should exhibit the same degree of weathering. 2) Studying the change in permeability with changes in weathering. This can be incorporated in 1 by selecting groups of samples of the same rock type with the groups showing different degrees of weathering. 3) Axial swelling. The permeameter has a diaphragm, fitted with strain gauges, machined in its base. Axial swelling can be monitored during radial permeability tests. A malfunctioning strain gauge negated the swelling information obtained in this series of tests. 4) Rate of erosion and changes in water chemistry. In many tests performed on intermediate quality rocks, water flow through fractures and pore spaces causes appreciable erosion. The magnitude and rate of erosion, together with changes in water chemistry, can be monitored by the chemistry and turbidity of the discharge. Water percolated through the system can have any initial chemistry desired so as to more closely simulate actual ground water conditions.

3.2 Slake-Durability Tests

a) Introduction: The main purpose of the slake-durability test is to determine the variation with depth of the weatherability of a rock mass. It is hypothesized that a series of tests performed on an entire core would delineate a low durability zone near the ground surface in rocks affected by weathering. Thus, results of a testing program, dealing with cut slopes of known age, could provide information concerning the rate of weathering of new excavations.

The performance of cut slopes in intermediate quality rocks depends largely upon the weatherability of the material. The term "weatherability" refers to the potential for a rock to deteriorate from atmospheric exposure during the expected life of the cutting. This is distinguished from "state of weathering," inherited from past weathering processes. A rock's resistance to weakening and disintegration (weathering) may be referred to as its durability.

It is dimensioned such that the unobstructed clearance between the base

ClibPDF - www.fastio.com

Because much of California undergoes relatively mild climatic changes, the slake-durability of rock masses is of primary interest for this study. Slaking refers to weakening or disintegration of a rock upon cyclic wetting and drying. The slake-durability test used for this project was developed by Franklin and Chandra (1972). The International Society of Rock Mechanics has included the method in its standardization of laboratory and field tests. Additional research on the slaking process has been performed by Gamble (1971). The slake-durability test consists of gently tumbling specified dry weight of rock through an air water interface and measuring the weight percentage of rock retained by its wire mesh container over a given time interval. The important variables, including specimen weight and shape, equipment dimensions, test duration, tumbling rate, water temperature, and drying oven temperature, have been standardized for the test and are detailed below.

b) Apparatus: The slake-durability test apparatus requires the following equipment:

1. The test drum is made from 2.00 mm standard mesh cylinder. The unobstructed length is 100 mm, with a diameter of 140 mm. The drum has a fixed solid base and a solid removable lid. It must withstand a temperature of 105° C.

2. A trough contains the slaking fluid and supports the test drum with its axis horizontal. The fluid level is 20 mm below the drum axis. It is dimensioned such that the unobstructed clearance between the base of the mesh and the trough is 40 mm.

3. A motor drive system rotates the drum at a speed of 20 revolutions per minute, the speed being held constant to within 5% for a period of ten minutes.

4. The drying oven maintains a temperature of 105° C to within 3° C for a period of at least 12 hours.

ClibPDF - www.fastio.com

5. The balance weighs the drum and sample to an accuracy of 0.5 gm.

Items a,b, and c, manufactured according to proposed standards of ISRM are marketed by Engineering Lab Equipment Company, Bracknell, Berkshire, England, and distributed in the United States through Soil Mechanics Equipment Company, Glen Ellyn, Illinois.

c) Procedures: The test is intended to provide an index useful in comparing rocks. In general, it cannot predict in situ rate of weathering, since this property may be influenced by factors other than slaking. It is assumed that a high degree of weathering by a combination of processes, will be reflected in a low slake-durability value.

Representative samples for the slake-durability tests were taken over contiguous core sections, such that a vertical profile of slake-durability values results for each bore hole. Each test sample represents from one to five feet of core length, depending on the recovery of adequately-sized rocks.

The following standard slake-durability testing procedure is suggested by Franklin and Chandra:

1. A representative sample is selected comprising ten rock lumps, each weighing 40-60 gm to yield a total sample weight of 450-550 gm. The lumps are roughly spherical in shape, with rough edges removed before testing.

2. The sample is placed in a clean drum and dried to constant weight at a temperature of 105° C. The weight of the drum plus sample is recorded and the test is conducted immediately afterwards.

3. The drum lid is replaced and the drive system is engaged for testing.

4. The trough is filled with slaking fluid, usually tap water at 20° C, to a level of 20 mm below the drum axis and the drum is rotated at 20 revolutions per minute for ten minutes.

5. The drum is removed from the trough, the lid is removed, and the drum

ClibPDF - www.fastio.com

plus retained portion of the sample is dried to constant weight at 105° C. The weight of the drum plus retained sample is recorded.

6. Steps 3 through 5 are repeated.

7. The drum is brushed clean and its weight is recorded.

The following variations from this standard procedure facilitated the testing for this project.

1. The lumps of rock deviated from the suggested shape. It was difficult to adhere to this standard since many of the rocks were easily broken apart during shaping. However, care was taken to remove rough or sharp edges from the lumps.

2. An initial submergence of the samples was necessary for calculating their bulk densities from the dry and buoyant weights. There were additional index values desired as supplementary data for the project. The samples were carefully submerged for a time short enough to prevent full saturation or significant slaking. Any small amount of material eroded by handling or submergence was easily recovered and included for the initial oven-dried sample weight. Slightly lower slake-durability values (less material retained) may be expected for this procedure.

3. Rock specimens were removed from the drums after washing so that other samples could be tested during the lengthy drying periods. Transfer of the retained rock was carefully done to prevent breakage or loss of material.

4. Samples 1-1 through 1-4 were washed for a single 20 minute period instead of the standard two cycles of 10 minutes each. The resulting slake-durability indexes probably lie somewhere between the normally expected first and second cycle values.

5. Water temperatures for core no. 1 samples were slightly higher than the standard 20° C, varying from 22° C to 23° C. The slake-durability indexes may be somewhat low as a result.

ClibPDF - www.fastio.com

d) Calculations: The slake-durability index for either cycle is calculated as the percentage ratio of the retained to initial dry sample weights as follows:

$$\text{slake-durability index} = \frac{\text{retained dry weight}}{\text{initial dry weight}} \times 100\%$$

The slake-durability indexes are plotted against borehole depth in the bar graphs of figures 3.6a,b,c. Typical test data, including in situ bulk densities and water contents, are presented in table 3.2.

e) Discussion: The slake-durability indexes for core samples 2 and 3 do not show well-defined zones of weathered rock near the surface of the cut slope. There is a general decrease in slake-durability with depth, probably due to some variation in the nauural rock properties rather than weathering at the surface. It is possible that the depth of weathering is less than three feet, to which depth samples were not retrieved. This would be difficult to confirm, since any method of sampling at a shallow depth, other than core drilling, would introduce a different amount of disturbance to the specimens.

Cores 1 and 4 yielded more useful slake-durability profiles. Samples 1-1 through 1-4 show a relatively weak rock zone, with gradually increasing slake-durability to a depth of about 18 feet. Although these first four test specimens underwent a single wash cycle of longer than normal duration, the relative values are meaningful. The slake-durability profile for core 4 is highly variable, but it indicates a weak zone down to about four feet. However, this sample may not actually indicate surficial weathering, since lower slake-durability values were obtained at greater depths.

For cores 1, 2, and 3 there appears to be a correlation between the slake-durability indexes and the bulk densities and water contents of the samples. Decreases in slake-durabilities are accompanied by a decrease in bulk density

ClibPDF - www.fastio.com

University of California Rock Mechanics Laboratory

TABLE 3.2. TYPICAL DATA SHEET - SLAKE DURABILITY TEST

Slake Durability Tests

Hole #4 - Hwy 27

Date: 7/16/74

R. Thorpe, K. Jenkins

Oven temp. 105°C

Water temp. ≈ 21°C

Sample No.	Approx. Depth	Init. Wt. (g)	Vol. (cc)	W (%)	γ (g/cc)	A (g)	B (g)	C (g)	I_{d_1} (%)	I_{d_2} (%)	Comments
#1	3.5-4'	465	201	13.7	2.31	409	108	42	26.4	10.3	Brown clay shale
#2	4-6'	492	217	13.6	2.27	433	244	124	56.4	28.6	Brown clay shale
#3	6-8'	539	240	14.4	2.25	471	215	74	45.6	15.7	Brown clay shale
#4	8-10.5'	466	205	15.1	2.27	405	255	136	63.0	33.6	Brown clay shale
#5	10.5-13'	513	216	8.7	2.38	472	225	98	47.7	20.8	Blue-grey clay shale
#6	13-17'	489	210	12.4	2.33	435	75	14	17.2	3.2	Brown clay shale
#7	17-19'	499	214	11.1	2.33	449	55	5	12.2	1.1	Brown clay shale
#8	19-22'	506	210	10.2	2.41	459	67	25	14.6	5.4	Brown clay shale
#9	22-24'	509	213	8.8	2.39	468	167	89	35.7	19.0	Brown clay shale
#10	24-26'	513	212	8.5	2.42	473	184	50	38.9	10.6	Brown clay shale
#11	26-28'	513	211	8.2	2.43	474	250	11	52.7	2.3	Brown clay shale
#12	28-30'	501	208	8.9	2.41	460	235	4	51.1	0.8	Brown clay shale
#13	30-31'	437	180	8.2	2.43	404	219	34	54.2	8.4	Brown clay shale
#14	31-33'	499	206	7.3	2.42	465	270	105	58.1	22.6	Brown clay shale

ClibPDF - www.fastio.com

TABLE 3.3. TYPICAL DATA SHEET - POINT LOAD TEST

Franklin Point Load Test

Hole #4 - Hwy 27

Date: 7/11/74

Richard Thorpe

Approx. Depth	Type of Test	Dip Angle	L (in)	D (in)	L/D	Hyd.Press. (psi)	I_s (psi)	I_{s50} (psi)	I_a	Description of Failure
3.5'	Diam.		1.0	1.97	.51	30	14	14		Plattens pushed into rock - poorly defined failure surf.
3.5'	Axial		1.0	1.10	.91	<10	<15	<15	-	axis (as above)
4'	Diam.		1.0	-	-	-	-	-	-	As above
5'	Diam.		-	-	-	-	-	-	-	As above
11'	Diam.		1.0	1.97	.51	<10	<5	<5		axis
11'	Axial		1.0	.79	1.27	<10	<30	-	-	axis
11'	Axial		1.0	.94	1.06	30	63	63		axis
12'	Diam.		1.5	1.97	.76	10	5	5		axis
12'	Axial		1.0	.94	1.06	<10	21	21	4.4	axis
12'	Axial		1.0	.89	1.13	10	23	23		axis
19'	Diam.		1.0	1.89	.53	40	21	21		axis
19'	Axial		1.0	.83	1.21	45	121	151	6.86	axis
19'	Diam.		1.0	2.00	.50	50	23	23		axis
23'	Diam.		1.0	2.00	.50	10	5	5		axis
23'	Diam.		1.0	2.00	.50	10	5	5		Failure dip ~45°
23'	Axial		1.0	.75	1.34	30	99	-		axis
23'	Axial		1.0	.98	1.02	<10	<19	<17		axis
23'	Diam.		1.0	1.97	.51	45	21	21		Failure dip 45°
25'	Diam.		1.0	2.00	.50	<10	<5	<5		axis
25'	Axial		1.0	.83	1.21	20	54	67	6.7	axis
25'	Diam.		1.0	1.89	.53	35	18	18		axis
25'	Diam.		1.0	1.93	.52	<10	<5	<5		axis

ClibPDF - www.fastio.com

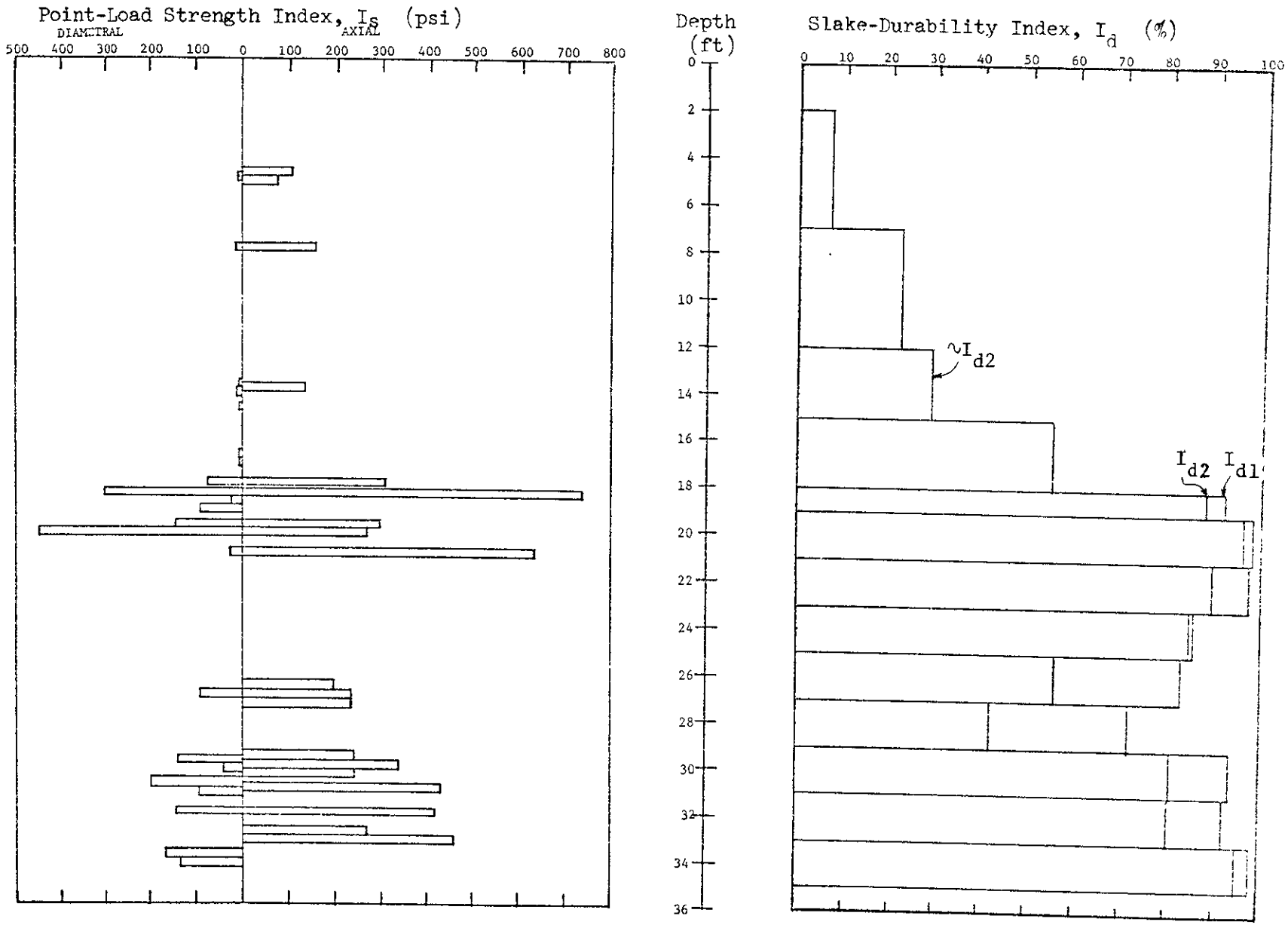

FIGURE 3.7a

Log of Point-Load Strengths
and Slake-Durability
Hole No. 1, Highway 680

ClibPDF - www.fastio.com

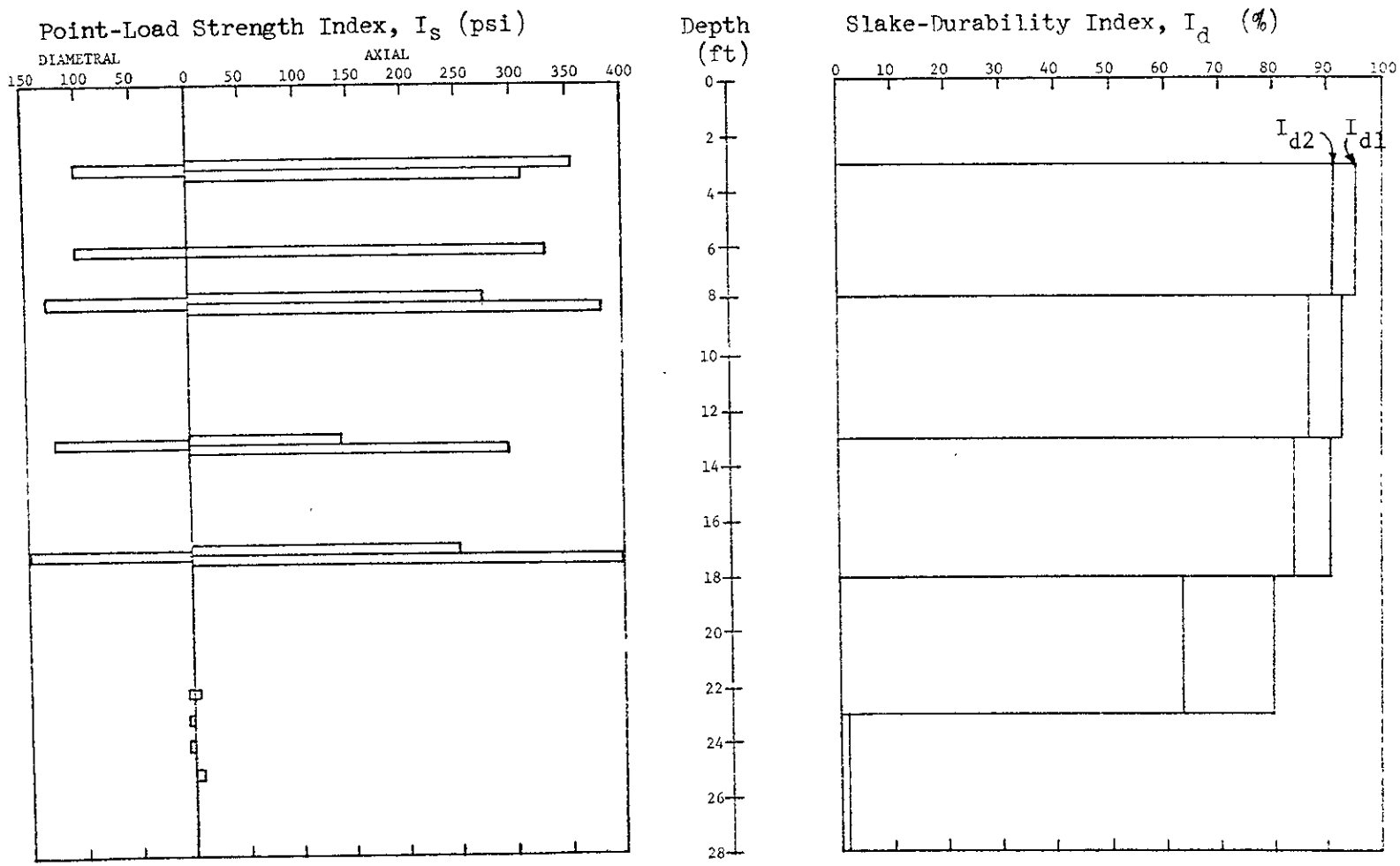

FIGURE 3.7b

Log of Point-Load Strengths
and Slake-Durability
Hole No. 2, Highway 4

ClibPDF - www.fastio.com

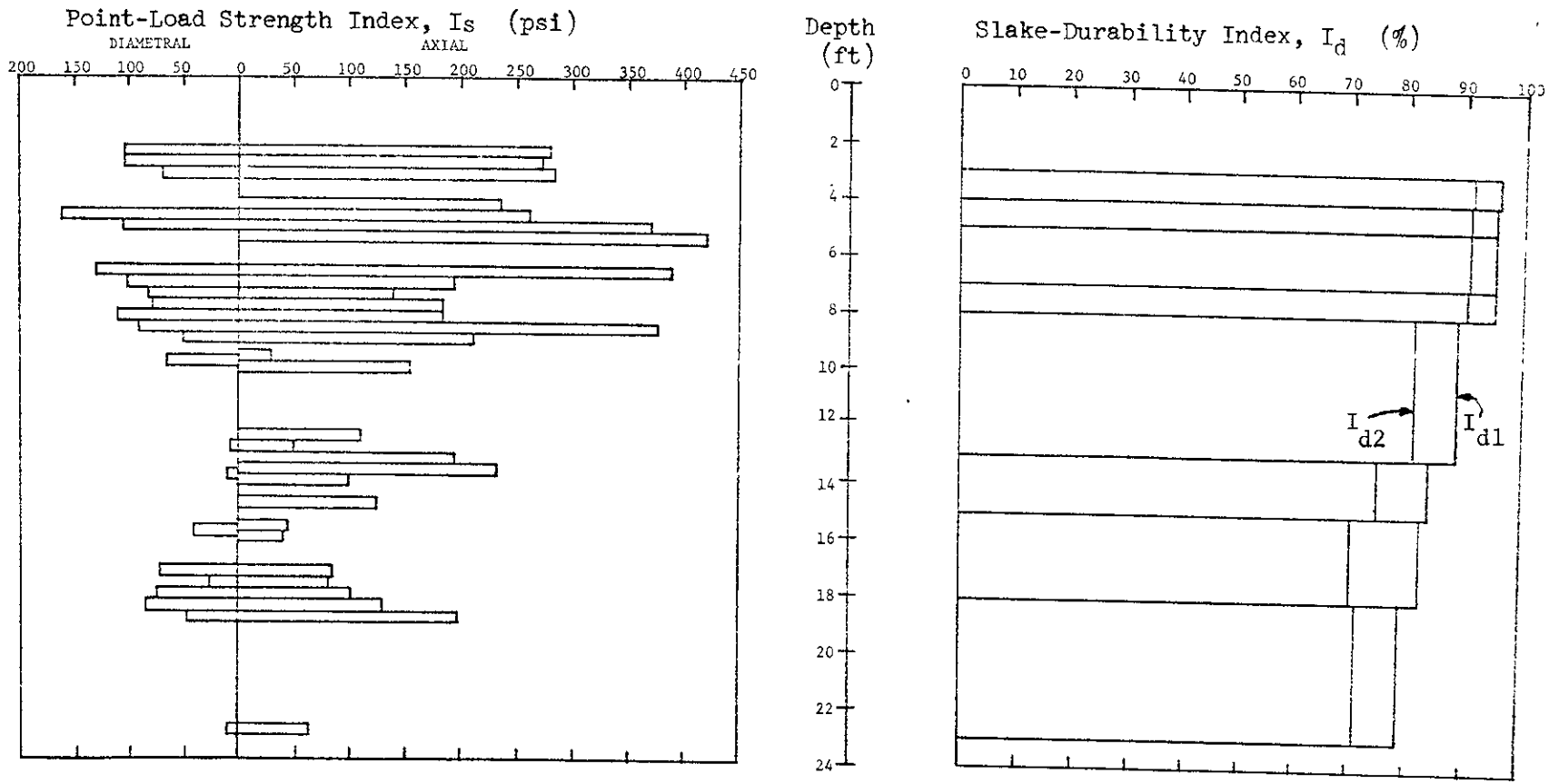

FIGURE 3.7c

Log of Point-Load Strengths
and Slake-Durability
Hole No. 3, Highway 4

ClibPDF - www.fastio.com

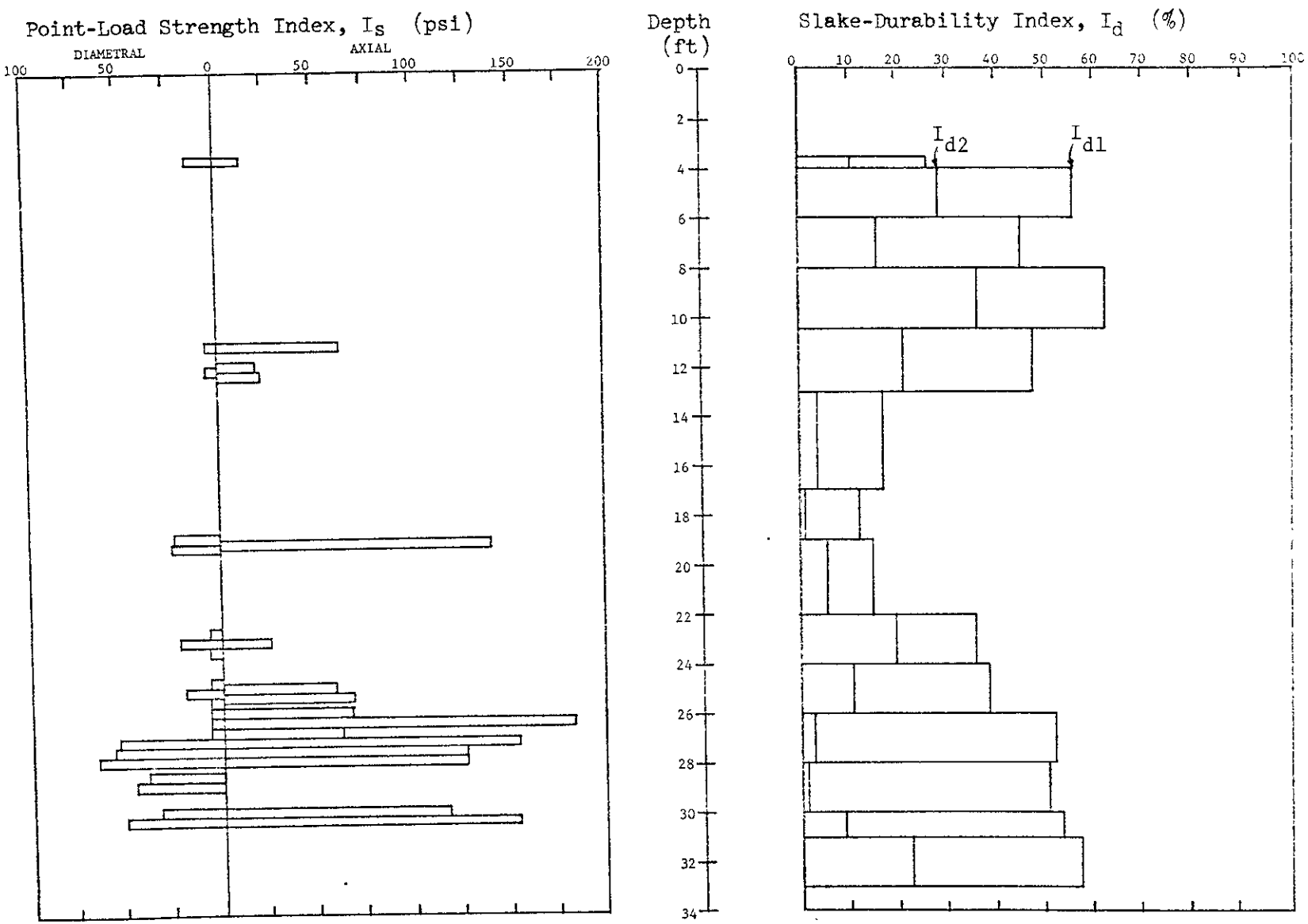

FIGURE 3.7d

Log of Point-Load Strengths
and Slake-Durability
Hole No. 4, Highway 24

ClibPDF - www.fastio.com

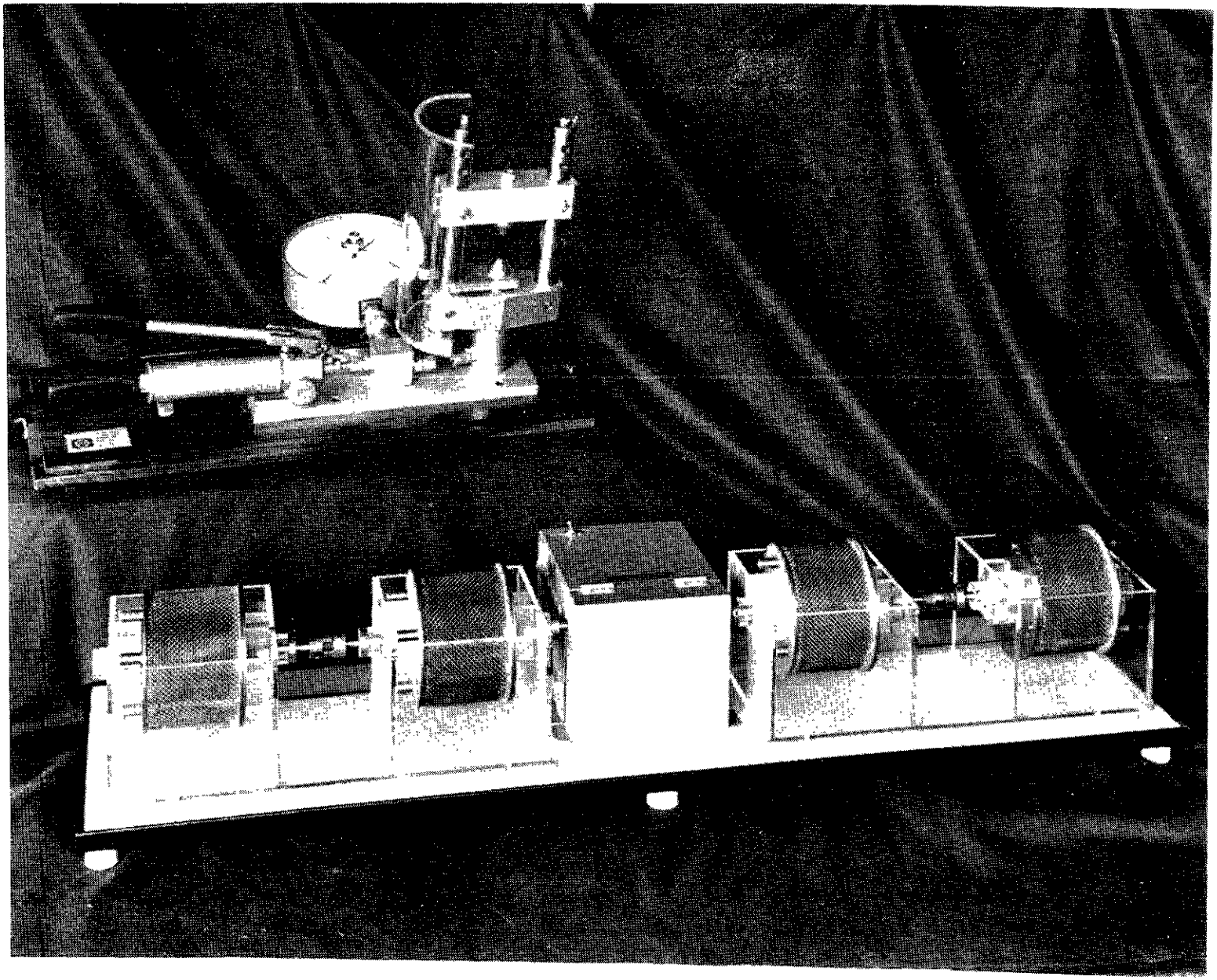

Figure 3.8. Slake Durability Machine and Point Load Apparatus. Photo courtesy of Photo Mechanics Equipment Company, Ltd., Glen Ellyn, Illinois, and Engineering Laboratory Equipment Ltd., Bracknell, Berkshire, England.

ClibPDF - www.fastio.com

and an increase in water content. This indicates an increase in pore space, which may be the result of the in situ weathering process. This relationship is not clearly shown in core sample 4, where the fine grained particles are more cohesive.

We compared the slake-durability index with a modification of the Division of Highways aggregate durability index (test method no. Calif. 229E). The latter index was calculated as the percentage of dry weight of material retained on a no. 10 sieve (2 mm openings) after a ten minute agitation period in the apparatus used in TM 229E. Two samples were selected for the test; one being a weathered sandstone, from hole no. 2 (depth about 23 feet) and the other a weak clay-shale from hole no. 4 (depth about 30 feet). The durability indexes obtained by the mofified TM 229E procedure are 10.6 percent and 54.2 percent for samples 2-23 and 4-30, respectively. These values agree fairly well with the slake-durability indexes shown in figures 3.7b and 3.7d at the same depth. On the basis of these two tests, it appears that the modified procedure for TM 229E may yield satisfactory durability indexes. However, a more extensive comparative study of the two test methods should be conducted before a definitive recommendation is made.

3.3 Point-Load Strength Testing

a) Introduction: The purpose of this program is to evaluate the reliability and practicality of the point-load test as a strength index for intermediate quality rocks. It was hypothesized that the test results would show variations of weatherability with depth as determined by correlations with other index tests.

The uniaxial unconfined compression test is commonly used to quantify rock strength. However, its value as a simple, inexpensive strength index is limited by the need for accurately machined specimens. Other testing methods,

ClibPDF - www.fastio.com

such as the Schmidt Rebound Test, yield results that may be correlated with the uniaxial compressive strength. Yet for the most part, these other tests are not standardized or are relatively insensitive to quantifiable strength changes.

The "indirect-tension" tests offer the closest correlation to rock compressive strength. The most familiar of this kind is probably the Brazilian cylinder splitting test in which line-loading is used. Point-loading is a similar method for determining indirect tensile strength. Although the point-load test has been used mainly for research, procedures and equipment suitable for field work have been developed by Broch and Franklin (1972). The factors governing the accuracy and repeatability of test results are discussed by these authors.

The point-load test consists of applying to the specimen two compressive loads concentrated at opposite points. The size and shape of the test specimen may vary, although standardization of this factor allows better reproducibility of results. The load is transmitted to the specimen hydraulically through platens of standard configuration.

b) Equipment: The testing machine suggested by Brock and Franklin consists of the following components:

1. The hydraulic loading system is adaptable to different sized specimens. A quick-retracting ram helps minimize delay between tests. Ram friction is low for accurate load measurement.

2. Two conical platens with spherical ends transmit the load to the specimen. The 5 mm radius spherical end joins the 60° conical section tangetially. The platens are hardened to resist deformation.

3. The accuracy of the failure load-measurement system is ± 2%. A device is provided for retaining the maximum load after failure.

4. The distance-measuring system monitors the platen separation distance to an accuracy of ± 0.5 mm.

ClibPDF - www.fastio.com

The testing apparatus previously obtained from Engineering Laboratory Equipment Company, Bracknell, England was used in this program. Although testing was performed in the laboratory, the machine is portable for field work. Figure 3.7 shows the assembled apparatus.

c) Procedures: Point-load strength tests were performed on core samples from the rock cut slopes observed earlier. Tests were made throughout the core lengths on specimens of adequate dimension, as discussed in the procedure.

Brock and Franklin detailed a standard testing procedure for the point-load test. This procedure was followed as closely as possible, with deviations required by the nature of the rock samples. For instance, the tests were made at natural water content, since rocks with low slake-durability would have disintegrated upon complete saturation. Also, the lack of adequately sized specimens often made it necessary to test somewhat shorter than standard core sections.

THE DIAMETRICAL TEST core specimens with length to diameter ratios of at least 1.0 were selected for the diametral test. Brock and Franklin suggest a ratio of 1.4 or greater, which seems too conservative in view of their data.[1] Ten or more tests per sample are required for rock classification, but this standard could not be met without more core sampling.

Once a specimen is measured and selected, it is inserted in the machine and the platens are closed to make contact along a core diameter. The distance from the contact point to the nearest free end must be at least half the diameter. The distance between the platens is recorded, and the load is increased to failure. The failure load is recorded and the test is repeated for samples of different depth.

THE AXIAL TEST. The testing procedure for the axial test is identical to the above, except that the platens make contact along the core axis. Core

[1] See their figure 8, page 678.

ClibPDF - www.fastio.com

sections broken in the diametral test may be used, with the radius/length ratio equaling 1.1 $\pm$ 0.05.

ANISOTROPIC ROCK cores with observable anisotropy were tested along and perpendicular to planes of weakness. Thus the platen separation in the axial test is measured perdendicular to the bedding, rather than axially. Generally the diametral strengths for such rocks are lower than the axial values.

d) Calculations: The point-load strength index I_s, is calculated as the ratio of the failure load in pounds to the square of the platen separation distance in inches. The failure load is obtained from the hydraulic pressure by a factor of 1.85 lbs/psi, which was derived experimentally with a Riehle testing machine.

Brock and Franklin suggest that a correlation be made for the indexes obtained from cores greater or less than 50 mm in diameter.[2] Since the core samples for this program generally conform to this size, the correlation is unnecessary here. For the axial test specimens a size correction is made for radius to length deviating by 10 to 20 percent from the standard value of 1.1.[3]

The anisotropy index may be calculated as the ratio of the average axial to diametral indexes. However, its value to this project is not important. Brock and Franklin suggest that the point-load strength index is approximately 1/24 the uniaxial compressive strength, due to the close correlation between the two tests.

e) Discussion of results: The point-load strength indexes are presented in the form of core logs in figures 3.7a to 3.7d. Typical Test data are included in table 3. . The core logs clearly show that

[2]See their figure 2.5.

[3]See their figure 12.

ClibPDF - www.fastio.com

insufficient results are available for development of reliable rock strength profiles. Although the indexes may tend to increase or decrease with depth, there is far too much scatter in the data to draw any quantitative conclusions concerning rock weatherability or depth of weathering.

The wide variance in the test results is not unreasonable since most of the cores were weak and fractured, thus altering the internal state of stress from that which would be expected for a homogeneous brittle material. Some specimens deform plastically around the loading platens before failure, as witnessed in the tests on core no. 4.

ClibPDF - www.fastio.com

Chapter 4. LABORATORY SHEAR TESTS

Design of cut slopes in hard rocks obviously requires assessment of the shear strength of the discontinuities along which sliding or toppling can develop. In intermediate quality rocks, it is likely that failure modes involve a complex of material failures and surface sliding events. In either case, the direct shear test is appropriate for study of the materials of highway cuts. Two types of shear tests were conducted in the course of this investigation. The small samples resulting from core borings were tested in the shear machine described in Appendix 4, in which normal load is supplied by a hydraulic piston and shearing is created by a screw jack. This machine has the unique capability of allowing control of water pressures inside the specimen during shear, but this capacity was not needed for the test program. In fact almost any soil mechanics laboratory direct shear machine of large capacity could be utilized for shear tests on samples of shales, up to normal pressures of the order of several hundred psi. Machines will differ in design details, as discussed briefly in Appendix 4, but the range of variability of rock materials is far greater than the individual differences between shearing machines. Thus we feel that direct shear testing for highway cut slope design on a routine basis is not an unreasonable procedure. Of course, the tests will be more meaningful if extended in size from the three or four square inches of the core specimen to several hundred square inches in shear area. Tests of such large size were also conducted, as part of this investigation using a simpler shear box of inside dimension 11-1/4 x 17-1/4", driven by hand-actuated hydraulic cylinders, as discribed later. Samples for such tests must be selected from outcrops.

4.1 Shear Tests on Specimens Selected from the Core Box

The direct shear machine tests a sample "potted" into a split metal box.

ClibPDF - www.fastio.com

The specimens were selected from the core samples according to what was available; they had to be intact lengths of core, three to four inches long. The locations of samples were suggested by the point-load and slake-durability results as it was hoped to be able to relate point-load strength and slake-durability with shear strength. The cores were sheared along planes of weakness; some specimens broke along these surfaces prior to testing. The specimens were saw-cut to fit the shear boxes and they were air dried on the bench before testing. They were then potted in the shear boxes using a sulfur compound ("cylcap"). Care was taken to try to insure that the mean plane of shear would be as close to the horizontal plane as possible. The potting is performed in two operations; the bottom half is potted first, then the top half is assembled after a bond breaker has been placed at the level of the expected shear plane to protect it from the sulfur. The specimen is then ready and protected, and the sulfur is poured into the top half through a hole in the bottom of this half box. Two additional holes provide for air escape.

The specimen is installed in the shear chamber, and the shear machine is positioned under the normal loading frame. The normal load cell is then applied and monitored visually on the load cell output bench. After zeroing the output on the digital printer and the XYY' recorder, the shear test is started at a constant speed of 0.1 in/min, while the normal load is maintained constant. Shearing continues until a residual value of shear strength is attained. In this program, some tests were followed by two subtests, at different normal pressures. This gave additional values of residual shear strength. (See table 4.1). During the tests, the following information was available, and was recorded:

normal load $P_n = \sigma_n \times A$ (area of shear)

shear force $T = \tau \times A$

ClibPDF - www.fastio.com

shear displacement (u)

normal displacement (v)

a) Results of the shear testing program: The results of the tests are summarized in Table 4.1. An explanation of the symbols follows:

A:	initial joint area; was corrected for shear displacement, in data analysis.
σ_n:	normal stress.
u_p:	shear displacement at peak shear load.
v_p:	normal displacement at peak shear load.
K_{ss}:	shear stiffness at peak shear load (τ_p/u_p).
τ_p, τ_r:	peak and residual shear strength.
ϕ_p, ϕ_r:	peak and residual friction angles assuming c = 0.
δ_p:	dilatancy at peak = $\tan^{-1}(v_p/u_p)$. Positive if dilation.
δ_r:	dilatancy during shear at residual strength. Positive if dilation.
ϕ_p^*, ϕ_r^*:	$(\phi_p - \delta_p)$ and $(\phi_r - \delta_r)$ respectively. They are the friction angles corrected for the effect of dilatancy or contraction. The dilatancy to peak load is not equal to that during shear at residual strength.

The results of shear tests provide data usable in analysis of highway cut slope safety. This will be considered further in Chapter 5.

4.2 Large Specimen Direct Shear Testing

a) Introduction: The shear strengths of discontinuities or joints in rock are important for estimating the stability of rock cut slopes. The roughness of the surface is important because it contributes to dilatancy and the dilatant component of strength. We cannot include the influence of *in situ* roughness in small laboratory tests, up to ca. 50 square inches of shear area.

ClibPDF - www.fastio.com

TABLE 4.1
SUMMARY OF SMALL SCALE SHEAR TESTS

Test No.	Sample No. (hole-depth)	A (in^2)	σ_n (psi)	u_p (10^{-2} in)	v_p (10^{-3} in)	K_{ss} (10^4 psi/in)	τ_p (psi)	τ_r (psi)	ϕ_p (deg)	ϕ_r (deg)	δ_p (deg)	δ_r (deg)	ϕ_p* (deg)	ϕ_r* (deg)	Comment
211	1-10	3.93	52	5.80	4.5	0.20	55		46.6		4.4		42.2		Peak
			53					71		53.3		11.4		41.9	Residual (1)
			110					153		54.3		2.1		52.2	Residual (2)
212	1-21	3.30	51	2.75	1.5	0.31	50		44.4		3.1		41.3		Peak
			53					29		28.7		5.8		22.9	Residual (1)
			109					83		37.2		1.4		35.8	Residual (2)
213	1-30	2.87	53	9.00	26.0	0.63	567		(84.7)		16.1		68.6		Peak,
			58					212	(Intact	74.7		--		--	Residual (1)
			116					235	(specimen)	63.7		--		--	Residual (2)
215	2-9	3.04	103	7.8	1.3	0.84	153		56.0		1.8		54.2		Peak
			106					146		54.0		6.1		47.9	Residual (1)
			165					167		45.3		0.3		45.0	Residual (2)
216	2-13	3.02	104	6.0	0.9	0.91	346		(73.3)		0.9		72.4		Peak,
			106					57	(Intact	28.3		3.3		25.0	Residual (1)
			176					155	(specimen)	41.4		-14.3		55.7	Resdiual (2)
217	2-20	3.15	105	8.4	-7.0	0.08	65		31.8		-4.8		36.6		Peak
			105					65		31.8		-4.8		36.6	Residual (1)
			178					180		45.4		--		--	Residual (2)
218	3-4	3.0	51	4.2	16.0	0.65	271		(79.3)		20.9		58.4		Peak
			55					63	(Intact	49.0		4.4		44.6	Residual (1)
			118					173	(specimen)	55.7		0.9		54.8	Residual (2)
219	3-10	3.0	52	6.2	-2.3	0.16	97		61.7		-2.1		63.8		Peak
			55					96		60.1		5.8		54.3	Residual (1)
			119					211		60.6		-6.2		66.8	Residual (2)
220	3-14	3.0	51	4.1	5.7	0.55	146		70.7		7.9		62.8		Peak
			55					115		64.4		3.7		60.7	Residual (1)
			120					289		67.5		4.2		63.3	Residual (2)
221	3-19	3.0	51	4.4	13.0	0.82	363		(82.0)		16.5		65.5		Peak,
			56					289	(Intact	79.0		6.8		85.8	Residual (1)
			120					426	(specimen)	74.2		0.4		74.6	Residual (2)
222	4-4	2.9	53	4.0	-1.0	0.14	54		45.5		1.4		44.1		Peak
			56					15		15.0		5.2		9.8	Residual (1)
			118					114		44.0		-5.0		49.0	Residual (2)
223	4-7	4.64	51	6.0	3.1	0.11	67		52.8		3.0		49.8		Peak, Recemented Joint
			53					24		24.4		9.1		15.3	Residual (1)
			111					91		39.3		0.5		38.8	Residual (2)

Continued...

ClibPDF - www.fastio.com

Table 4.1 Continued. Summary of Small Scale Shear Tests

Test No.	Sample No. (hole-depth)	A (in^2)	σ_n (psi)	u_{p-2} (10in)	v_{p-3} (10in)	K_{ss} (10^4psi/in)	τ_p (psi)	τ_r (psi)	ϕ_p (deg)	ϕ_r (deg)	δ_p (deg)	δ_r (deg)	ϕ_p* (deg)	ϕ_r* (deg)	Comment
224	4-7	4.64	49	3.2	3.3	0.34	92		62.0		5.8		56.2		Peak,Recemented Joint
			50					40.7		39.1		9.7		29.4	Residual (1)
			109					129		49.9		1.8		48.1	Residual (2)
225	4-20	3.1	49	3.7	1.7	0.30	109		65.8		2.6		63.2		Peak
			54					87		58.3		5.8		52.5	Residual (1)
			114					198		60.0		0.4		59.6	Residual (2)
226	4-26	3.1	50	5.1	5.6	0.12	62		51.1		6.2		44.9		Peak
			51					35		34.5		4.6		29.9	Residual (1)
			109					120		42.2		-2.3		44.5	Residual (2)

* Note: All stresses corrected for shear displacement.

ClibPDF - www.fastio.com

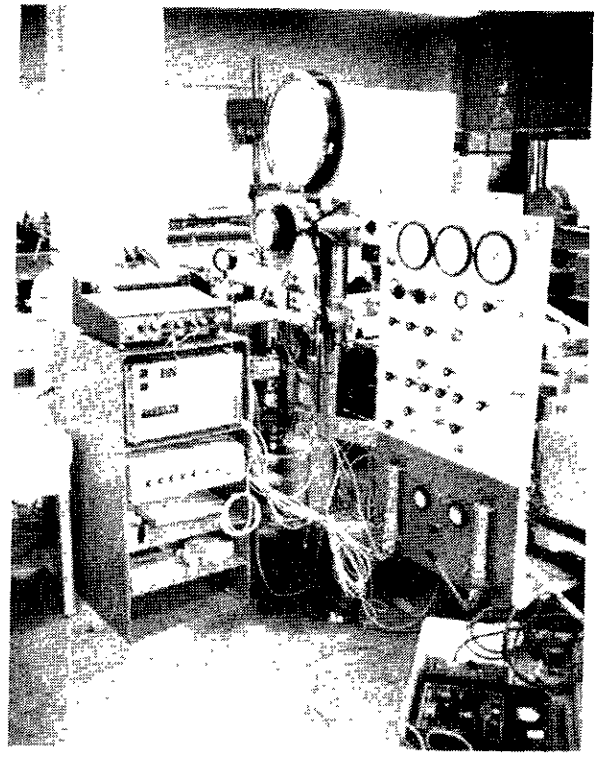

Figure 4.1. Shear machine for samples up to 5 inches x 5 inches. Normal stress is provided hydraulically. Shear displacement of the lower part of the specimen is forced by a motor driven screw. Water pressure can be monitored during the test.

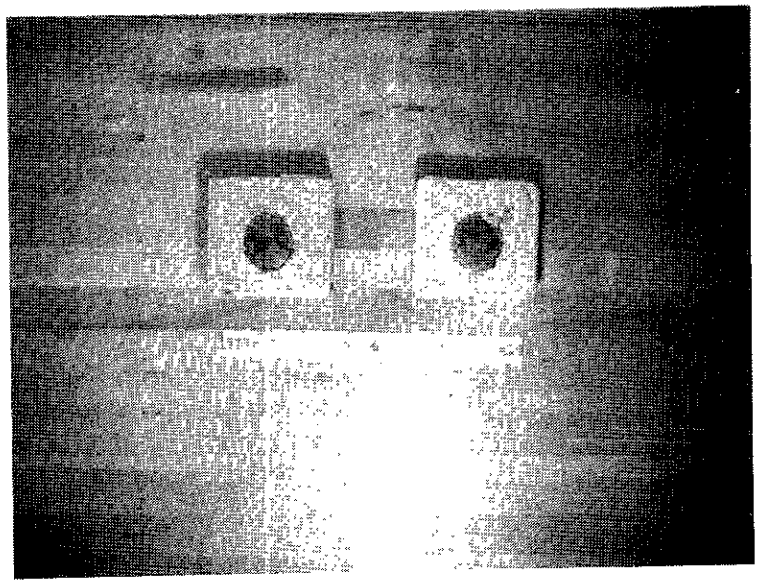

Note:
This picture is to be replaced by a better one as soon as it is available.

Figure 4.2. Potted samples of core before shear test. (upper and lower halves).

ClibPDF - www.fastio.com

However, if samples can be obtained, it is practical to conduct large specimen shear tests in the laboratory to obtain data basic for design of cut-slopes in intermediate quality rock. Our intention here is to demonstrate such a test and present the type of data that may be extracted from it.

b) Equipment: The equipment described here (figure 4.3), manufactured by Golder Brawner and Associates, of Vancouver, Canada, consists of the following components:

1. Shear box: The shear box is composed of an upper and a lower chamber. The units are constructed from 1/2 inch steel plates and may be completely disassembled. The inside dimensions of the shear box are 11-1/4" by 17-1/4"; the lower half being 5" deep, while the upper half is 8" deep.

2. Loading system: The shear and normal loads are applied by means of two manually controlled hydraulic jacks. The normal load reaction member is attached to the frame housing the lower chamber. The shear load jack is attached to the frame also, with its reaction member linked to the upper chamber. A manual pressure generator, serving as a regulator, is included in the normal load circuit. The loading system is easily disassembled.

3. Monitoring system: The shear and normal hydraulic pressures are monitored by two bourdon gauges. Shear displacement of the upper chamber is measured horizontally by a dial gauge (0.001" accuracy) mounted opposite the shear load jack. Normal displacement during shearing is monitored by three dial gauges (0.001" accuracy) on the top of the upper chamber. These gauges define the orientation and displacement of the upper shearing surface relative to the lower surface.

4. Spacers: Spacers are needed for isolating the shear plane from the upper and lower chambers. The spacers are "L" shaped, two inches wide and 1/4" thick. When in position, four such plates are continuous with the inside

ClibPDF - www.fastio.com

perimeter of the shear box. A total of twelve spacers may be used, achieving a separation of 3/4".

5. Potting material: Hydrastone is used to encase the specimen within the upper and lower chambers. The material is mixed in dry form with water. The tests performed in the project each required about one sack (100 lbs) of dry hydrastone.

c) Procedures: Due to the fact that larger specimens are needed for the test, rock samples, rather than cores were retrieved from surface outcroppings. Sample no. 1, sandstone is from the vicinity of borehole no. 4, and sample no. 2, a soft claystone, was taken near borehole no. 2. Both samples were intact, with no predetermined joint surface.

1. The test specimens are first broken down to a size accomodated by the shear box. The maximum dimensions are approximately 10" by 17" for the shear surface. A maximum height of 12" is recommended. The specimen should be somewhat smaller than the size of the box so that adequate penetration of the potting material is ensured.

2. With the upper shear chamber removed, the specimen is seated on small blocks so that the desired shear plane is horizontal and slightly higher than the top of the lower chamber. The potting material is placed around the specimen to within about 1/4" of the shear plane.

3. After the lower specimen half is set (about 1/2 hour), the spacers are positioned for the desired separation. The area bounded by the spacers is filled with sand to act as a "bond-breaker" between the upper and lower halfs. The surface of the sand should be continuous with the top of the spacers.

4. The spacers are wiped clean and the upper chamber is positioned directly over the lower. The respective sides of the chambers must be parallel. The base of the normal load jack is removed to expose two rectangular openings.

ClibPDF - www.fastio.com

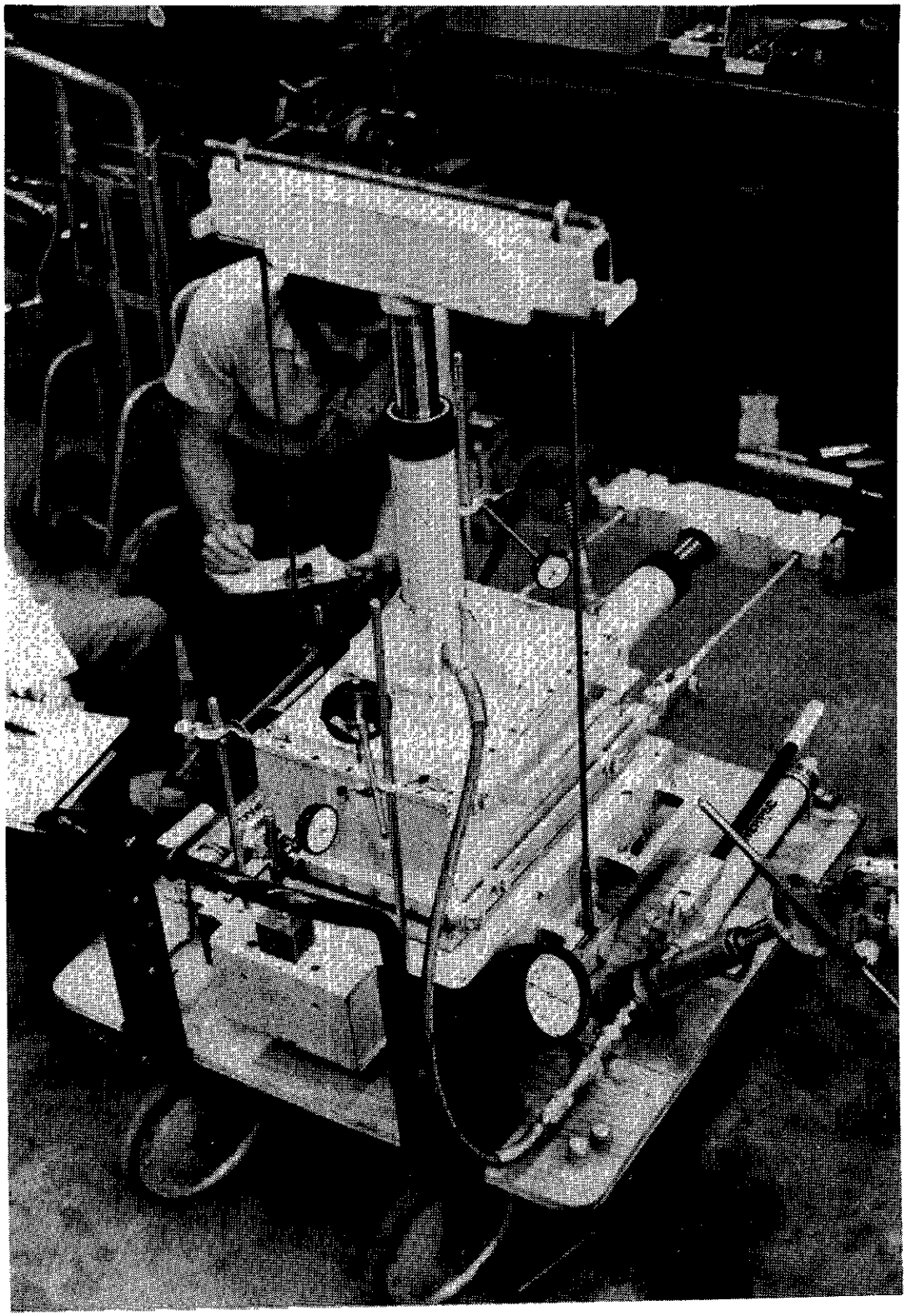

Figure 4.3 Shear machine for samples up to 11 3/4" x 17 3/4", with maximum normal and shear load 20 tons. Built for U.C. Rock Mechanics Laboratory by Golder & Brawner Associates, Vancouver.

ClibPDF - www.fastio.com

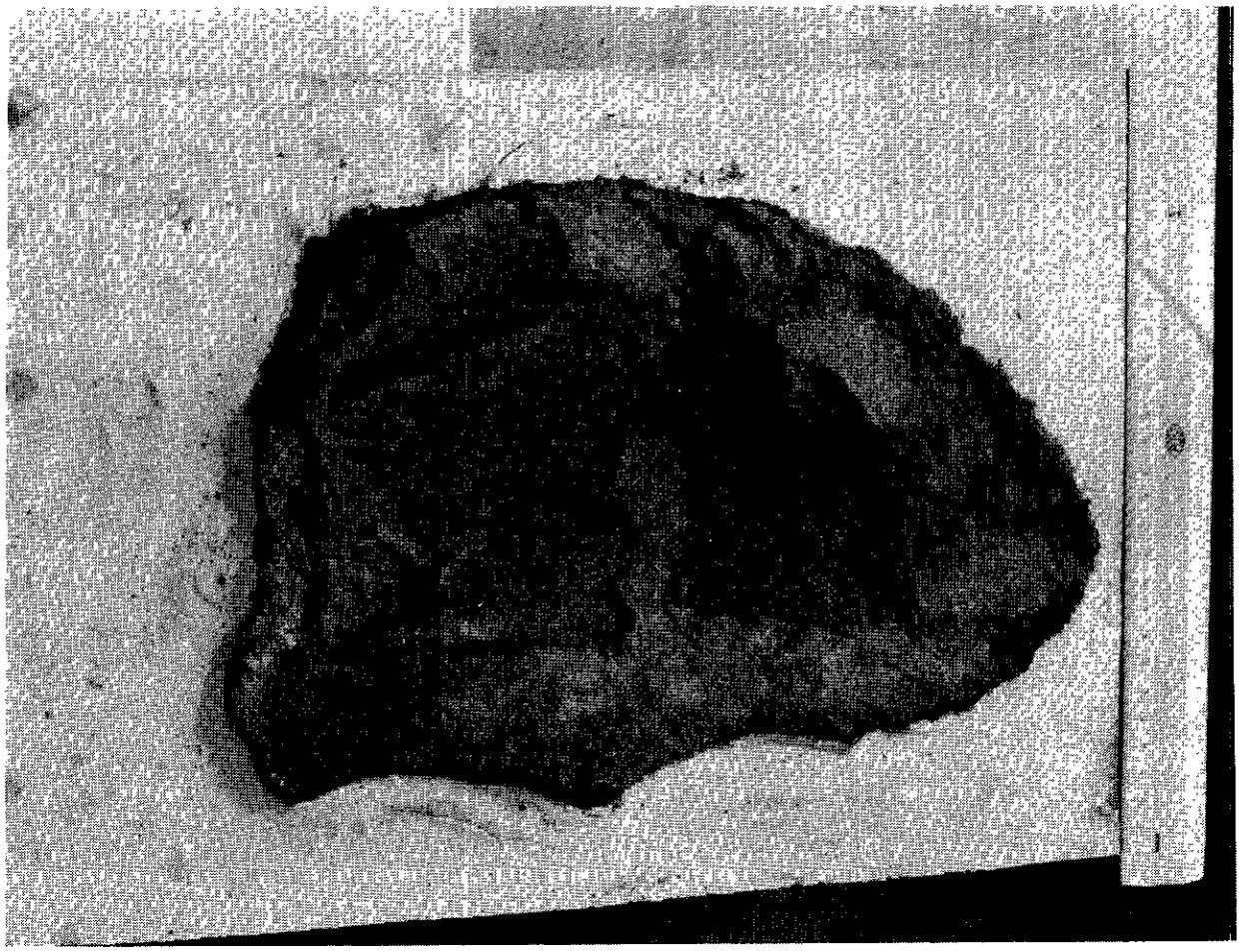

Figure 4.4 Half of shear sample no. 1 (sandstone) potted in plaster. (gradation on ruler is centimeters).

ClibPDF - www.fastio.com

The potting compound is poured through these, until the chamber is filled and contact with the top is made. Any exposed potting material must be scraped flush with the top of the chamber.

5. After the potting material has cured for about twelve hours, the spacers and sand are removed and the apparatus is assembled for testing. The shear load reaction member must be supported to prevent premature shearing of the specimen.

6. The normal load is applied in convenient increments and all four dial gauges are read and recorded correspondingly.

7. When the desired normal load is attained, the shear load is applied. Again, all four dial gauges are recorded at increments of shear load. After the residual shear strength is reached, the normal load may be increased as in test no. 2, to obtain additional shear strengths.

8. At the completion of the test, the upper and lower chambers are separated. The contact area of the specimen is determined and a roughness analysis may be performed, as described in the appendix.

9. The encased specimen is removed by disassembling the chambers.

d) Results: The results of the two large-scale shear tests are summarized in table 4.2. An explanation of the symbols follows:

A:	Initial shear surface area. Corrected for shear displacement in data analysis.
σ_n:	Normal stress, corrected for shear displacement.
u_p:	Shear displacement at peak shear load.
v_p:	Normal displacement at peak shear load.
τ_p, τ_r:	Peak and residual shear strenghts, corrected for shear displacement.
ϕ_p, ϕ_r:	Peak and ultimate internal friction angles $\mp \tan^{-1}(\frac{\tau_p}{\sigma_p})$ zero cohesion is assumed.

ClibPDF - www.fastio.com

δ_p: Dilatancy at peak = $\tan^{-1}\left(\frac{v_p}{u_p}\right)$. Positive if dilation.

Figures 4.5 and 4.6 give the two test curves (τ vs u). Shear test data sheets are given in appendix 5.

ClibPDF - www.fastio.com

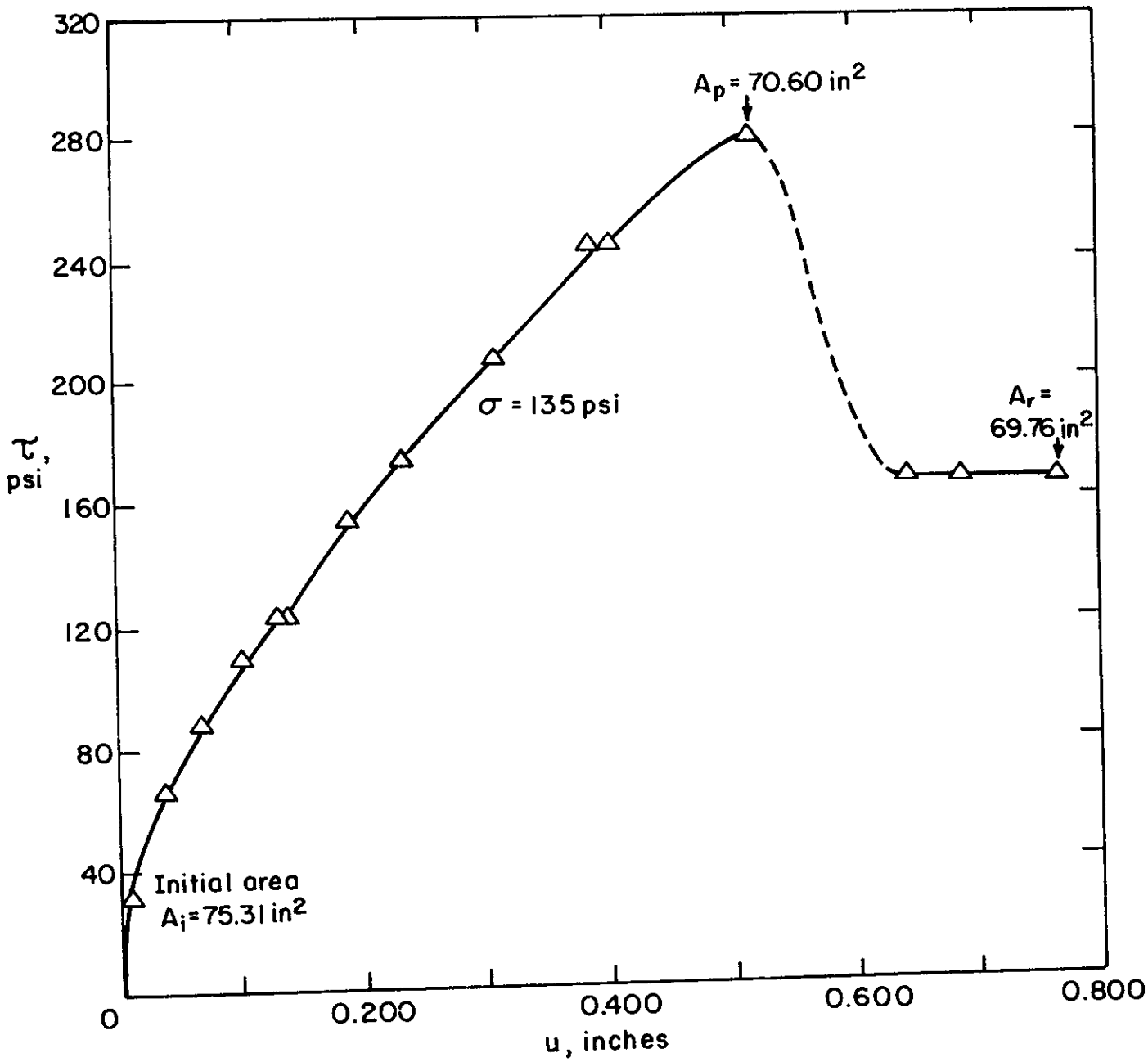

Figure 4.5. Shear test data for large specimen of sandstone (#4) σ = 135 psi.

ClibPDF - www.fastio.com

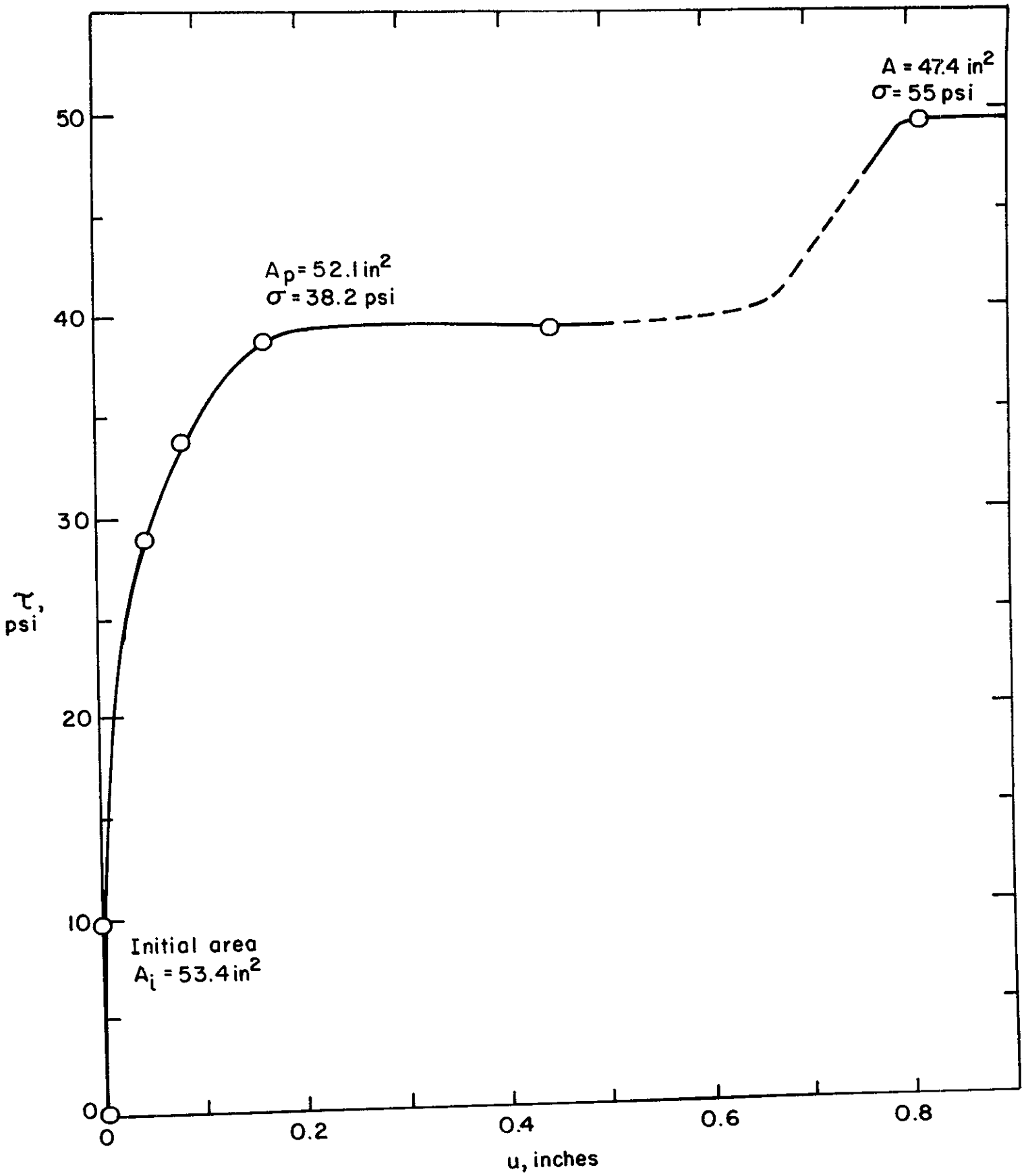

Figure 4.6. Shear test data for soft claystone (sample #2) from Highway #4 cut.

ClibPDF - www.fastio.com

TABLE 4.2
SUMMARY OF LARGE SCALE SHEAR TESTS ON INTACT SAMPLES

Test No.	Initial A (in^2)	σ_n (psi)	u_p (in)	v_p (10^{-2} in)	τ_p (psi)	τ_r (psi)	δ_p (deg)	ϕ_p^* (deg)	ϕ_r (deg)	Comment
1	75.3	144	0.515	+12.1	297		13.2	64.1		First Test, Peak
		146				178			50.6	First Test, Residual
2	53.4	16.5	0.165	-1.6	12.9		-5.5	38.0		First Test, Peak
		17.2				13.4			38.0	First Test, Residual
		27.5				17.9			33.0	First Test, Residual; σ_n increased to 27.5 psi

ClibPDF - www.fastio.com

Chapter 5. DISCUSSION AND RECOMMENDATIONS FOR FURTHER STUDIES

5.1 Results of the Test Program

By design, all of the boreholes penetrated essentially the same types of rocks -- mudstone and claystone with some clayey sandstone. In borehole 1, the rock generally became harder with depth. The shear strength, slake durability, point load index and bore hole jack deformability all showed a gradual increase with depth. These all all independent tests measuring different things and they need not vary in the same direction; however as the rock became harder, it also became stronger, stiffer, and more durable. In borehole 2, the rock near the surface was soft and it became moderately hard in the middle, then softer toward the bottom. The point load and slake durability tests show a gradual decrease with depth, without registering the moderately hard interval in the mid section. The friction angle correlated well with the geology, reaching its highest value in the center. There were no bore hole jack results. In bore hole 3, the rock was a relatively hard silty sandstone, becoming softer with depth. The slake durability and point load tests showed this trend. The friction angle did not agree with this trend. Only 2 borehole jack tests were run. Borehole 4 was in soft to moderately hard claystone, with a harder shale layer at mid depth and a soft, highly weathered claystone layer towards the bottom. The results are more scattered and harder to generalize than in the other locations.

In general, there were too few tests, in view of the great variability of the rock properties, to be able to develop strong correlations between the different tests, since all were not performed on the same specimens. Also, as noted above, the rock parameters influencing the test results are different in each case and need not show any correlation at all. All the tests were essentially in the same rock type. It can be expected that with more heterogeneous stratigraphy, there would have been more dramatic changes in test results

ClibPDF - www.fastio.com

with strong correlationships from one test technique to another. The shear test results, it should be noted, relate primarily to the strength of weak surfaces within the bedrock; this is fundamentally different from the point load tests which reflect the behaviour of the intact material. An insufficient number of radial permeability tests were run to allow discussion of the relationship of this test to other measurements.

In summary, a number of potentially useful techniques have been elaborated. Cross correlation of the typical test results presented was not an objective, but it is of interest to observe that the results show some degree of consistency. We believe these test techniques can be potentially helpful in transportation engineering, particularly as regards design of surface excavations.

5.2 Application of the Test Methods Discussed to the Design of Excavations in Intermediate Quality Rocks.

When a transportation route traverses hilly terrain, the engineer has to decide between tunnels and open cuts. In regard to cuts, he may have the freedom to choose the direction and he usually will be able to choose the precise location and the elevation (hence the height) of the cut. Then, he will have to select the rock slope angles, the numbers and widths of benches, and if called for, the types of drainage and supporting structures required. The test methods introduced here can assist the engineer in making some of these decisions because they help to evaluate rock behaviour and failure modes related to the performance of intermediate quality rocks in surface excavations.

An excavation can prove to be unsatisfactory in service in a number of ways. Erodible, silty materials may be carried away by rain-water as the cut is destroyed by gullies. Clayey materials, softened by water, may slump and become remoulded, causing the formation of flow slides. Though both of these "failure modes" can occur in bedrock formations, in weathered or hydrothermally altered

ClibPDF - www.fastio.com

zones, we regard such behaviour as essentially soil-like and the causative materials as soils in the strict engineering sense; therefore discussion of these problems is outside the scope of this report. In intermediate, and in hard rocks, undercut, daylighting surfaces of discontinuity may allow blocks of material to slide, or topple into the excavation. This is usually considered to be a hard rock problem, but a certain degree of structural control can be expected in any sedimentary formation wherein clay seams, faults, and contacts between dissimilar strata can control the location of sliding. Sliding in these rocks, however, invariably involves internal shearing, since the rock asperities will crush. The intermediate quality rocks, additionally, present a failure mode consisting of accelerated weathering followed by gravity transportation and water erosion of the loosened and weakened material. For example, in the cuts on the east side of the Caldecott tunnel, figure 5.1a,b, mudstone members ten to thirty feet wide are slaking and the loosened material runs down on the benches so that the harder conglomerate layers now stand out in relief of as much as five feet. Thus undermined, some of the stronger conglomerate members may eventually work their way onto the benches.

Thus, the intermediate rocks are divisible into two groups; the first tend to fail by sliding internally or on structurally controlled surfaces, and the second by weathering and erosion. In order to evaluate the magnitude of potential problems with slaking and erosion, some form of durability test is essential. It will remain for a future investigation to attempt to link the response of different rocks in slake durability tests to weather in actual excavations. Methods for designing cut slopes so as to minimize sliding hazards are discussed by Hoek and Bray (1974). We will show how to use point load or NX jack tests, together with a small number of shear tests to friction angles required for such analytical procedures.

ClibPDF - www.fastio.com

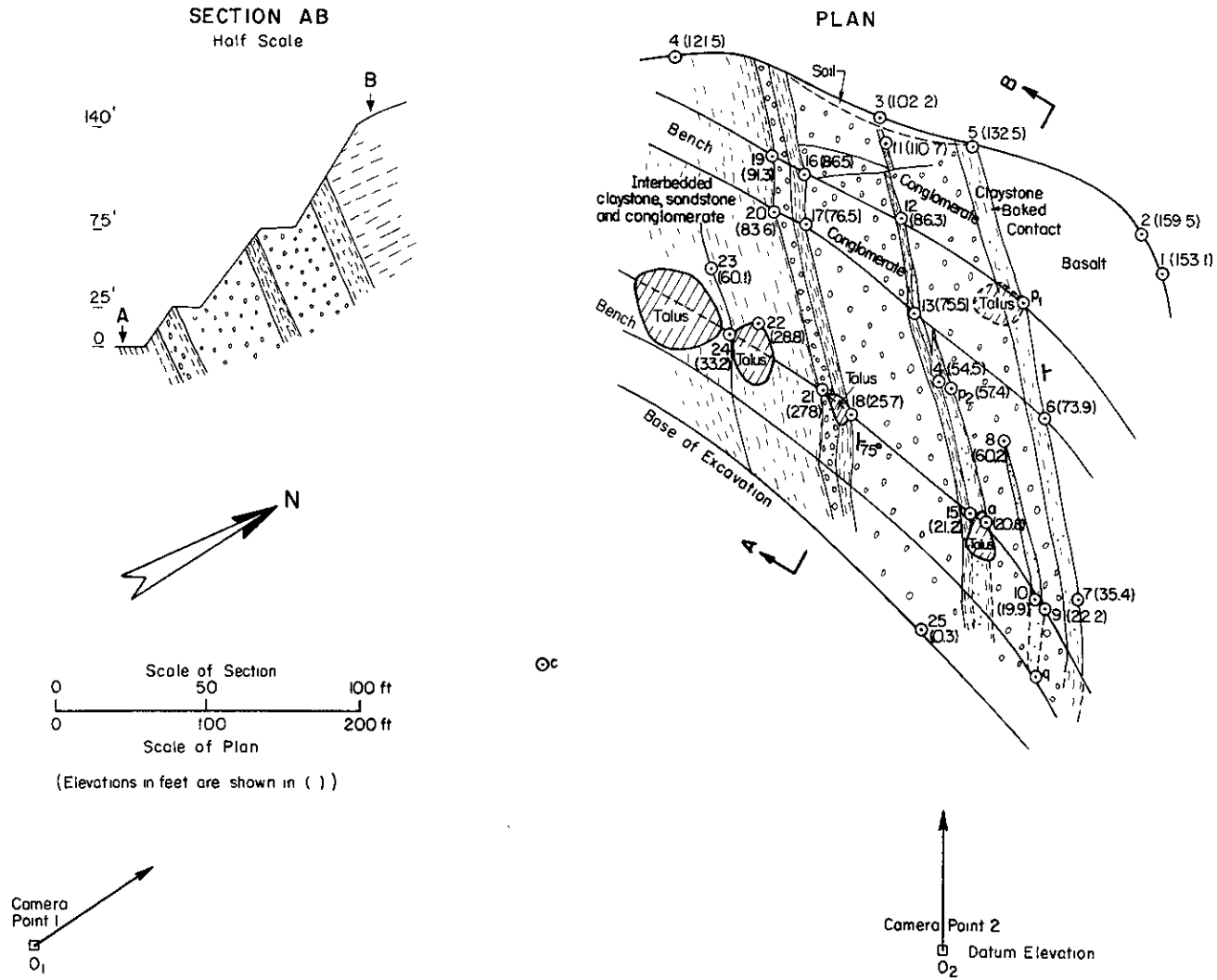

Figure 5.1a Geologic sketch map and cross section of the rock cut on highway 24, to the east of the Caldecott Tunnel (north side of freeway).

ClibPDF - www.fastio.com

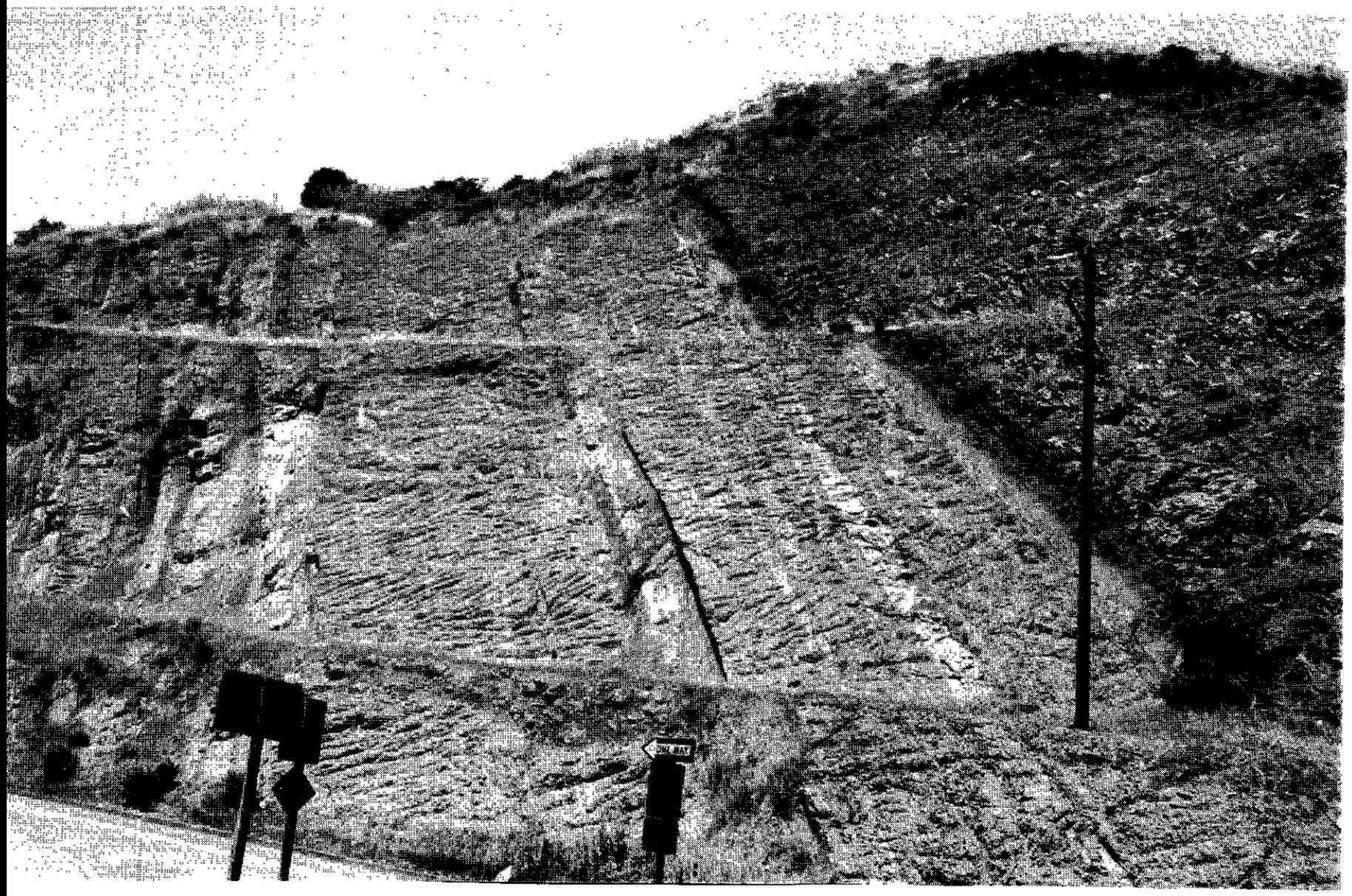

Figure 5.1b Photograph of cut of figure 5.1a. This photo, taken from camera point 2, was used together with another similar photo taken from camera point 1, to make the map. Note the erosion in the steeply dipping beds of mudstone.

ClibPDF - www.fastio.com

It is usually not possible to perform enough shear tests on samples of representative weakness surfaces to characterize the shear strength versus normal pressure relationship. Shear strength on rough natural surfaces originates from bond, from friction and from interlocking. It is possible to determine or to estimate the sliding friction coefficient ϕ from shear tests on sawed surfaces. The geometric interlocking contribution to shear strength can then be added on, as suggested by Patton if the roughness angle i can be characterized $\tau_p = \sigma \tan(\phi + i)$. This is discussed by Goodman (1974), and also by Hoek and Bray (1974). However, this procedure is not correct for intermediate quality rocks because the asperities can be sheared off at relatively low normal pressures. Patton showed that as σ is increased, the energy to shear through the asperities of a rough rock surface eventually becomes less than the energy to override them. Rough joints in granite reach this transition at a normal stress of the order of five to ten thousand pounds per square inch. However, sliding on multiple fissures in a Tertiary mudstone or along a bedding surface in a clay shale, will cause shearing through most high points of rock at normal stresses of only several hundred pounds per square inch. In order to develop the proper combination of frictional sliding, and rock shearing, one can try to perform numerous tests on similar specimens. However, since this is not usually feasible, and since identical specimens of natural surfaces cannot be obtained, we prefer an interpretive procedure based upon a shear strength equation presented by Barton (1974). Barton's equation accounts for friction of the rock surfaces in contact, over-sliding of asperities, and shear through asperities, as follows:

$$\tau_p = \sigma(\tan \phi_p^* + J_R \log_{10}(q_u/\sigma)) \qquad (1)$$

in which:

τ_p is the peak shear strength at a normal pressure of σ.

ClibPDF - www.fastio.com

ϕ_p^* is the friction angle for sliding on smooth surfaces of the rock in question.

J_R is a roughness index, increasing from 0 as the roughness increases.

q_u is the compressive strength of the rock comprising the asperities.

Barton suggested the following values for the roughness index:

J_R = 0 for perfectly smooth plane surfaces.

5 for smooth, nearly planar surfaces.

10 for smooth undulating surfaces.

20 for rough, undulating surfaces.

Suppose a shear test is performed and both peak dilatancy displacement (v_p) and peak shear displacement (u_r) are measured. As shown in chapter 4, table 4.1, we can calculate the dilatancy angle $\delta_p(\sigma)$ by

$$\delta_p(\sigma) = \tan^{-1}\left(\frac{v_p}{u_p}\right) \tag{2}$$

and we can calculate the friction for smooth surfaces ϕ_p^* from

$$\phi_p^* = \tan^{-1}\left(\frac{\tau_p}{\sigma}\right) - \delta_p \tag{3}$$

then we use Barton's equation (1) as the defining equation for J_R, that is

$$J_R = \frac{(\tau_p/\sigma - \tan\phi_p^*)}{\log_{10}(q_u/\sigma)} \tag{4}$$

In this case, the quantity q_u will be evaluated independently. The compressive strength q_u can be obtained from point load tests, or from NX jack tests by means of an established correlation. In the case of the point load tests as noted in section 3.3, the compressive strength is approximately 24 times the point load index. In the case of NX jack tests, Deere, et al (1967) give the "modulus ratio" E/q_u for many different rock types; it is usually in the range from 200 to 500. Since the modulus of elasticity is obtainable from borehole jack or dilatometer results, the compressive strength for rocks at inacessible points can be estimated from such results. It is also possible to estimate the

ClibPDF - www.fastio.com

compressive strength from hardness measurements or from engineering rock descriptions.

Consider the shear test results on discontinuity surfaces previously reported in section 4.1. The results are summarized in table 5.1, together with the applicable point load test results. An unconfined compressive strength was calculated from the point load index for each shear test specimen. Then, the dilatancy angle actually measured at the normal stress of the test (δ_p) was used in equation (4) to calculate J_R for each shear test. These values ranged from a low of 1.0 to a high of 6.7. Barton's strength equation (1) was used, with J_R, q_u, and ϕ_p^* defined for each test, to compute shear strength curves ($\tau_p(\sigma)$ versus σ) for each sample. These curves, figure 5.2, extrapolate the single measurement in a much more satisfactory way than a Mohr Coulomb relationship, which we know to be incorrect for weak rocks.

To analyze potential sliding in a formation with the shear strength corresponding to one of the curves in question, we can proceed in a simplified manner by finding an overall single friction angle ($\phi_{equivalent}$) giving the correct shear strength at the average normal stress of the potential slide. Consider the hypothetical case of figure 5.3. The shear strength test has given point B, through which a shear strength curve (τ_p versus σ) has been plotted, assuming a value of sliding friction ϕ_p^* equal to 26 degrees. Secants from the origin to different points on this curve are inclined at angles $\phi_{equivalent}$ which decrease from 59 degrees, at very low normal stress, to 26 degrees at high normal stress. The potential sliding mass produces an average normal stress of 95 psi on the plane surface of sliding, and corresponding to this normal stress, the equivalent friction angle is 46 degrees. The stability of this mass can now be assessed using a simple technique, of the type proposed by Hoek and Bray. Or, if a method of analysis is used in which variable shear strength along the sliding surface can be input, the actual shear strength curve can be used.

ClibPDF - www.fastio.com

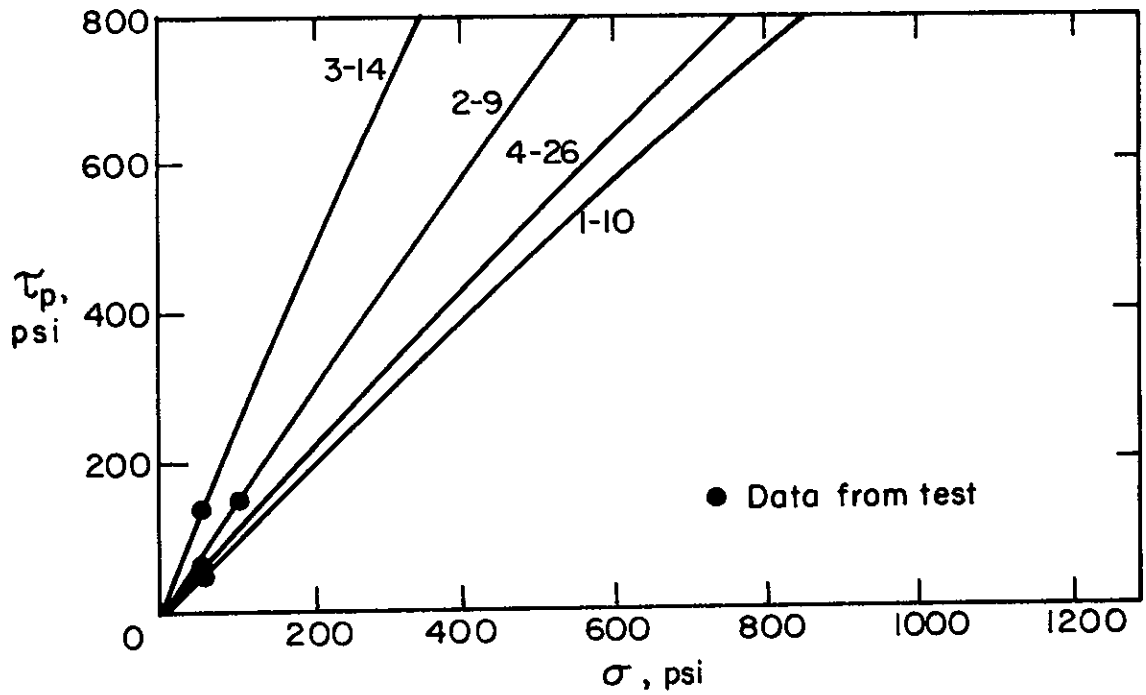

Figure 5.2. Extrapolated shear test curves.

ClibPDF - www.fastio.com

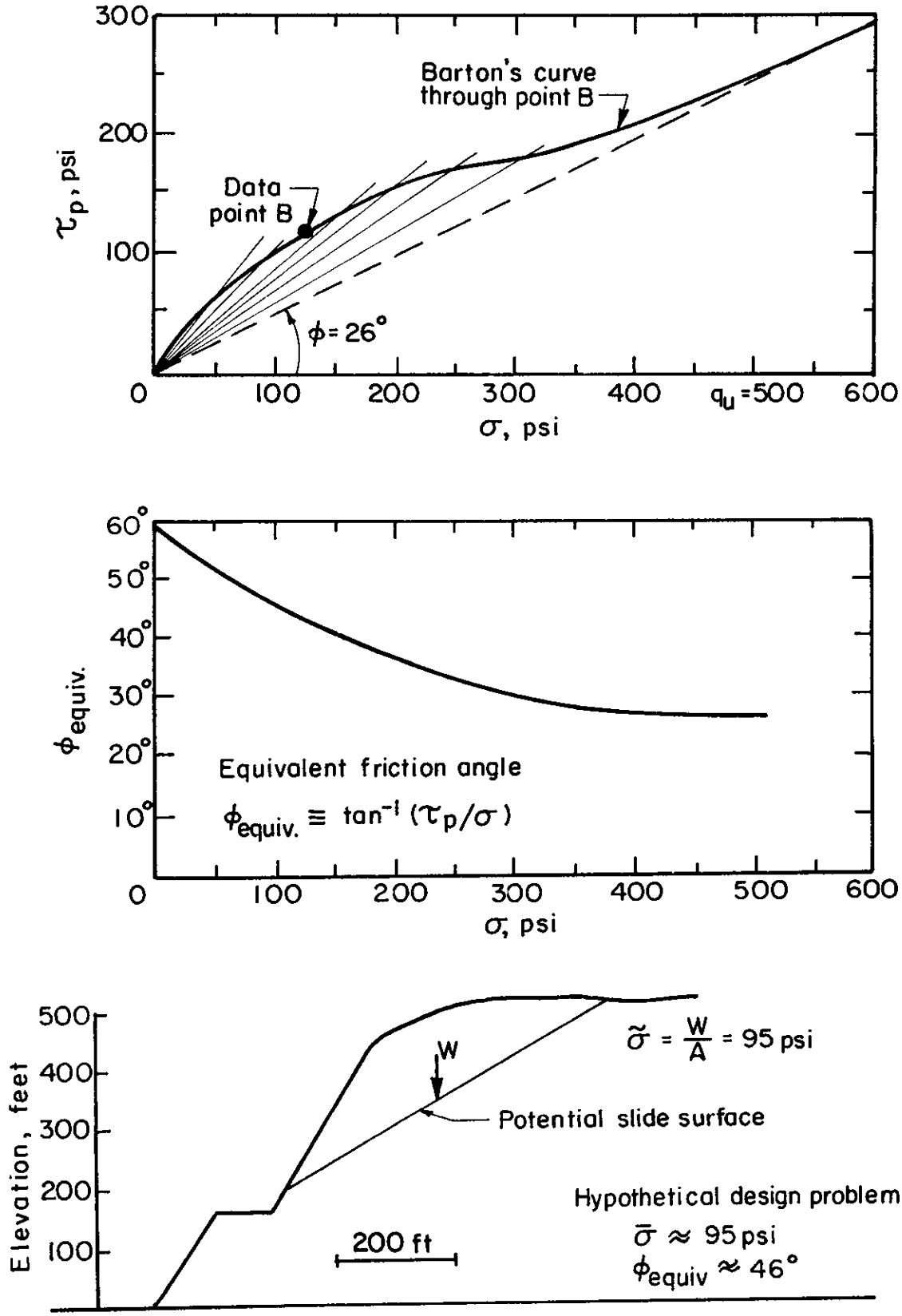

Figure 5.3. Determination of a single overall friction angle ($\phi_{equivalent}$) for rock of intermediate quality (ϕ = 26° in sliding on smooth surfaces).

ClibPDF - www.fastio.com

TABLE 5.1

PEAK SHEAR STRENGTH ROUGHNESS PARAMETER J_R CALCULATED FOR SHEAR TEST RESULTS ON DISCONTINUITY SURFACES

Test No.	Sample No.	(1) I_s(psi)	(2) q_u(psi)	σ_n(psi)	τ_p(psi)	(4) δ_p(o)	J_R
211	1-10	85	2040	52	55	4.4	2.8
212	1-21	310	7440	51	50	3.1	1.4
215	2-9	260	6210	103	153	1.8	1.0
220	3-14	115	2760	51	146	7.9	4.6
222	4-4	15	360	53	54	1.4	1.7
223	4-7	15 (3)	360	51	67	3.0	3.5
224	4-13	15	360	49	92	5.8	6.7
225	4-20	65	1560	49	109	2.6	1.7
226	4-26	55	1320	50	62	6.2	4.4

(1) I_s is the average of diametral and axial point load strengths.

(2) $q_u \approx 24\ I_s$.

(3) Approximate value assumed as no. I_s value available at respective depth.

(4) From Table 4.1.

ClibPDF - www.fastio.com

TABLE 5.2

COMPUTATION OF BARTON'S $\tau - \sigma$ CURVES FOR SHEAR TESTS ON DISCONTINUITY SURFACES

Sample	q_u	J_R	ϕ_p^*	$\tau_p(\sigma)$ 100	200	400	1000
1-10	2040	2.8	42.2	103	200	389	935
1-21	7440	1.4	41.3	96	190	374	917
2-9	6240	1.0	54.2	148	293	580	1428
3-14	2760	4.6	62.8	266	496	927	2128
4-4	360	1.7	44.1	100	196	--	--
4-7	360	3.5	49.8	127	244	--	--
4-13	360	6.7	56.2	173	319	--	--
4-20	1560	1.7	63.2	217	423	828	2008
4-26	1320	4.4	44.9	118	226	432	1015

$$\tau_p = \sigma \tan \left(\phi_p^* + J_R \log \frac{q_u}{\sigma}\right)$$

ClibPDF - www.fastio.com

5.3 Recommended Future Investigations

This report has introduced the subject of the mechanical properties of rocks which we have chosen to term "intermediate" in quality, because of their position intermediate between soils and hard rocks. Such rocks are very common in California and it is hoped further work can continue some of the investigations initiated here. Some areas of particular relevance to the design of surface excavations for transportation routes are the following.

a) The shear strength of California rock formations: Methods of testing and interpreting the results of shear tests have been introduced here. It would be helpful now to gather a large number of samples representative of different formations up and down the state and report shear strength characteristics -- peak and residual strength versus normal pressure relationships for intermediate rocks of different ages and types. We should also evaluate Barton's shear strength relationship.

b) Swelling of California mudstones and related rocks: The radial permeability test has particular promise for evaluating swelling characteristics of rocks. This potential of the radial permeability test was not investigated here but the equipment for the swelling measurement was assembled and is now available. A comprehensive series of tests should be performed to develop this technique for routine investigation. Also, the relationship between the occurrence of swelling clay-rocks and highway cut failures should be determined by a program of sampling and testing.

c) Terrestrial photogrammetric mapping of geology in cuts and exposures: The geologic map of figure 5.1a was made using the photograph of figure 5.1b and another similar photograph. It is often difficult to make goelogical maps of cuts, because of inaccessibility, steepness, and lack of planimetrical topographic control. The photogrammetric technique uses a hand held camera and/or requires

ClibPDF - www.fastio.com

a set up and control procedure of less than an hour duration. Thereafter, the map can be made in the convenience of the office. The procedure can be improved and a field instrument can be developed, including a Polaroid camera back, so that photo-interpretation of the geological features can be completed in the field. This is a promising development for the transportation geologist, because it will allow him to document geology as it is momentarily uncovered, during construction operations.

d) Involvement of rock mechanics investigator in a current design problem: The fastest way to advance the design procedures with respect to rock mechanics and geological input is to create real need through a current design problem. Field study, sampling, testing, and measurement will provide the complete case record by which the ideas introduced here can be weaved into practical engineering work.

ClibPDF - www.fastio.com

APPENDIX 1

GEOLOGICAL LOGS OF BORINGS

ClibPDF - www.fastio.com

Location: Vicinity of Sheridan Road, Alameda County - Site 1
Borehole: 1

LOG OF MATERIAL

Depth

0
1 No recovery
2
3 Light brown mudstone. Very soft, becoming slightly stronger with depth;
4 contains small (3/16" dia.), rounded clasts of light brown silty shale
5 which are less weathered portions of the matrix material.
6
7
8 No recovery
9
10 Light, greyish-brown slilty shale. Laminations dip about 30°; fractures
11 oriented perpendicular and subparallel to laminations; dark brown stains
12 on fracture planes; weakly cemented, can be broken down to a powder by
13 rubbing between fingers.
14
15
16 Dark, brownish-grey shale. No apparent laminations; fractured with dark
17 brown stains on fracture planes; blocky and conchoidal fracturing
18 Medium brown shale. Core samples consist of rounded to subangular aggre-
19 gates up to 1 inch diameter; easily broken, by rubbing with fingers, to
20 small, platy chips less than 1/16 inch long.
21 Dark, brownish grey shale. Laminations dip about 30 degrees; moderately
22 hard; core lengths about 6 inches; moderately fractured; yellowish-brown
23 stains along the fracture planes are slightly calcareous; fissile.
24
25
26
27
28
29
30
31
32 Dark grey shale. Faintly laminated; hard; occasional randomly oriented.
33 Fractures; reddish-brown alteration to 1mm thick, along some fracture
34 planes while silica coatings occur along others.
35 Bottom of hole

ClibPDF - www.fastio.com

Location: Franklin Canyon, Contra Costa County - Site 2
Borehole: 2

LOG OF MATERIAL

Depth

0
1
2
3
4
5
6 Yellowish-brown, massive siltstone. Highly altered but still moderately well cemented.
7 Light yellowish-grey, silty clay. Soft; pulls apart easily, revealing
8 slickensided shear fractures dipping about 15 degrees.
9
10 Yellowish-brown, massive siltstone. Very fine-grained, well sorted, subangular
11 to subrounded clear quartz grains comprising about 55-60% of the rock; feld-
12 spar altered to yellowish-brown clay, about 30-35% of the rock; very fine-
13 grained, subrounded ferromagnesium and minor accessory minerals the balance
14 moderately well cemented, cementing agent not calcerous;
15
16 Yellowish-brown, massive siltsone. Soft, subangular to subrounded pieces.
17 up to 1 1/2" diameter; poorly cemented; breaks down easily to a silty powder.
18
19
20
21
22
23
24
25 Light, yellowish-brown to dark grey clayey shale. Highly weathered; the
26 clayey parts are yellowish-brown and the more competent portions dark grey;
27 Slickensided fracture planes dip about 30°; the sample pulls apart easily along fracture planes; dessication cracks develop upon drying.
28 Bottom of hole.

ClibPDF - www.fastio.com

Location: Franklin Canyon, Contra Costa County - Site 2
Borehole: 3

LOG OF MATERIAL

Depth	
0	
1	No recovery
2	
3	
4	Light yellowish brown, very fine-grained, massive, silty sandstone.
5	Very fine-grained, subangular to subrounded, clear quartz grains comprising
6	60-65% of the rock, very fine-grained feldspar altered to light yellowish-
7	brown clay 25-30% of the rock; and ferromagnesium and minor accessory minerals
8	about 12%; moderately hard,
9	cores up to six inches long.
10	
11	
12	
13	
14	
15	
16	
17	
18	
19	
20	
21	Bottom of hole

ClibPDF - www.fastio.com

Location: East End of Caldecott Tunnel, Contra Costa County
Site 3
Borehole: 4

LOG OF MATERIAL

Depth

0
1 No recovery.
2
3
4 Reddish-brown claystone. Contains light grey, subrounded, siltstone
5 clasts up to 3/8" diameter; recovery ranges from soft, clayey aggregates
6 about 3/4" diameter to moderately hard, intact cores 10" long (most
7 cores are 3-4" long); clayey portions
8 are slightly cohesive.
9
10 Nearly vertical contact, dipping about 85°, between a reddish
11 brown claystone (top unit) and a grey, moderately hard, friable
12 shale. The brown claystone contains small, subrounded siltstone
13 clasts.
14 Same as for 4' to 10'.
15
16
17
18
19
20
21
22
23 Same as above except that it is highly weathered. Soft, like a
24 dense, moist clay; parting parallel and perpendicular to the
25 core axis-may have been caused by the coring.
26 Same as for 4' to 10' except recovery consists of angular chips
27 to 1" diameter.
28 Chocolate brown claystone. Moist; occasional, random fractures;
29 no apparent mineralization along fracture planes; intact cores
30 up to 12" long.
31 Same as above except recovery consists of angular piece.
22 to 1 1/2" in diameter.
33 Bottom of hole.

ClibPDF - www.fastio.com

Appendix 2.1

Curves of Borehole Jack (NX Jack) Test Results

ClibPDF - www.fastio.com

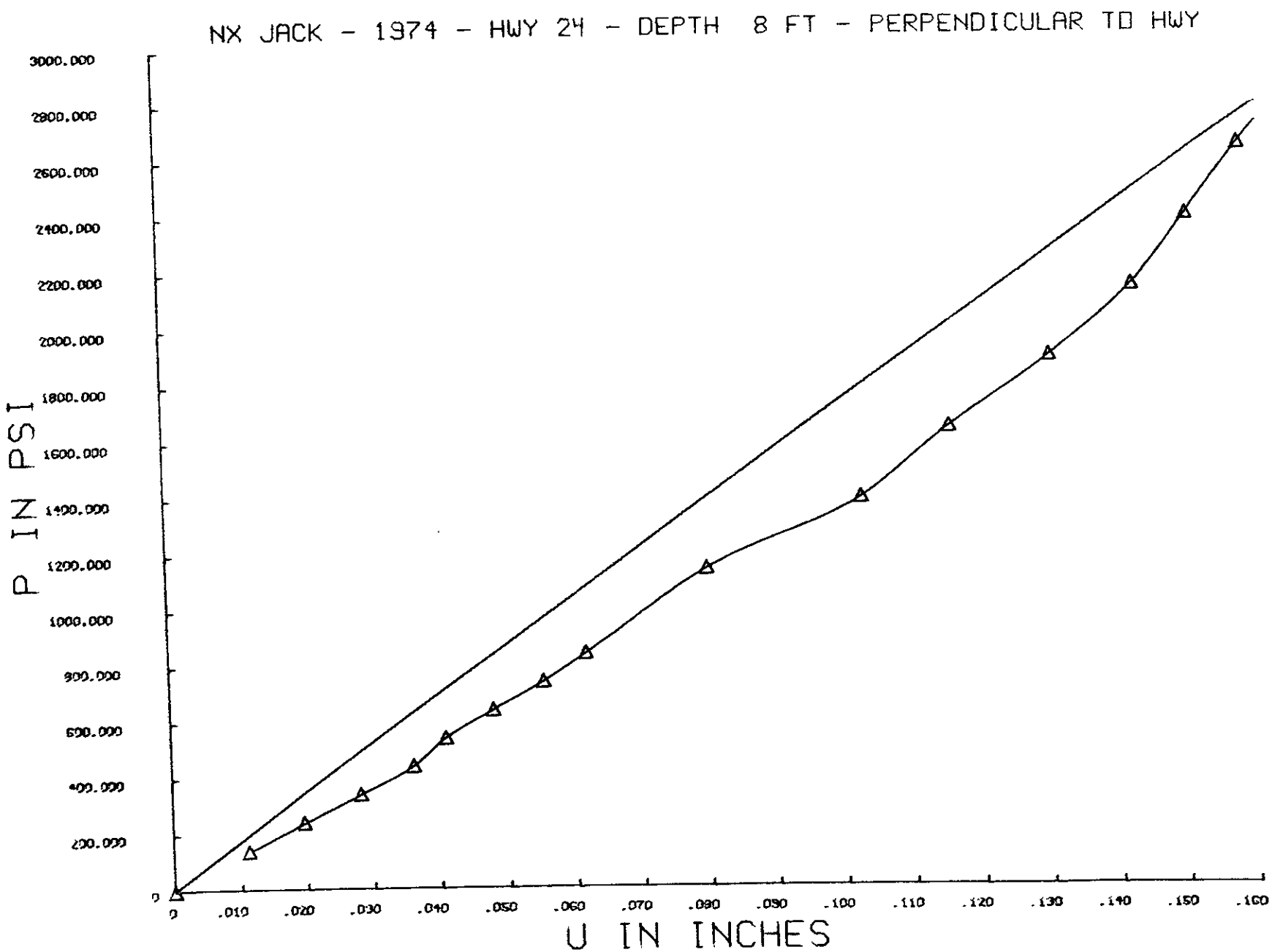

ClibPDF - www.fastio.com

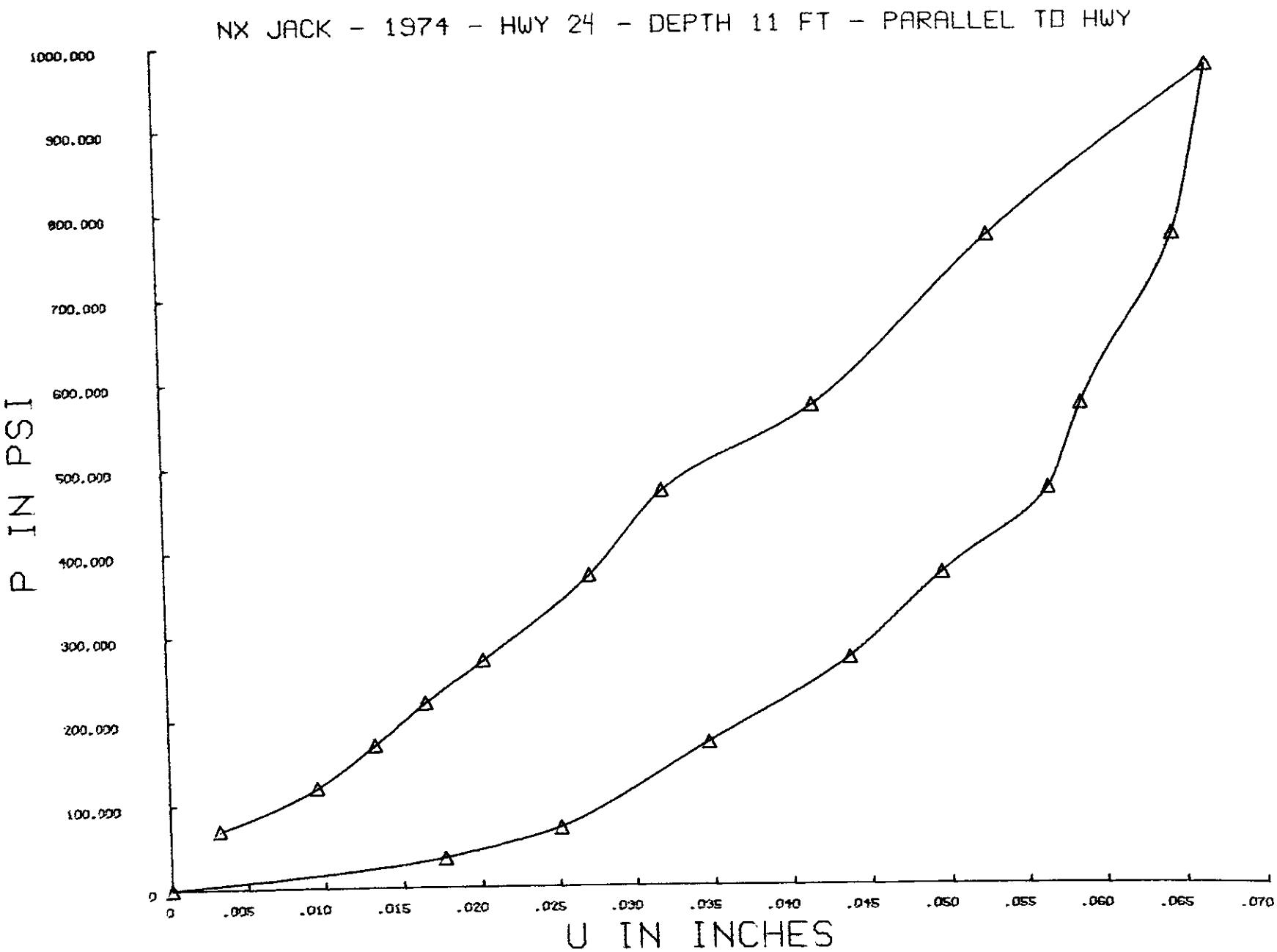

ClibPDF - www.fastio.com

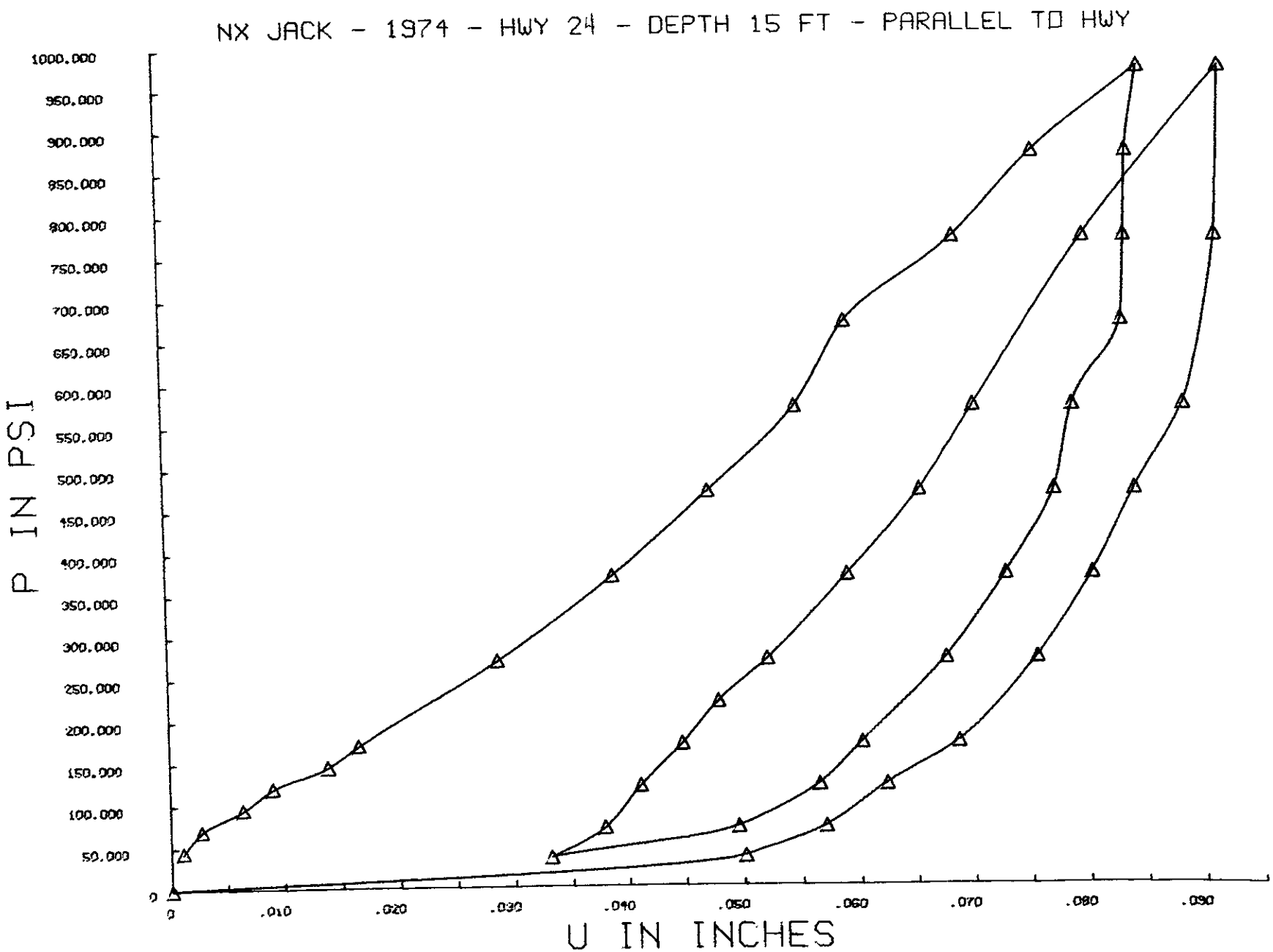

ClibPDF - www.fastio.com

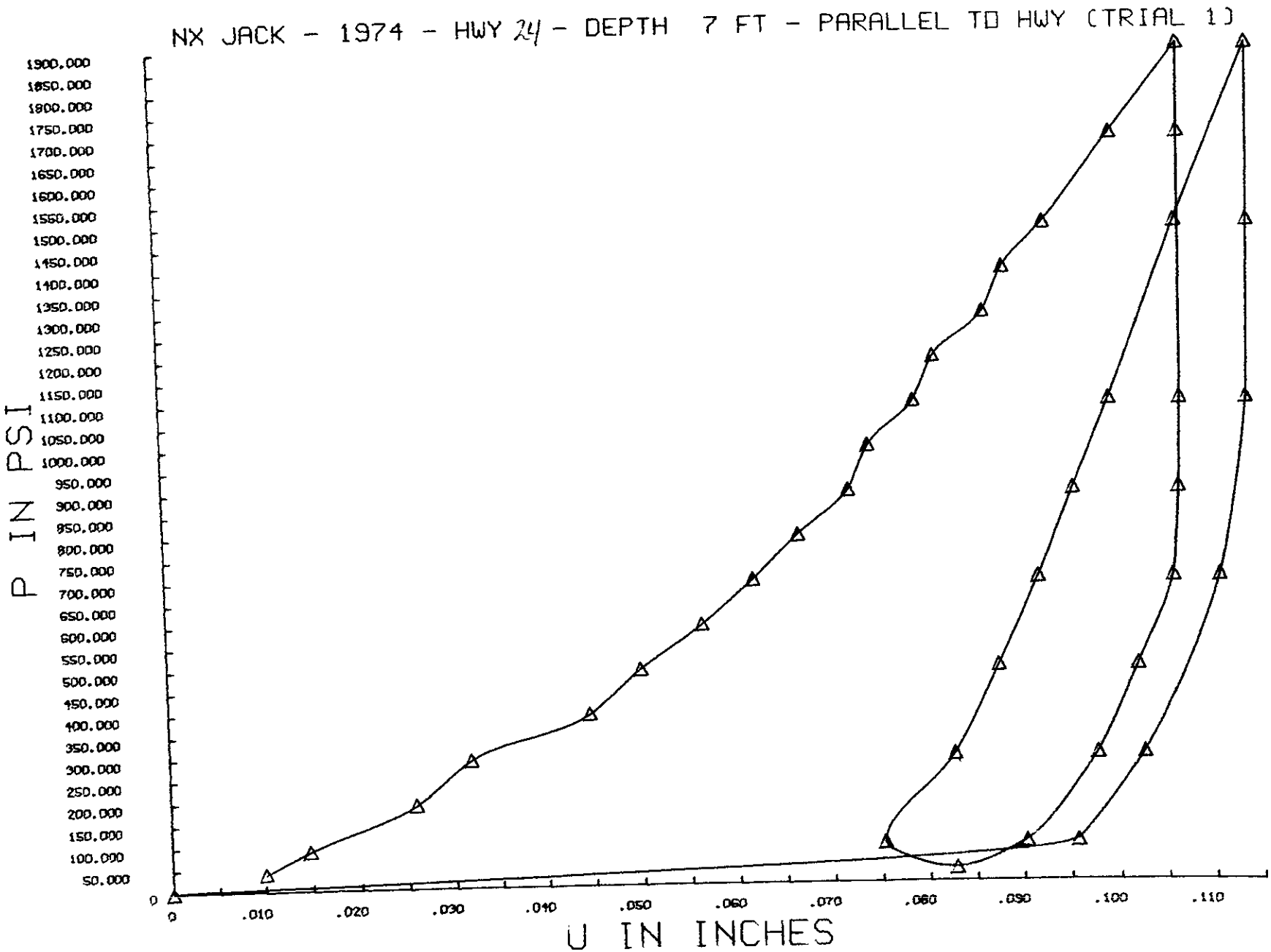

ClibPDF - www.fastio.com

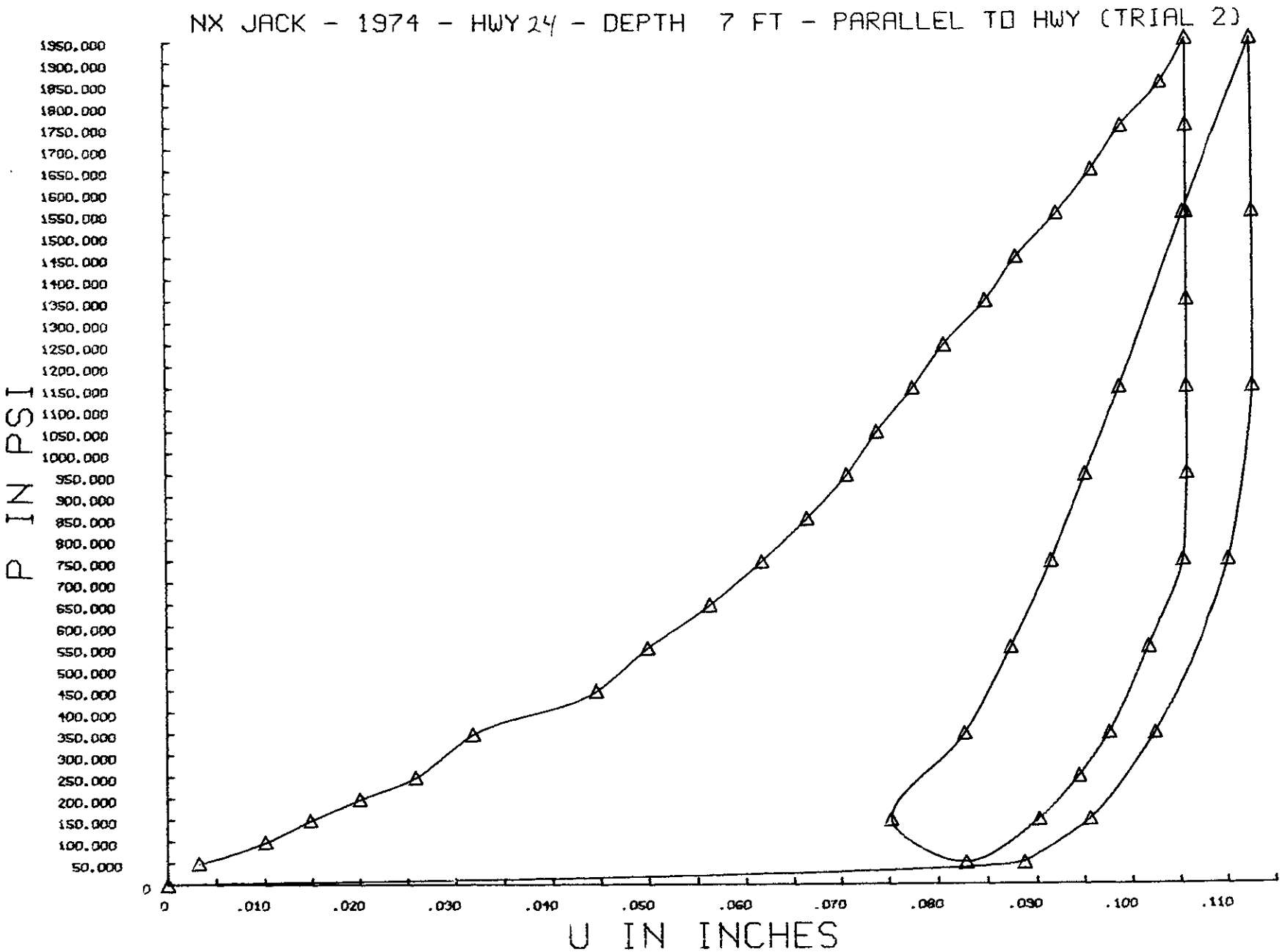

ClibPDF - www.fastio.com

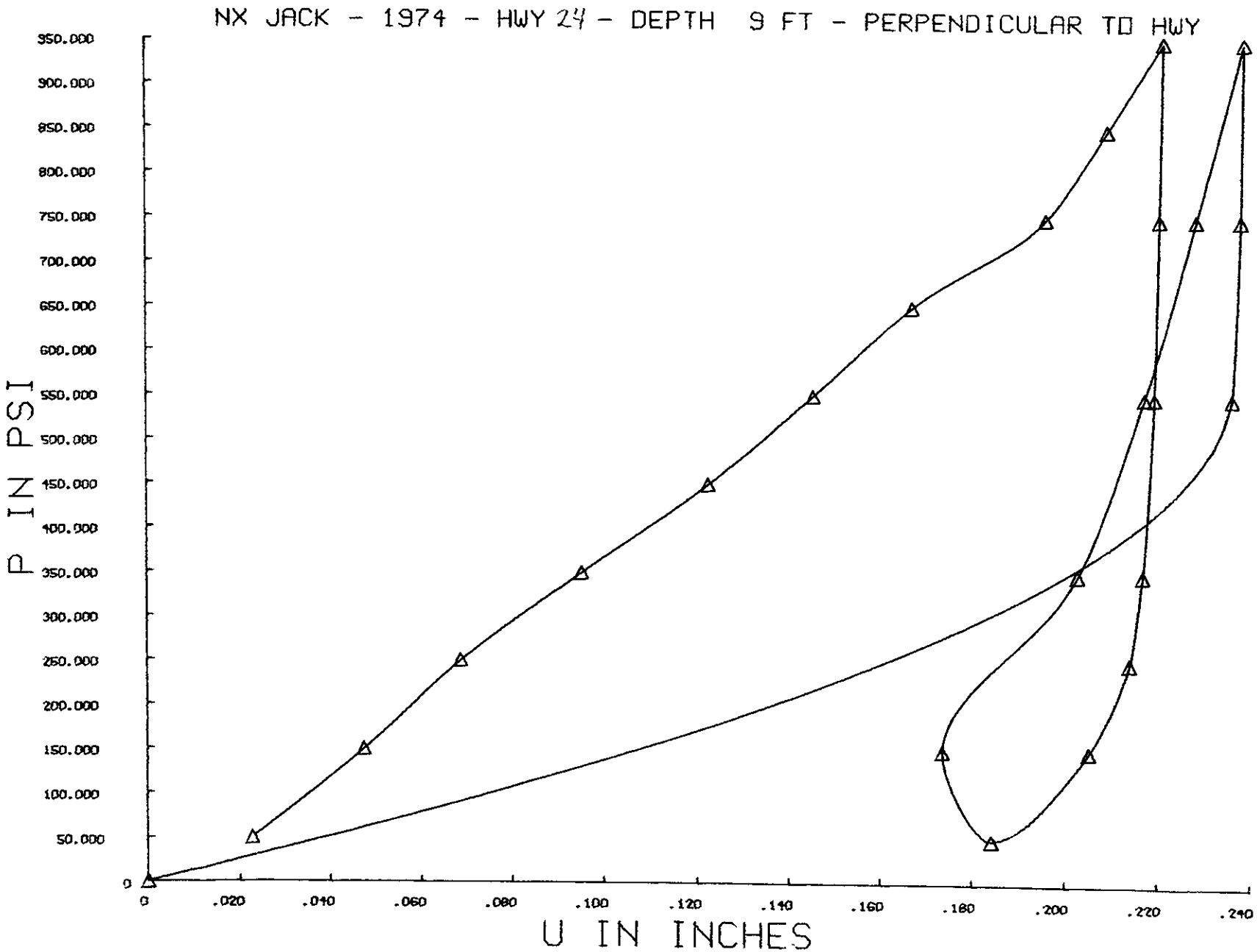

ClibPDF - www.fastio.com

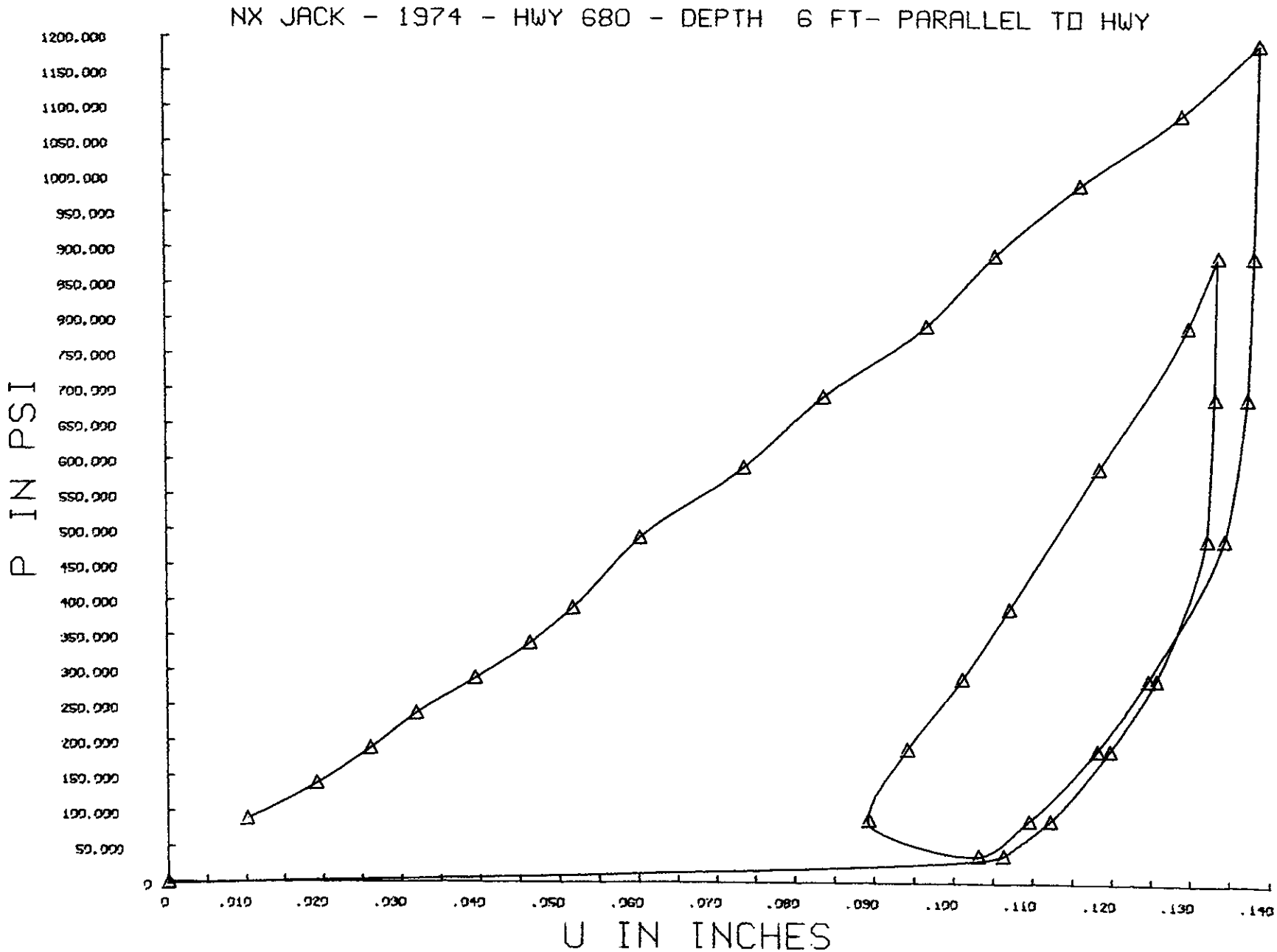

ClibPDF - www.fastio.com

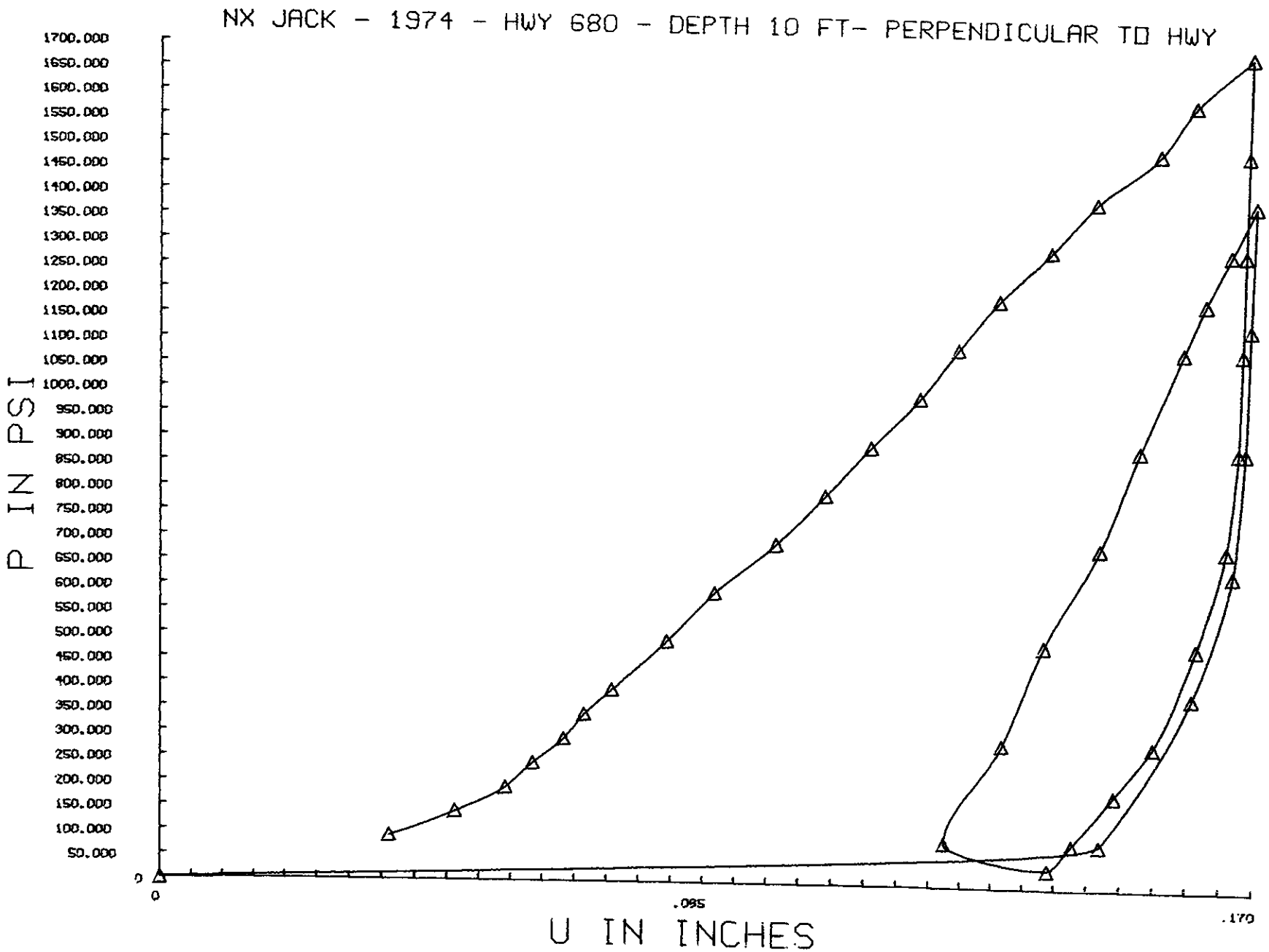

ClibPDF - www.fastio.com

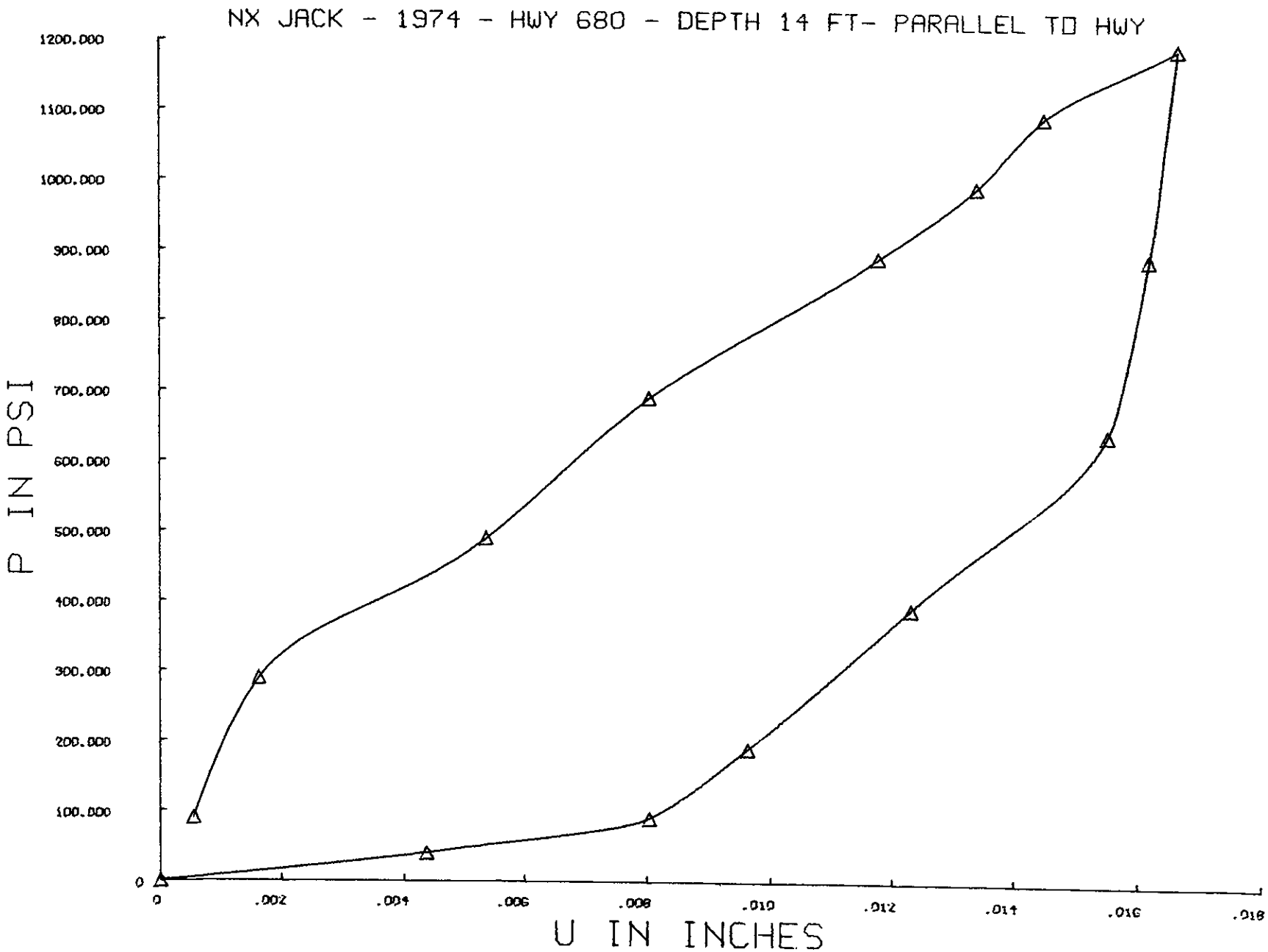

ClibPDF - www.fastio.com

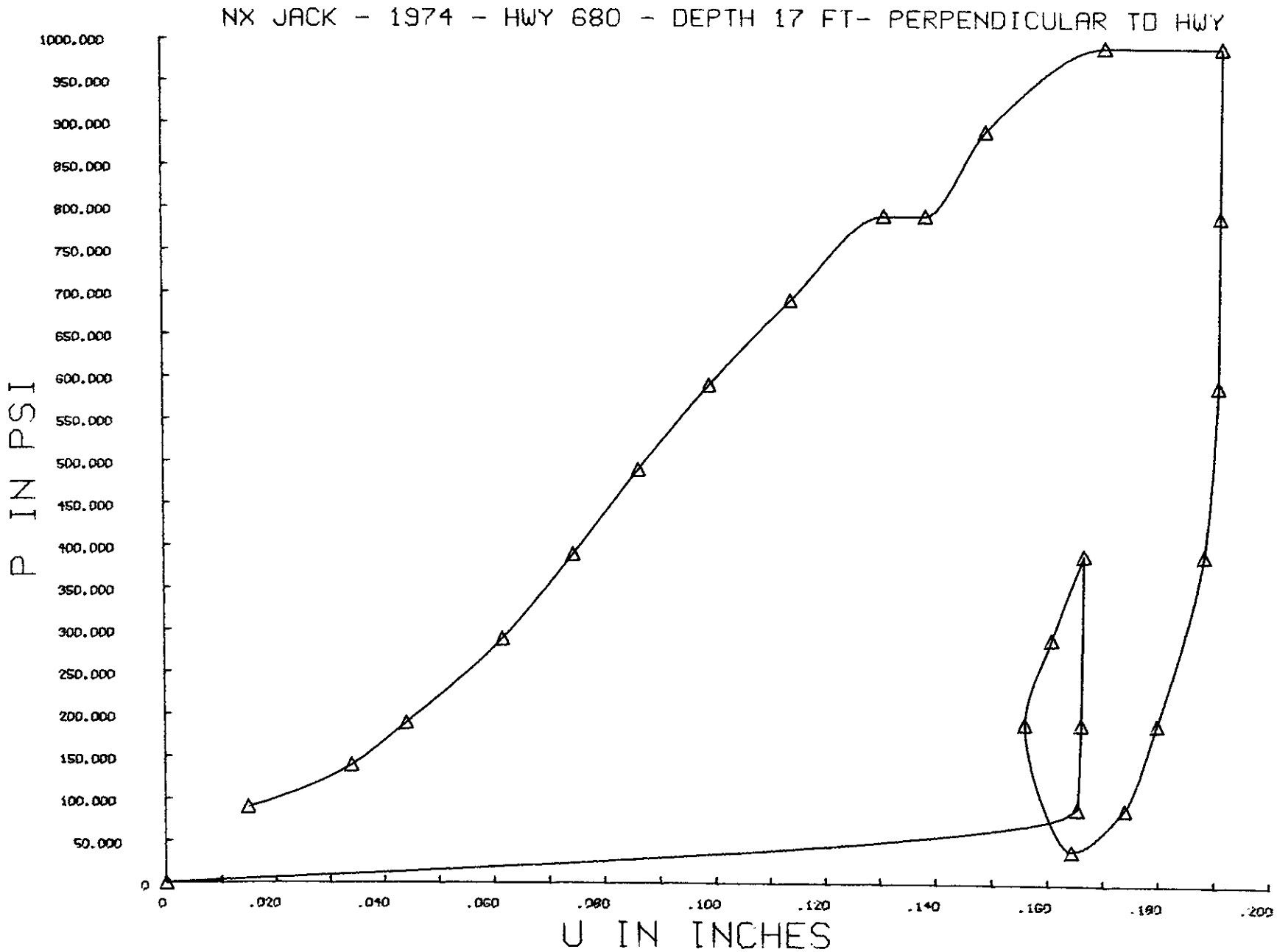

ClibPDF - www.fastio.com

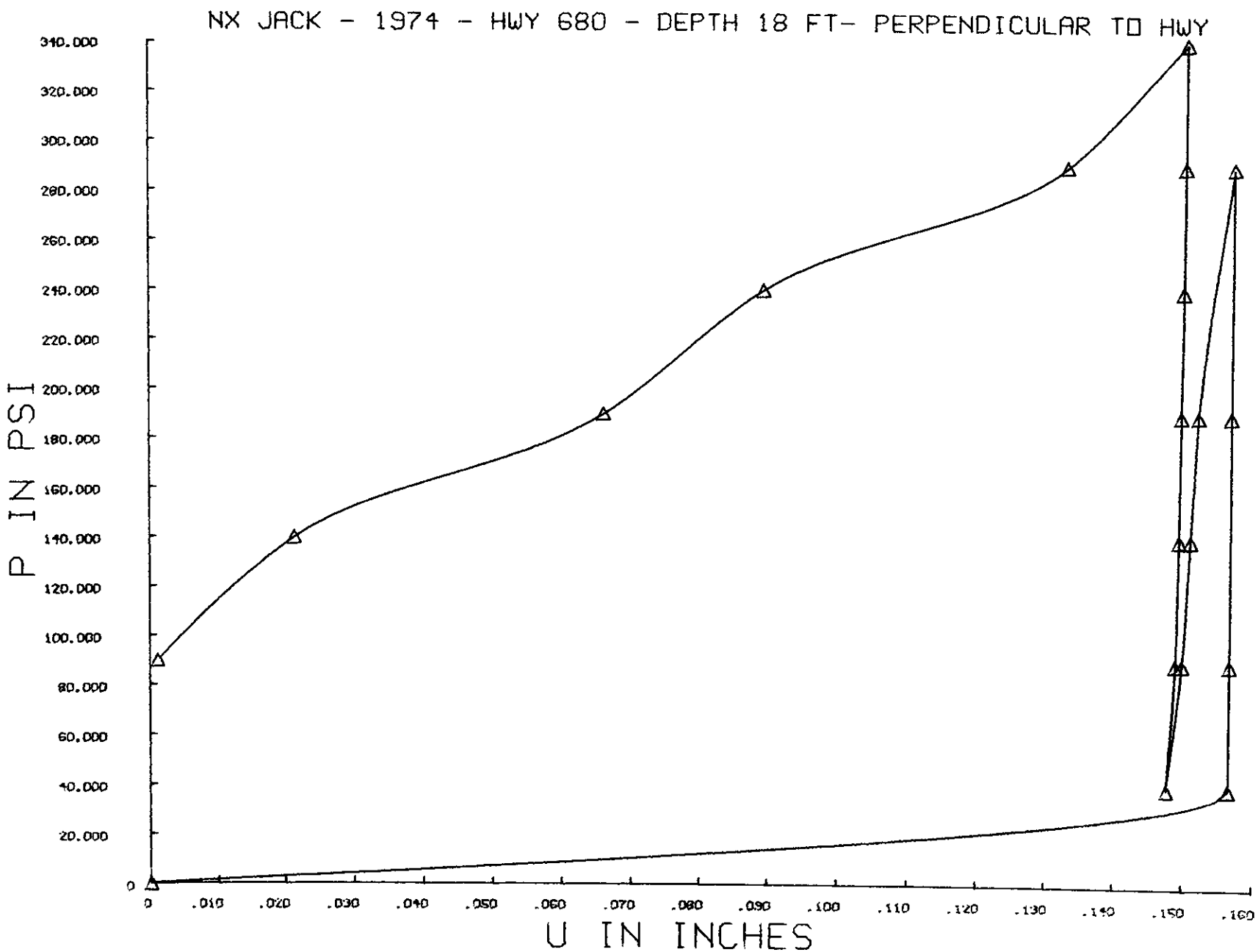

ClibPDF - www.fastio.com

Appendix 2.2

Computer Program for NX-Jack Test Analysis, and a Typical Output, Including a Printer Plot.

ClibPDF - www.fastio.com

```
      PROGRAM NXJACK (INPUT,OUTPUT,TAPE99)
      COMMON UTOT(100),PRESS(100),NREAD,UMAX,PMAX,LINE(8)
      INTEGER WORD(2),WORD1
      DIMENSION SRVA(100),SRVB(100),EMOD(100),UA(100),UB(100),UAV(100),
     1PRHYD(100)
C
C SET UP TO ANALYZE SEVERAL TESTS. EACH TEST DATA DECK STARTS WITH A
C START CARD, BEFORE THE TITLE CARD. THE LAST CARD IN THE DECK IS A
C STOP CARD
C THE TITLE MUST FIT IN THE FIRST 70 COLUMNS.
C
      DATA WORD /6HSTART ,6HSTOP  /
    6 READ 100,WORD1
      IF (WORD1.EQ.WORD(1)) GO TO 7
      IF (WORD1.EQ.WORD(2)) STOP
      GO TO 6
    7 READ 101,LINE
      PRINT 102
      PRINT 104,LINE
      LINE(8) = 0
C
C NREAD IS THE NUMBER OF READINGS, INCLUDING THE ONE AT ZERO PRESSURE.
C THE SERVO CALIBRATIONS ARE IN 10(-4) IN PER DIVISION.
C HERE NEAR=2.16E-04 AND FAR=4.18E-04
C THE HYDRAULIC EFFICIENCY(HYDEFF)MAY VARY FROM INSTRUMENT TO INSTRUMENT
C IT IS THE RATIO OF AVERAGE PRESSURE UNDER THE PLATE TO THE PRESSURE
C IN THE HYDRAULIC LINE.
C
      READ 108,NREAD,CALIBA,CALIBB,PMAX,HYDEFF
      READ 103,(PRHYD(I),SRVA(I),SRVB(I),I=1,NREAD)
      DO 300 I=1,NREAD
      UA(I) = 0.0
      UB(I) = 0.0
      UAV(I) = 0.0
      EMOD(I) = 0.0
      UTOT(I) = 0.0
      PRESS(I) = 0.0
  300 CONTINUE
C
C PMAX IS THE HIGHEST HYDRAULIC PRESSURE USED IN THE JACKING TEST
C READINGS OF THE SERVO INDICATORS SHALL BE INPUT AS FLOATING POINTS.
C THE INITIAL READINGS UPON CONTACT AT ZERO PRESSURE SHALL BE INCLUDED.
C DATA REDUCTION IS MADE BY ASSUMING PLANE STRAIN CONDITION UNDER THE
C PLATE. WITH BETA=45 DEGREES, AND NU=0.25, THEN K(NU,BETA)=1.630.
C THIS INCLUDES THE EFFECT OF CRACKING AND STRESS REDISTRIBUTION.
C THE COMPLETE FORMULA IS EMOD = K*HYDEFF*PRHYD*D/UAV
C THE HOLE DIAMETER IS 3 INCHES. THE DIAMETRAL DEFORMATION IS COMPUTED
C AS THE AVERAGE OF TWO SERVO READINGS.
C UA = SRVA*CALIBA , AND UB = SRVB*CALIBB.
C THEN, UAV = (UA+UB)/2.0 AND EMOD = 4.89*HYDEFF*PRHYD/UAV
C
      J= NREAD-1
      UMAX= 0.
```

ClibPDF - www.fastio.com

```
      SRVAMX=0.0
      SRVBMX=0.0
    2 DO 200 I=1,J
      UA(I) = (SRVA(I+1)-SRVA(I))*CALIBA
      UB(I) = (SRVB(I+1)-SRVB(I))*CALIBB
      UAV(I) = (UA(I)+UB(I))/2.
      EMOD(I) = 4.89*HYDEFF*(PRHYD(I+1)-PRHYD(I))/UAV(I)
      PRESS(I) = PRHYD(I+1)
C
C FIND UMAX
C
      IF(SRVA(I).GT.SRVAMX) SRVAMX=SRVA(I)
      IF (SRVB(I).GT.SRVBMX) SRVBMX=SRVB(I)
  200 CONTINUE
      DELTA = SRVAMX-SRVA(1)
      DELTB = SRVBMX-SRVB(1)
      UMXA = DELTA*CALIBA
      UMXB = DELTB*CALIBB
      UMAX = (UMXA+UMXB)/2.
C
C FIND UTOT(I)
C
      UTOT(1) = UAV(1)
      DO 400 I=2,J
      UTOT(I) = UTOT(I-1)+UAV(I)
  400 CONTINUE
      PRINT 105
      PRINT 106
      PRINT 107,(PRHYD(I),SRVA(I),SRVB(I),UA(I),UB(I),UAV(I),EMOD(I),I=1
     1,NREAD)
C
      CALL PLOT
      GO TO 6
C
  100 FORMAT (A6)
  101 FORMAT (8A10)
  102 FORMAT (1H1)
  103 FORMAT (3F5.0)
  104 FORMAT (//,5X,8A10,//)
  105 FORMAT (//,5X,10HHYDR PRESS,5X,7HSERVO A,5X,7HSERVO B,5X,7HDISPL A
     1,5X,7HDISPL B,9X,3HUAV,5X,13HMOD OF DEFORM)
  106 FORMAT   (8X,5H PSI ,7X,7HREADING,5X,7HREADING,6X,4H IN ,8X,4H IN
     1,10X,4H  IN,9X,3HPSI,//)
  107 FORMAT(5X,F10.0,7X,F5.0,7X,F5.0,1PE12.1,2E12.1,E15.1,0P,/)
  108 FORMAT (I5,2E10.2,F10.0,F5.0)
      END
```

ClibPDF - www.fastio.com

```
      SUBROUTINE PLOT
      COMMON UTOT(100),PRESS(100),NREAD,UMAX,PMAX,LINE(8)
      DIMENSION SPECS(30),BUFX(500),BUFY(500),GIVEN(3)
C
C SET UP SPECS ARRAY
C SET XDIST,YDIST
      SPECS(1) = 1.5
      SPECS(2) = 1.0
C SET UP THE GIVEN ARRAY FOR FABLIX
      GIVEN(1) =  UMAX
      GIVEN(2) = 0.0
      GIVEN(3) = NREAD-1.0
C FABLIX THEN COMPUTES SPECS(3), SPECS(4), SPECS(9)
C SET XLENGTH, YLENGTH
      SPECS(7) = 8.0
      SPECS(8) = 6.0
C SPECIFY TOOL
      SPECS(11) = 1.0
C SPECIFY INTERMEDIATE FILE NUMBER
      SPECS(12) = 99.0
C POINTS WILL BE SPECIFIED LATER
C SET XSKIPS, YSKIPS
      SPECS(14) = 1.0
      SPECS(15) = 1.0
C SPECIFY POINTS
      SPECS(13) = NREAD
C FABLIX FINDS A NICE SCALE RANGE
      CALL FABLIX (GIVEN,SPECS)
C RESET THE GIVEN ARRAY FOR FABLIY
      GIVEN(1) = PMAX
      GIVEN(2) = 0.0
      CALL FABLIY (GIVEN,SPECS)
C FABLIY COMPUTES SPECS(5), SPECS(6), SPECS(10)
C SPECIFY THE SYMBOL NUMBER
      SPECS(16) = 1.0
C SPECIFY CHARACTER SIZE, ROTATION AND FONT TYPE
      SPECS(17) = 0.1
      SPECS(18) = 0.1
      SPECS(19) = 0.0
      SPECS(20) = 0.0
      SPECS(21) = 2.0
C SPECIFY THE NUMBER OF DECIMAL PLACES
      SPECS(28) = 3.0
C INITIALIZE THE ZONE VALUES
      SPECS(24) = 0.05
      SPECS(25) = 0.05
      SPECS(26) = 0.05
C NODLIB AND NODLIL NUMBER THE X AND Y AXES RESPECTIVELY
      CALL NODLIB(SPECS)
      CALL NODLIL(SPECS)
C AXLILI DRAWS AN AXIS PAIR WITH TICK MARKS
      CALL AXLILI(SPECS)
C PSLILI PLOTS A SYMBOL AT EACH DATA POINT
```

ClibPDF - www.fastio.com

```
      CALL PSLILI (UTOT,PRESS,SPECS)
C PFLILI DRAWS A SMOOTH CURVE THROUGH THE DATA POINTS
      CALL PFLILI (UTOT,PRESS,BUFX,BUFY,SPECS)
C RESET THE CHARACTER SIZE FOR LEFT AND BOTTOM TITLES
      SPECS(17) = 0.2
      SPECS(18) = 0.2
C TITLEB CONSTRUCTS A BOTTOM CENTERED TITLE
      CALL TITLEB (11HU IN INCHES,SPECS)
C TITLEL CONSTRUCTS A LEFT CENTERED TITLE
      CALL TITLEL (8HP IN PSI,SPECS)
C RESET THE CHARACTER SIZE FOR THE TOP CENTERED TITLE
      SPECS(17) = 0.12
      SPECS(18) = 0.12
C TILTET CONSTRUCTS A TOP CENTERED TITLE
      CALL TITLET (LINE,SPECS)
C
      CALL GDSEND(SPECS)
      RETURN
      END
```

ClibPDF - www.fastio.com

TYP[illegible] OOT

MX JACK - 1974 - MAY 27 - DEPTH 6 FT - PARALLEL TO HWY

HYDR PRESS PSI	SERVO A READING	SERVO B READING	DISPL A IN	DISPL B IN	DAV IN	MOD OF DEFORM PSI
30.	0.	0.	6.5E-03	0.	3.2E-03	8.[illegible]E+03
40.	30.	0.	3.2E-03	2.1E-03	2.7E-03	1.0E+04
50.	40.	5.	3.2E-03	0.	1.6E-03	3.3E+04
70.	60.	5.	2.2E-03	0.	1.1E-03	5.0E+04
90.	70.	5.	3.2E-03	4.2E-03	3.7E-03	1.4E+04
110.	85.	15.	1.1E-03	0.	5.4E-04	1.0E+05
130.	90.	15.	2.2E-03	2.1E-03	2.1E-03	5.1E+04
170.	100.	20.	6.5E-03	8.4E-03	7.4E-03	3.6E+04
270.	130.	40.	7.6E-03	6.3E-03	6.9E-03	3.9E+04
370.	165.	55.	4.3E-03	4.2E-03	4.2E-03	6.3E+04
470.	185.	65.	9.7E-03	6.3E-03	8.0E-03	3.4E+04
570.	230.	80.	7.6E-03	6.3E-03	6.9E-03	3.9E+04
670.	265.	95.	7.6E-03	4.2E-03	5.9E-03	4.6E+04
770.	300.	105.	6.5E-03	4.2E-03	5.3E-03	5.0E+04
870.	330.	115.	8.6E-03	8.4E-03	8.5E-03	3.2E+04
970.	370.	135.	-2.2E-04	0.	-1.1E-04	2.5E+06
870.	369.	135.	-8.6E-04	0.	-4.3E-04	6.2E+05
770.	365.	135.	-3.2E-03	-2.1E-03	-2.7E-03	1.0E+05
670.	350.	130.	-4.3E-03	0.	-2.2E-03	1.2E+05
570.	330.	130.	-5.4E-03	-2.1E-03	-3.7E-03	7.2E+04
470.	305.	125.	-5.4E-03	-2.1E-03	-3.7E-03	7.2E+04
370.	280.	120.	-5.4E-03	-4.2E-03	-4.8E-03	5.6E+04

ClibPDF - www.fastio.com

270.	245.	110.	-8.5E-03	-6.2E-03	-7.5E-03	3.5E+04
170.	215.	95.	-7.5E-03	-6.3E-03	-6.9E-03	3.9E+04
70.	180.	80.	-6.5E-03	-4.2E-03	-5.3E-03	1.3E+04
35.	150.	70.	5.4E-02	-6.3E-03	-4.4E-04	-8.3E+03
170.	175.	55.	1.4E-02	8.4E-03	1.1E-02	4.3E+04
370.	240.	75.	1.2E-02	1.0E-02	1.1E-02	4.8E+04
570.	285.	100.	1.1E-02	6.3E-03	8.5E-03	6.2E+04
770.	345.	115.	1.1E-02	1.0E-02	1.1E-02	5.1E+04
970.	395.	140.	-1.1E-02	0.	-5.4E-03	2.0E+05
570.	345.	140.	-2.5E-02	-1.7E-02	-2.1E-02	5.2E+04
170.	230.	100.	-8.6E-03	-6.3E-03	-7.5E-03	3.6E+04
70.	190.	85.	0.	0.	0.	0.

ClibPDF - www.fastio.com

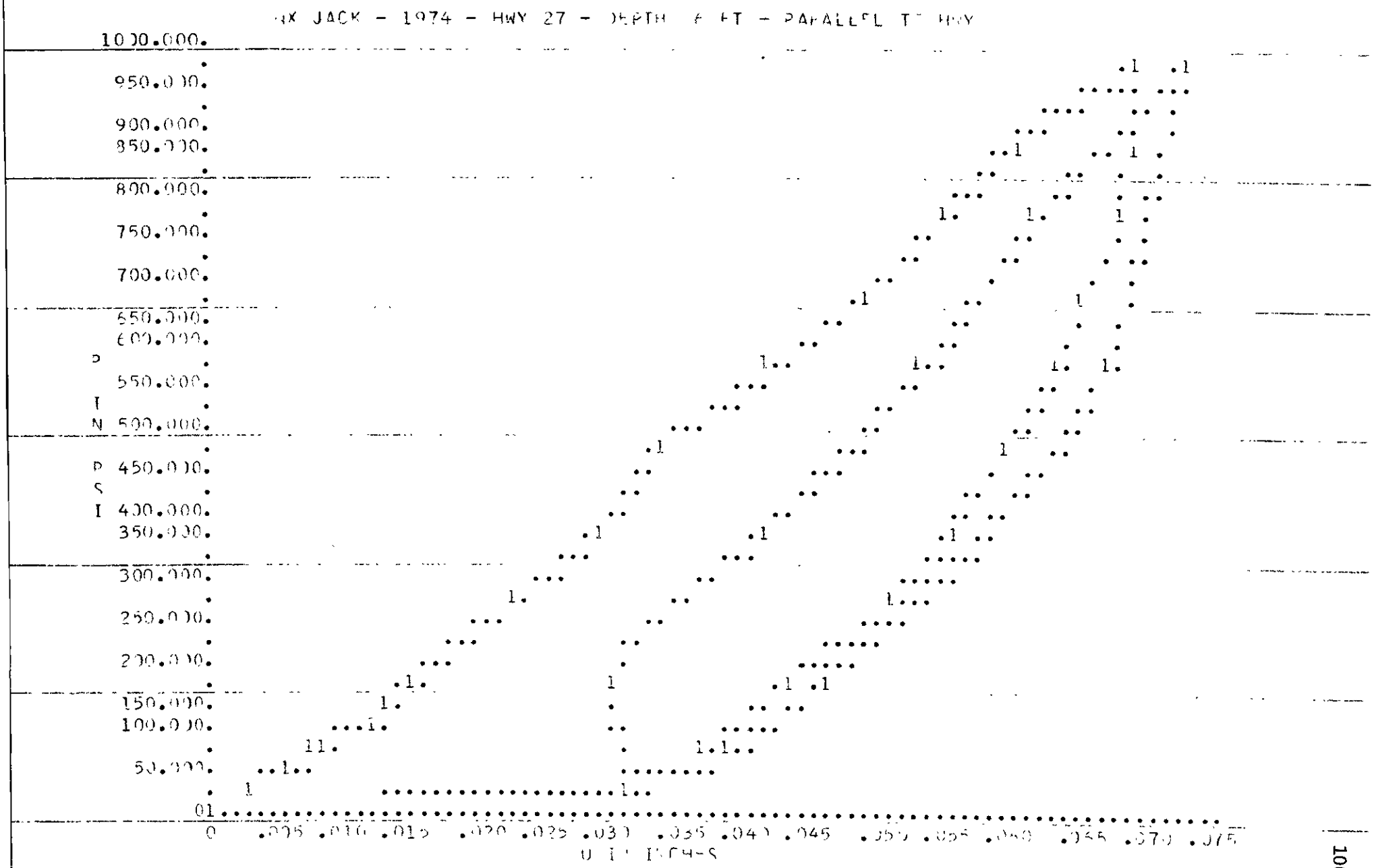

ClibPDF - www.fastio.com

Appendix 3

Detailed Procedures for Radial Permeability Tests

ClibPDF - www.fastio.com

Appendix 3: DETAILED PROCEDURES FOR RADIAL PERMEABILITY TEST

a) Sample Preparation: Test specimens are prepared from NX-sized cores. The core is cut to the desired length using a diamond rotary saw blade. Soft samples that are sensitive to lubricants used with diamond tipped blades can usually be cut using a hacksaw or, for very clayey samples a razor blade. Samples should be cut to a standardized length and care must be taken to assure that the ends are smooth and coplanar. This is necessary to insure a uniform loading of the sample and establish a standardized flow pattern. If the sample ends are not in full contact with the load cell the sample will not be uniformly loading and flow may occur through its ends. Both conditions will affect the flow path and rate, producing results that cannot be properly interpreted. If the cut ends are not coplanar they can be ground until parallel using lapidary equipment or they can be capped with sulfur or hydrostone. Sulfur capping is advantageous in that it is quick and the needed apparatus is cheaper than the lapidary equipment. When working with intermediate quality rocks sulfur capping has the added advantage of keeping the ends intact and, when properly prepared, will only ovver the sides of each end by about 0.06 inches. The capped ends are seldom exactly coplanar but the deviation is so slight that it can be compensated for by the use of thin, impermeable rubber pads at both the top and bottom ends. Since the top plate of the permeameter is secured by the use of three cap nuts, it can be tightened in a manner that will take it coplanar with the upper surface of the sample.

After preparing the end pieces an axial hole 0.375 inches in diameter is drilled through all but the bottom 0.75 inches of the sample. It is generally best to secure the sample before drilling. The method used during the project consists of placing the sample in a collar that can be tightened to prevent the sample from rotating. The collar assembly is then secured to the drill press table by clamping it in a vise that has been bolted to the table. It is

ClibPDF - www.fastio.com

aligned so that the hole will be drilled through the center of the sample and parallel to its axis (figure A3.1).

Two types of 0.375 inch drill bits are used. A diamond core drill bit is used to drill into the more competent rocks while a carbide-tipped masonry drill bit is used to drill into soft rocks. The masonry bit is also used where running water (the lubricant used with the diamond core drill) might erode the sample or cause it to swell.

The hole is cleaned out after drilling. This is usually accomplished by inserting a small air hose down the hole. When working with clayey samples it may be necessary to gently run a brush along the hole to dislodge small patches.

The upper 0.75 inches of the hole is sealed, with the remaining portion of the hole connected to the outside through a tube (see figure 3.4 of chapter 3). Place a 1.5 inch piece of 0.25"O.D. copper tubing 0.75 inches down the drilled hole. This is done by flaring one end of the tube and fitting it with a 0.25 inch "O" ring. The flare is used to retain the "O" ring. Place the flared end of the tube and the "O" ring 0.75 inches into the hole.
The "O" ring fits snugly between the tube and sample walls, forming a seal between the two and holding the tube in place. Fill the space between the walls of the sample and tube with epoxy and let stand until hard. The epoxy completely seals the upper 0.75 inches of the sample wall and holds the tube rigidly in place. Devcon's "5 minute" epoxy works well and hardens in less than 10 minutes Care must be taken to insure that the copper tube is perpendicular to the end of the sample.

Problems sometimes arise in obtaining a good bond between the epoxy and rock. This usually occurs when the sample is soft and/or friable and the epoxy cannot form an effective bond with the sample. Should this occur water seepage

ClibPDF - www.fastio.com

may be a secondary problem. During tests where the sample/epoxy bond was unsatisfactory the tube was sucked down the hole, invalidating the test. Problems also arise when working with an oversized hole. This may occur when the hole is drilled with a carbide tipped masonary drill bit. New drill bits used during the project were oversized enough that the "0" rings were too small to make contact with the hole walls.

A second sealing and tube retaining system has been developed to overcome these problems (figure A3.2). The axial hole is drilled using an oversized 0.375 inch carbide tipped masonary drill bit. A 1.5 inch piece of 0.25 inch O.D. copper tubing is fitted with a flared eyelet having a 0.25 inch diameter central hole. The eyelet is fitted so that the flared end is up and the bottom of the retaining washer is 0.75 inches from the bottom end of the tube. The eyelet is then epoxied to the tube, forming a rigid assembly. The retaining washer and then a 0.75 inch piece of 0.25 inch I.D., impermeable, rubber tubing are placed on the bottom portion of the tube. The complete assembly is then inserted into the hole. The assembly fits snugly and must be inserted carefully to avoid damaging the sample. An impermeable rubber gasket, with a centered hole the size of the retaining wash, is placed on top of the sample. It should be slightly thicker than the retaining washer and at least as large as the top of the sample.

The sample is then saturated by submerging it in deaired water and subjecting the two to a vacuum.

b) Test Preparation: The strain indicator is hooked up to the strain gauges and "zeroed." This only needs to be done when axial strain and/or normal load are monitored.

A prepared sample is placed in the permeameter. It is best accomplished using the following procedures. The top plate of the permeameter is inverted and set on a stand. A 0.25 inch "0" ring is placed in the notch in the top

ClibPDF - www.fastio.com

plate's central hole (figure 3.2). The sample is then placed on the top plate, with the tube extending out of its axial hole being inserted into the top plate's central hole. Do not dislodge the "O" ring. The permeameter is lowered over the sample and fitted over the top plate. It should be positioned so that its ends are coplanar with those of the sample. If this cannot be done, remove the permeameter, insert thin, permeable rubber pads, and reposition the permeameter. Remove the complete assembly from the stand, turn it right-side-up, and tighten the cap nuts to provide the desired axial load. When running a simple radial permeability test (no strain measurements) the cap nuts can be tightened "finger tight." The permeameter is then hooked up to the water and drain lines in preparation to run the convergent test.

Air in the permeameter, axial hole in the sample, and water lines is removed by introducing water into the openings. The permeameter and high pressure water line are deaired in one operation. The permeameter air-bleed valve is opened (valve A, figure A3.3). The high pressure water source is pressurized (10 to 20 psi is sufficient). Turning the valve above the high pressure water gauge (valve A in figure 3.1) to "convergent flow" allows the pressurized water to flow through the high pressure water line and into the permeameter. When the permeameter is filled with water, tap it until all air bubbles are dislodged and have escaped through the air bleed-valve, then close the valve.

The axial hole in the sample and the drain line are deaired next. Remove the plug over the central hole in the permeameter's top plate (figure A3.3). Insert a water hose down the hole, to the base of the axial hole in the sample (figure A3.4). With water flowing slowly through the hose, remove the hose slow enough to insure that all air bubbles are removed. Next, fasten the water line to the coupling next to the plug hole (figure A3.3). Open the coupling valve (valve B, figure A3.3). Run water gently through the apparatus and,

ClibPDF - www.fastio.com

when water is flowing out of the central hole, reinsert the plug (put plumber's tape on the plug threads to be sure of a complete seal). Allow water to continue to flow through the tubing that connects the permeameter to the measuring apparatus until all air is removed. Close the coupling valve, turn off the water, and remove the water hose.

The convergent test is ready to run.

c) Test Procedures: The convergent test is run first as there is a greater chance of sample failure during the divergent test since it is subjected to tensional forces.

Convergent test

1. Turn off valves A,B,C (figures 3.1 and A3.6).
2. Pressurize high pressure water source to 25 psi.
3. Turn valve A all the way to the right.
4. If the pipette is hooked up to measure flow, turn valve C (figure 3.1) to the "on" position (figure A3.6a). If the copper tube/graduated cylinder system is used to measure flow, turn valve B (figure 3.1) all the way to the right.
5. Monitor the flow rate. (Note: if flow rate is too slow or fast to monitor properly change the pipette (or beaker) to a more appropriate size).
6. Record the water pressure, flow volume, and time in the data sheet (figure A3.5).
7. Drain the pipette (figure A3.6c) or beaker.
8. Increase the water pressure 25 psi.
9. Repeat steps 4-8 until the maximum water pressure is reached (300 psi for this instrument).
10. Release pressure (bring back to zero). Turn off all valves.

ClibPDF - www.fastio.com

Divergent test

If the rock permeability is large enough to have used the copper tube/ valve system during the convergent test, no preparation is necessary as all the lines are poorly hooked up and deaired. The procedure is the same as for the convergent test except that the low pressure water source is used, pressure increases are in increments of 5 psi, and the valves are turned differently. Start the test with all valves in the off posiiion. Pressurize the low pressure water source to 5 psi. Turn valve B (figure 3.1) all the way to the left. Turn valve A (figure 3.1) all the way to the left. Proceed with the test as outlined for the convergent test, using pressure increments of 5 psi, until the maximum pressure is reached (30 psi for our equipment).

If the pipette was used to measure flow during the convergent test, the lines must be reconnected. The low pressure water source is connected to the permeameter top plate's central opening (figure A3.3) while the pipette is connected to its outer opening (figure A3.3). The lines must be deaired before starting the test. The low pressure line can be deaired by running water through it before connecting it to the permeameter. After the air has been expelled and with the water still flowing, connect the line to the permeameter. If care is taken when disconnecting and reconnecting the tube leading to the pipette, no air will be introduced into the line. As a precaution it is best to start the operation with the pipette full (10 ml pipette is best) and with valve c turned off. Disconnect the tube leading to the pipette. Just before the tube is reconnected to the outer fitting, turn valve c to "on" (figure A3.6a) and allow the water to drain form the pipette while the fitting is secured. Do not allow the pipette to drain completely as air will become trapped in neck of the valve and will be hard to dislodge. After the lines have been reconnected and deaired the divergent test can be run as previously outlined.

ClibPDF - www.fastio.com

The sample's permeability for each pressure level p is calculated after the test, using the formula:

$$k = \frac{Q}{2\pi\ell p} \text{Ln} \frac{R_2}{R_1}$$ After Bernaix (1969).

where:

Q = flow rate in cm^3/sec.

ℓ = sample length over which radial flow occurs, in cm.

p = percolation head (pressure head), in cm.

R_2 = core radius, in cm.

R_1 = axial hole radius, in cm.

k = permeability, in cm/sec.

Note: 1 psi corresponds to the pressure of 2.307 feet of water or 70.317 cm of water.

Table 3.1 (in Chapter 3) shows a typical data sheet, and the variation of permeability with pressure for the selected test. Sample calculations are given in table A3.1.

ClibPDF - www.fastio.com

TABLE A3.1

SAMPLE CALCULATIONS

1) Test sample dimensions $\ell = L - 2L_1 = 11.11 \text{ cm} - 2(1.91 \text{ cm}) = 7.30 \text{ cm}$

$R_2 = 2.51 \text{ cm}$

$R_1 = 0.48 \text{ cm}$

2) a) $k = \frac{q}{2\pi\ell P} \text{Ln} \frac{R_2}{R_1}$

since $q = Q/T$,

$k = \frac{Q}{2\pi\ell PT} \text{Ln} \frac{R_2}{R_1}$

b) for the water pressure at 30 psi (convergent test),

$P = (30 \text{ psi})\ (70.317 \text{ cm/psi}) = 2109.2 \text{ cm}$

$Q = 100 \text{ cm}$

$T = 516.8 \text{ sec}$

and $k_{30} = \frac{Q}{2\pi\ell PT} \text{Ln} \frac{R_2}{R_1} = \frac{100}{2\pi(7.30)(2109.2)(516.8)} \text{Ln} \frac{2.51}{.48} =$

$= 3.30 \times 10^{-6} \text{ cm/sec}$

ClibPDF - www.fastio.com

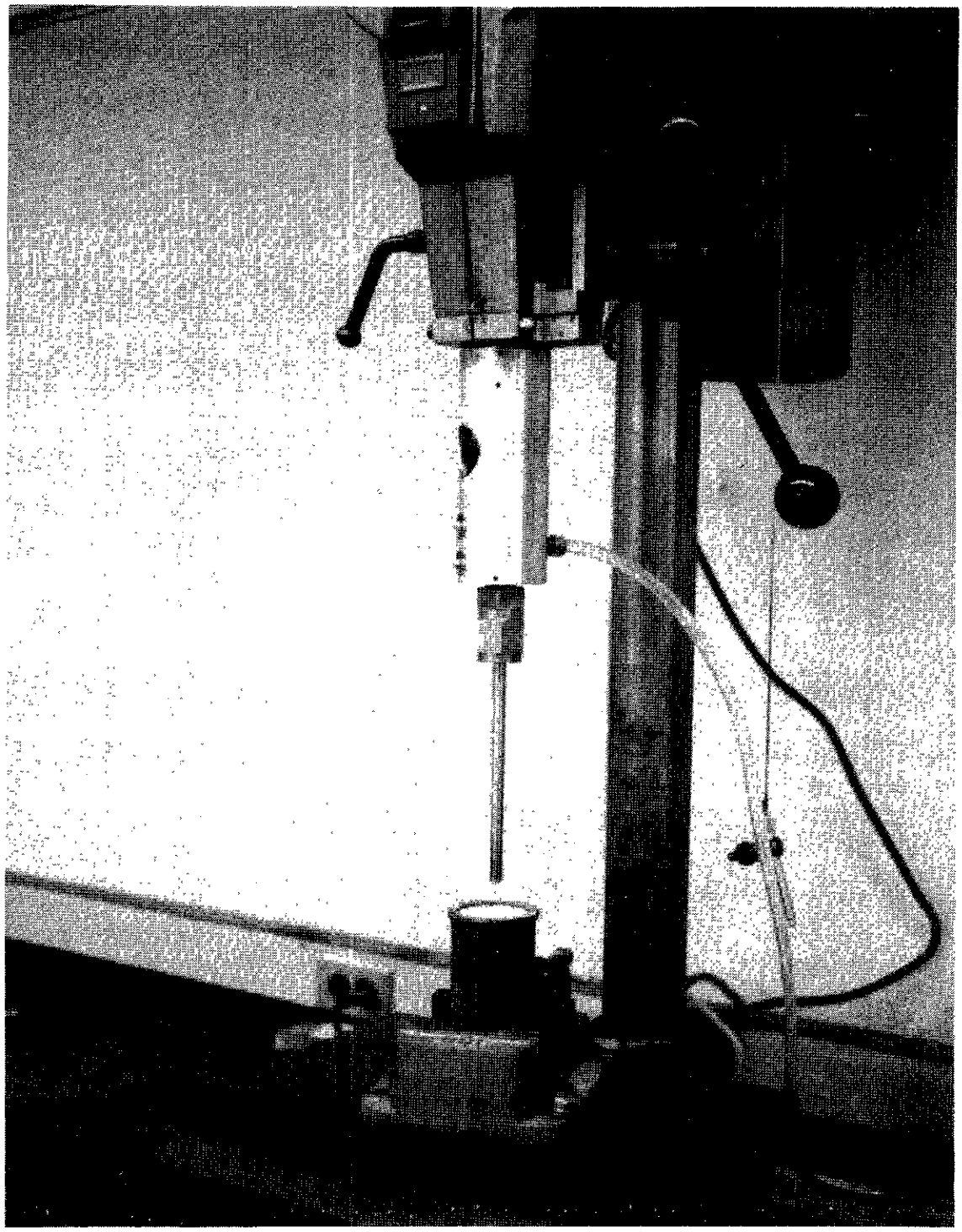

Figure A3.1 Drill Press Set Up Used to Drill the Axial Hole.

ClibPDF - www.fastio.com

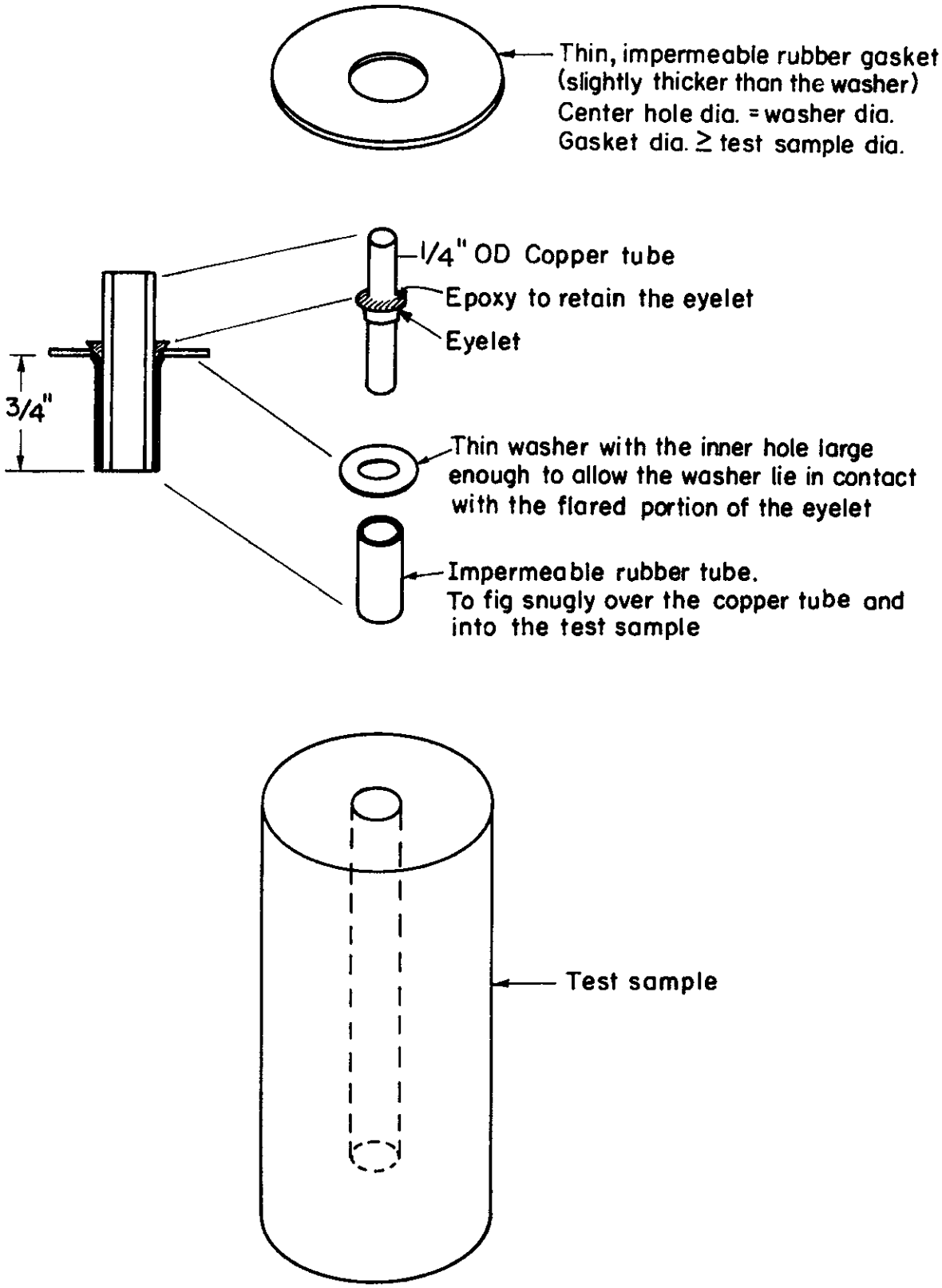

Figure A3.2. Alternate sealing and tube retaining system.

ClibPDF - www.fastio.com

To coupling

Valve B

Plug

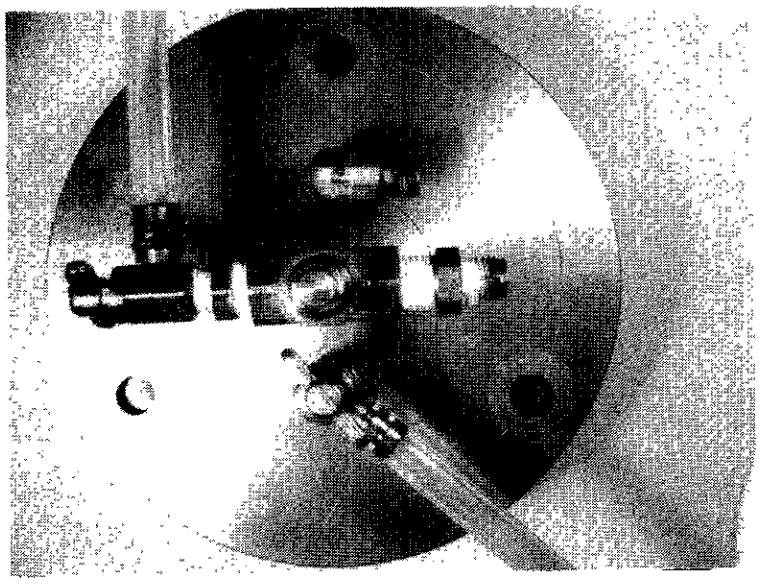

Water line hookup for flow into (or out of) the outside of the sample.

Water line hookup for flow into (or out of) the axial hole.

Valve A

Figure A3.3. Radial Permeameter Top Plate.

ClibPDF - www.fastio.com

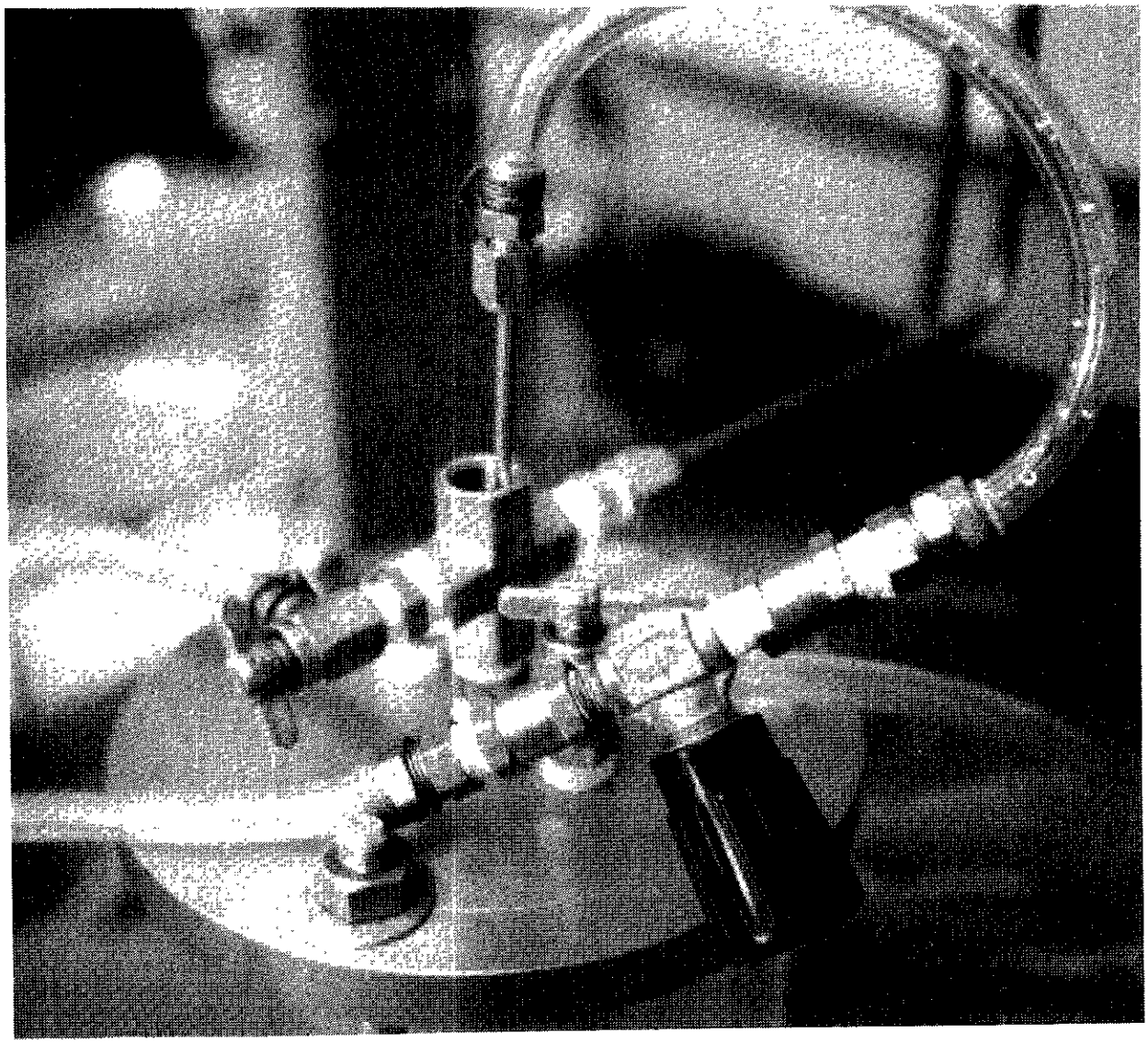

Figure A3.4. Deairing the Axial Hole

ClibPDF - www.fastio.com

University of California RADIAL PERMEABILITY TEST Rock Mechanics Laboratory

Sample Description: _____

_____

_____

Location: _____

Boring No.: _____

Sample Depth: _____

Test No. _____

Date: _____

Tested by: _____

Strain Indicator No. _____

Gage Factor: _____

Sample Dimensions (cm):

L _____ L_1 _____

ℓ _____

R_1 _____ R_2 _____

Test	Strain Indicator Reading (Micro Inch/Inch) Static	Strain Indicator Reading (Micro Inch/Inch) Steady State	Water Pressure (lb/in^2) Static	Water Pressure (lb/in^2) Steady State	Head (cm)	Q (cc)	Time (sec)	k cm/sec	

Figure A3.5. Radial Permeability Data Sheet.

ClibPDF - www.fastio.com

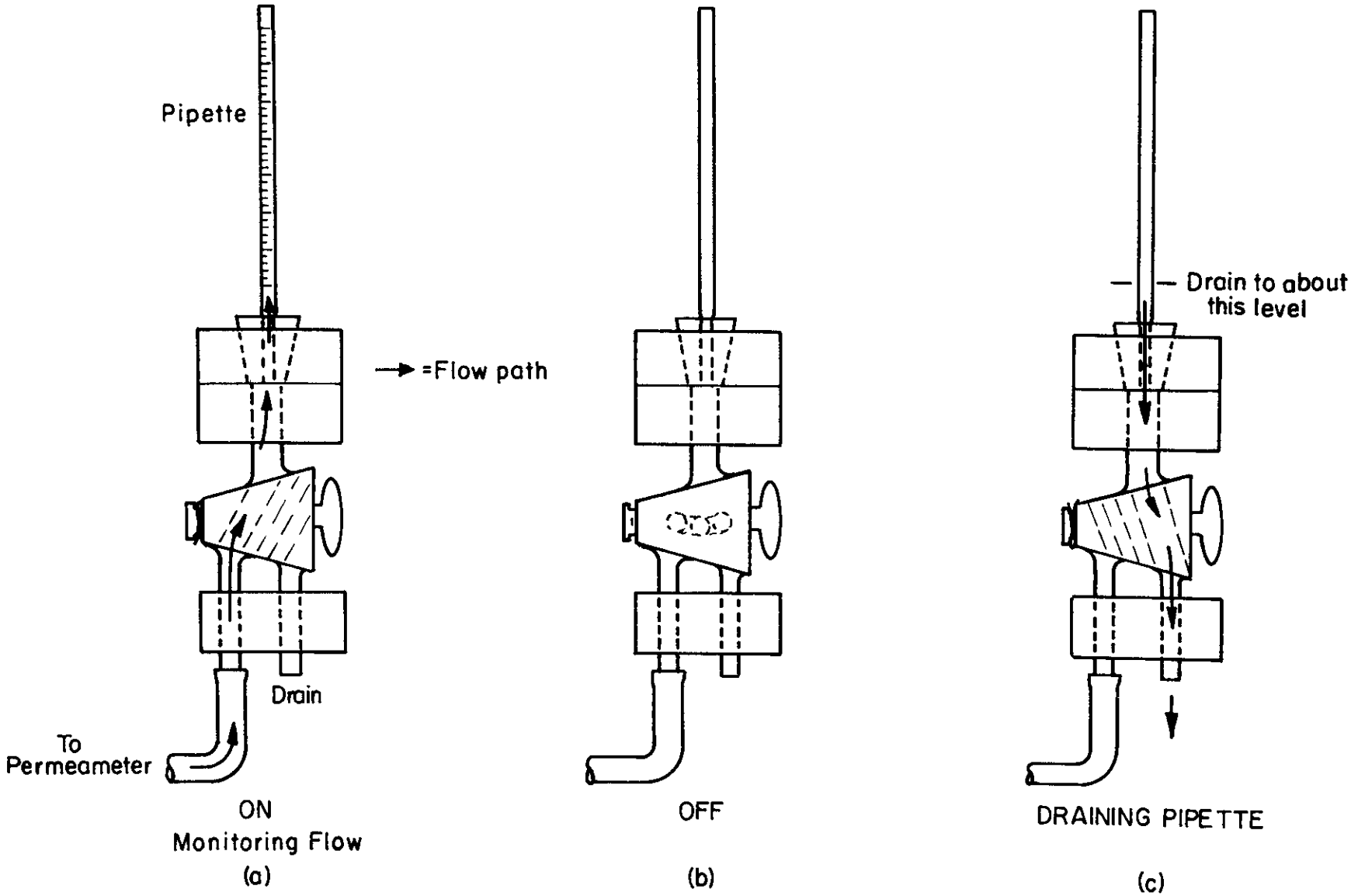

Figure A3.6. Pipette flow measuring system.

ClibPDF - www.fastio.com

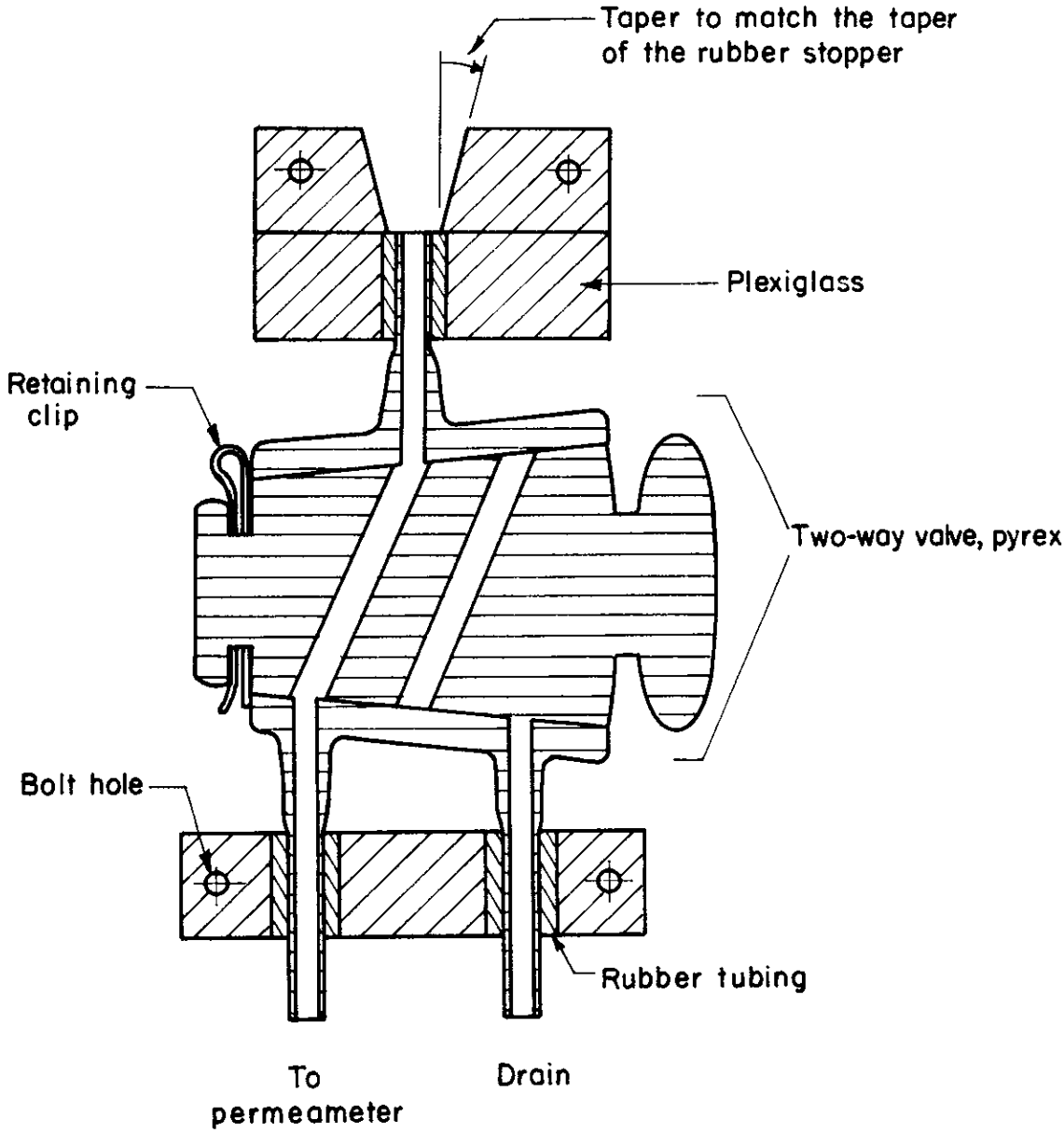

Figure A3.7. Pipette valve and brackets.

ClibPDF - www.fastio.com

Appendix 4

Direct Shear Testing with the (σ,u) Machine

ClibPDF - www.fastio.com

Appendix 4. Direct Shear Testing with the (σ,u) Machine

a) Equipment: The (σ,u) direct shear machine of the U.C. Berkeley Rock Mechanics laboratory was built to permit shearing of joint samples up to 22 square inches in undrained conditions with simultaneous measurements of joint water pressures (Goodman, Heuzé, Ohnishi, 1972), (Goodman, Ohnishi, 1973). Design of any direct shear test represents a selection of priorities from among competing constraints including desire for independent control of: the three translational and three rotational modes of relative displacement, or their reaction forces; environmental conditions; the position and orientation of the applied load vector with respect to the joint plane through large displacements; and load or displacement rates. The selected design provides for control of shearing displacement and normal force. Lateral shear translation is prevented as are all rotations. The limitations on displacement and rotation are needed to permit sealing of the test chamber for internal water pressure. The normal load is stationary whereas the center of the contact area travels; thus large displacements are not feasible. Figure A4-1 shows a schematic section through the machine. Shearing is conducted within a water-tight test chamber which is opened for inputting the sample by removing 8 machine bolts (11*). The sample with a horizontal joint plane up to 4.7 by 4.7 inches (12 by 12 cm) in area, is potted within a steel box which is rigidly connected to the horizontally travelling piston (4) through a saddle (12). The thrust of the front of the saddle against the lower half of the sample is resisted by the rear of the water chamber (13); the chamber and therefore the top of the sample is held stationary horizontally by reaction rods (6). These rods can rotate freely in the vertical plane to allow the water chamber to move vertically through a maximum applitude of 3/8 of an inch (0.95 cm) as the joint contracts, dilates,

*Number referenced here refer to annotations on the appropriate figures.

ClibPDF - www.fastio.com

or closes. The maximum horizontal shear displacement of the bottom of the sample past the top is 0.5 inch (1.27 cm). The horizontal displacement is created by a motor and variable speed transmission, yielding a maximum shearing speed of 0.275 inches per minute (0.012 cm/sec). The normal load is supplied by a hydraulic piston maintained at constant pressure by a hand operated regulator.

The maximum normal and shear loads are both 40,000 pounds (0.178 MN). This provides a maximum normal or shear stress on the largest specimen of 2000 psi (13.8 MN/m^2). Loads are measured by strain gauge load cells (2) and (3) and displayed on a digital voltmeter, a printer, and an XYY plotter. Manual feedback of the normal pressure permits fine control on the normal force as in the present program. The relative normal displacement between the top and bottom of the specimen was measured by sensing the movement of the top half, with a sensor attached to the normal loading frame. Shear deformation is measured by a linear potentiometer (15) between a point on the base (10) and the piston. (Jewelled dial gauges also give direct readings of these displacements). During a test the outputs of potentiometers (14) and (15) are connected to Y_1 and X_2 of the plotter while Y_2 receives either the output of load cell (2) or (3) according to the stage of the test.

The unique feature of the machine is the sealing mechanism for the water chamber, which sustains water pressure inside the chamber of up to 700 psi (4.83 MN/m^2) throughout the test, despite differential displacement across the sample of 0.5 inches (1.28 cm) horizontally and 0.375 inches (0.95 cm) vertically. Figure 2 shows how the seals work. The sides of the box have an opening larger than the actual piston (8) by the amount of the allowable vertical motion (3/8 inch) (0.95 cm). Close fitting seal plates (3) are pressed against the sides of the chamber by adjustable tension rods (4). The vertical motion of the chamber is accomodated by sliding between the seal plates and the sides of the chamber while

ClibPDF - www.fastio.com

horizontal motion of the piston is accomodated by sliding between the seal plates and the piston. The friction introduced by "0" rings (6) is significant at higher pressures, even though teflon "0" rings are used.

The direct shear chamber is shown with the cover and load cell removed in figure 3a. Figure 3b shows a side view. Figure 3c shows the machine during a test.

Notes on Figures A4.3:

1. Normal load cell and cover plate.
2. Test chamber - can move only vertically.
3. Seal plate.
4. Seal plate compression rod (to put vertical motion "0" rings in compression).
5. Roller bearings for horizontal motion of pistons inside chamber.
6. Shear force reaction rods, flexible in vertical plane.
7. Normal load system.
8. Specimen saddle; moves horizontally inside chamber.
9. Outlets, intra-specimen pore pressure lines.
10. Pore pressure transducers.
11. Roller bearings to maintain horizontal motion direction.
12. Piston.

ClibPDF - www.fastio.com

ClibPDF - www.fastio.com

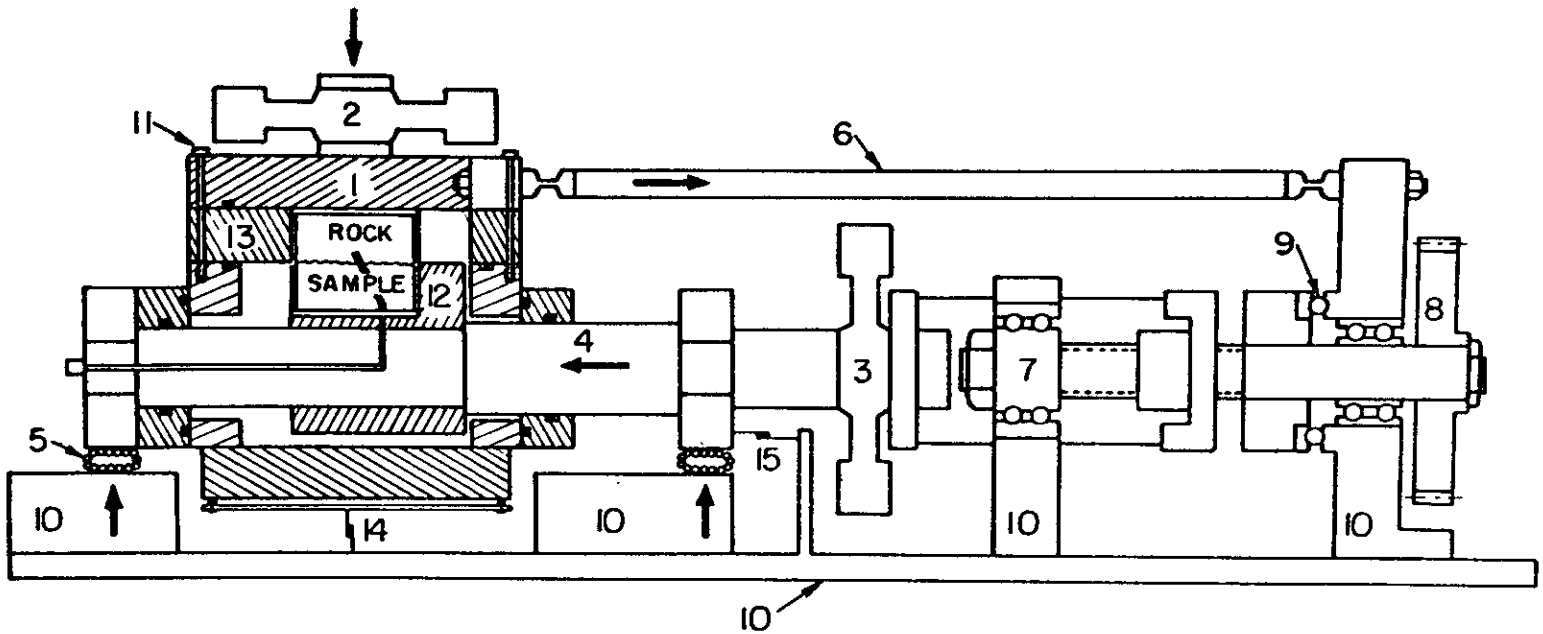

Fig. A4.1. Schematic section through direct shear machine

(1) Test chamber - see Fig.
(2) Normal force load cell
(3) Shear force load cell
(4) Shear force piston
(5) Roller bearings
(6) Flexible reaction rod
(7) Ball and screw assembly
(8) Drive gear
(9) Bearings
(10) Base - (stationary)
(11) Chamber sealing bolts
(12) Saddle
(13) Resisting abutment
(14) & (15) Linear potentiometers

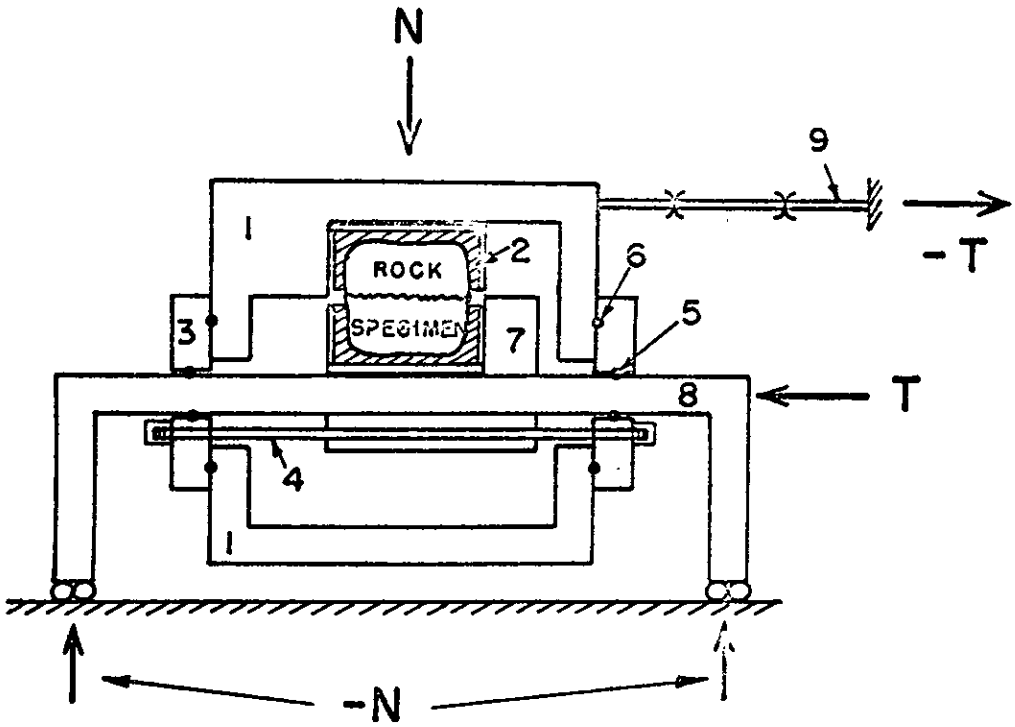

Fig. A 4.2 Sealing scheme for water-tight test chamber (Diagrammatic).

(1) Water-tight test chamber - free to move up and down
(2) Shear box with potted rock specimens.
(3) Seal plate
(4) Seal plate pressure rods; adjustable (actually centered on seal plate)
(5) "0" rings for horizontal motion
(6) "0" rings for vertical motion
(7) Saddle - moves only horizontally with piston
(8) Piston
(9) Reaction rod (see Fig.

ClibPDF - www.fastio.com

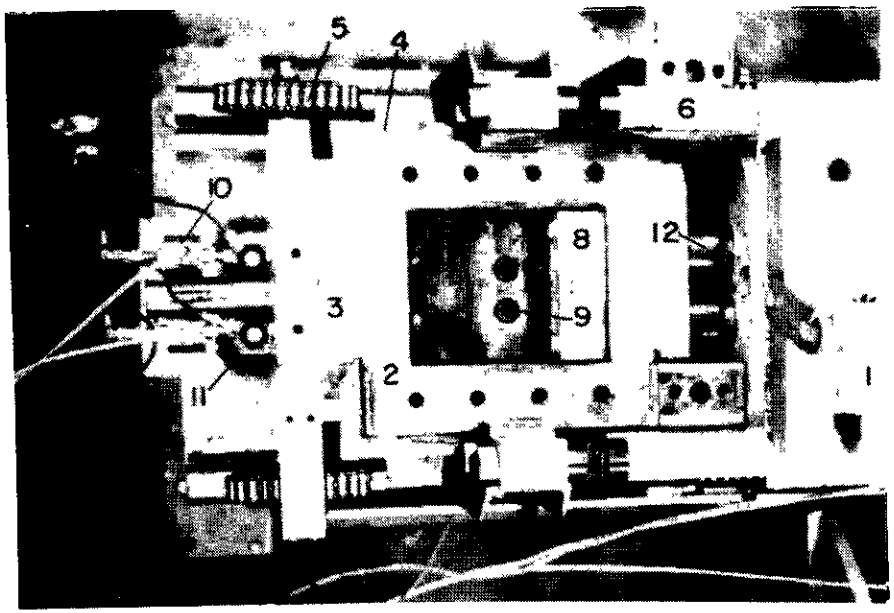

(a)

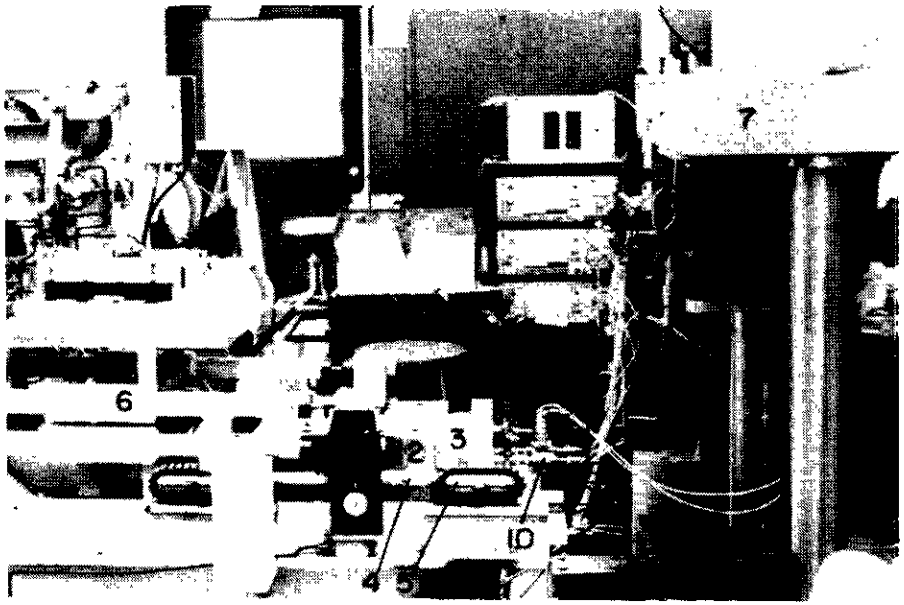

(b)

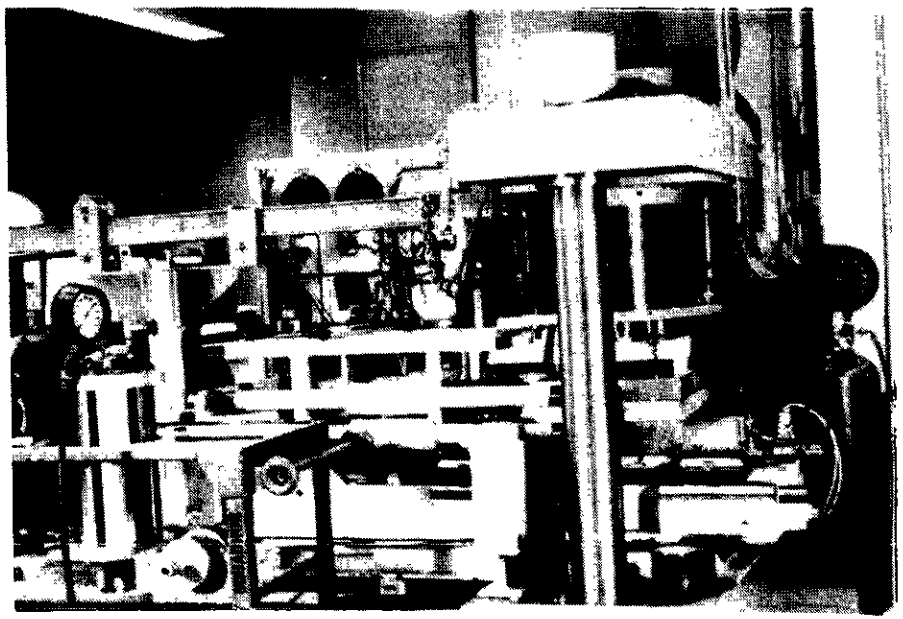

(c)

Fig.A4.3.

Photographs of Direct Shear Machine

(a) Top view with cover removed

(b) Side view

(c) During test

ClibPDF - www.fastio.com

APPENDIX 5

DATA SHEETS FOR LARGE SHEAR TESTS

ClibPDF - www.fastio.com

4-25-74
Borrero
Heuzé
Thorpe

Large Scale Shear Test No. 1 - Sandstone from Caldecott Hole Area = 75.31 in^2

Corr. u	Shear Hyd.Pres.	Shear Load	* τ(psi)	u	Normal Hyd.Pres.	Normal Load	* σ(psi)	V_1	V_2	V_3	V_c
	0psi	0lbs	0	0"	0psi	(+300)	4	0"	0"	0"	0"
	0	0	0	-.0130"	500	2100	28	-.032	-.024	-.001	-0.022
	0	0	0	-.0190	1000	4900	65	-.043	-.034	-.006	-0.031
	0	0	0	-.0220	1500	7500	100	-.057	--	-.010	--
0	0	0	0	-.0245	2000	10200	135	-.080	-.060	-.019	-0.059
.0065	500	2300	31	-.0180	2000	10200	135	-.075	-.064	-.023	-0.059
.0380	1000	5000	66	+.0135	↓	↓	↓	-.068	-.066	-.037	-0.060
.0695	1300	6600	88	+.0450	↓	↓	↓	-.057	-.065	-.049	-0.058
.1005	1600	8200	109	+.0760	↓	↓	↓	-.042	-.062	-.062	-0.054
.1325	1800	9250	123	+.1080	↓	↓	↓	-.022	-.056	-.077	-0.047
.1395	1800	9250	123	+.1150	↓	↓	↓	-.017	--	-.080	--
.1885	2200	11500	153	+.1640	↓	↓	↓	+.013	-.041	-.100	-0.033
.2335	2500	13000	173	+.2090	↓	↓	↓	+.050	-.025	-.114	-0.035
.3115	3000	15600	207	+.2870	↓	↓	↓	+.119	+.012	-.135	+0.022
.3885	3500	18400	244	+.3640	↓	↓	↓	+.184	+.047	-.144	+0.059
.4025	3500	18400	244	+.3780	↓	↓	↓	+.185	+.052	-.144	+0.061
.5145	4000	21000	279	+.4900	↓	↓	↓	--	+.041	--	(+0.062)
.6445	2400	12400	165	+.6200	↓	↓	↓	--	--	--	--
.6875	2400	12400	165	+.6630	↓	↓	↓	--	--	--	--
.7665	2400	12400	165	+.7420	2000	10200	135	--	--	--	--

(Dead wt of top half = 300#)
γ = 2.48 gm/cc

* τ and σ are uncorrected for changes in area of contact.

ClibPDF - www.fastio.com

5-22-74
Borrero
Perdicaris
Thorpe

Large Scale Shear Test No. 2 - Hwy 4 Sample No. 1
$A_i = 53.43\ in^2$

(A) Shear Hyd.Pres. (psi)	Shear Load (lbs)	τ (psi)	u (in)	( ) Normal Hyd.Pres. (psi)	Normal Load (lbs)	σ (psi)	V_1	V_2	V_3	V_c
0	0	0	0	0	300	5.6	0	0	0	0
0	0	0	0	50	558	10.4	0	0	0	0
0	0	0	0	100	815	15.3	-0.001	-0.001	-0.001	-.001
0	0	0	0	150	1073	20.1	-0.002	-0.002	-0.004	-.002
0	0	0	0	200	1330	24.9	-0.005	-0.006	-0.006	-.006
0	0	0	0	250	1588	29.7	-0.008	-0.014	-0.007	-.010
0	0	0	0	300	1845	34.5	-0.009	-0.035	-0.004	-.018
100	515	9.6	0	300	1845	34.5	-0.010	-0.051	+0.003	-.023
300	1545	28.9	0.048	300	1845	34.5	-0.019	-0.067	+0.010	-.031
350	1803	33.7	0.087	300	1845	34.5	-0.026	-0.068	+0.009	-.035
400	2060	38.6	0.165	300	1845	34.5	-0.030	-0.067	+0.017	-.034
400	2060	38.6	0.450	300	1845	34.5	-0.036	-0.059	+0.020	-.033
400	2060	38.6	--	300	1845	34.5	--	-0.049	--	--
400	2060	38.6	--	500	2875	53.8	-0.010	-0.044	-0.001	-0.21
500	2575	48.2	0.813	500	2875	53.8				

(Dead wt ≈ 300 lbs)
γ = 2.05 gm/cc
w = 69%

ClibPDF - www.fastio.com

References

Barton, N., (1974) "Estimating the Shear Strength of Discontinuities in Rock," Proc. 3rd. Congress of International Society for Rock Mechanics, (Denver) Vol. 2.

Bernaix, J., (1969) "New Laboratory Methods of Studying the Mechanical Properties of Rocks," International Journal of Rock Mechanics, Mining Sci., Vol. 6, pp. 43-90.

Broch, E., and Franklin, J. A., (1972) "The Point Load Strength Test", International Journal of Rock Mechanics, Min. Sci., Vol. 9, pp. 669-697.

Deere, D., Hendron, A., Patton, F., and Cording, F., (1967) "Design of Surface and Near Surface Construction in Rock," Proc. 8th Symposium on Rock Mechanics, (AIME), pp. 237-302.

Duncan, J. M., and Goodman, R. E., (1968) "Finite Element Analysis of Slopes in Jointed Rock," U.S. Army Corps of Engineers, Waterways Experiment Station, Contract Report S-68-3.

Franklin, J. A., and Chandra, R., (1972) "The Slake-Durability Index," International Journal of Rock Mechanics, Min. Sci., Vol. 9, No. 3.

Gamble, J. C., (1971) "Durability-Plasticity Classification of Shales and Other Argillaceous Rocks," Ph.D. Thesis, University of Illinois.

Goodman, R. E., Van, T. K. and Heuzé, F. E., (1968) "The Measurement of Rock Deformability in Boreholes," Proc. 10th Symposium on Rock Mechanics, Austin, Texas, (AIME) Ed.

Goodman, R. E., Heuzé, F. E. and Ohnishi, Y., (1972) "Research on Strength-Deformability-Water Pressure Relationships for Faults in Direct Shear," Final Report from Geological Engineering, University of California, Berkeley, to U.S. Bureau of Mines, Denver on ARPA Contract H0210020.

Goodman, R. E., and Ohnishi, Y., (1973) "Undrained Shear Testing of Jointed Rocks," Rock Mechanics, No. 5, pp. 129-149.

Goodman, R. E., (1974) "The Mechanical Properties of Joints," Proc. 3rd. Congress of the International Society of Rock Mechanics, Vol. 1, pp. 127-140.

Habib, P., Baron, G., and Castel Y., (1963) "Deformation des Roches sous Contrainte," Revue Inst. Fr. Petrole, 18, December.

Heuzé, F. E., Goodman, R. E., and Bornstein, A., (1971) "Numerical Analysis of Deformability Tests in Jointed Rock. Joint Perturbation and No-Tension Finite Element Analyses," Rock Mechanics, Vol. 3, No. 1.

Heuzé, F. E., and Goodman, R. E., (1971) "Three-Dimensional Approach for the Design of Cuts in Rock," Proc. 13th Symposium on Rock Mechanics, Urbana, Illinois, (ASCE) Ed.

ClibPDF - www.fastio.com

Hoek, E., and Bray, J., (1974) "Rock Slope Engineering," Inst. Mining and Metallurgy, London.

International Society for Rock Mechanics, "Suggested Methods for Determination of the Slake-Durability Index," Standardization of Laboratory and Field Tests of the International Society for Rock Mechanics, Volume in preparation.

Mearns, R. W., Hoover, T. P. and McCauley, M. L., (1973) "Design Variables for Cut Slopes," Transportation Laboratory, California Division of Highways, Sacramento, Research Report CA-DOT-TL-2882-1-73-27, September.

Mogi, K., (1962) "The Influence of the Dimension of Specimens on the Fracture Strength of Rocks," Bull. Earthq. Res. Inst. Tokyo University, Vol. 40.

Patton, F., (1966) "Multiple Modes of Shear Failure in Rock," Proc. 1st Congress of International Society for Rock Mechanics, Lisbon, Vol. 1, pp. 509-513.

Reichmuth, D. R., (1968) "Point Load Testing of Brittle Materials to Determine Tensile Strength and Relative Brittleness," Proc. 9th Symposium on Rock Mechanics, (AIME).

State of California, Division of Highways, Materials and Research Department, (1967) "Method of Test for Durability Index," TM 229-E.

Weight, S. G., (1971) "A General Computer Program for Slope Stability Analysis in Soils," Department of Civil Engineering, The University of Texas, Austin.

ClibPDF - www.fastio.com